ABSTRACT

GOJANOVICH, GREGORY STEVEN. Investigating and Manipulating Major Histocompatibility Complex (MHC) Class I-Restricted Peptide Epitopes and Cognate T-cell Responses. (Under the direction of Dr. Paul R. Hess.)

The major histocompatibility complex class I (MHCI) molecules are restrictive elements for responses by natural killer (NK) and cluster of differentiation (CD)8+ T cells, which are cytotoxic immune cell effectors that assist in the containment of intracellular pathogens and the destruction of foreign tissues. While studies have shown the existence of antigen-specific CD8+ T-cell responses in cats and dogs, data regarding the capability of putative classical MHCI allomorphs to restrict such responses are lacking. Thus, one objective of this dissertation is to characterize genes critical to normal peptide:MHCI (pMHCI) expression, the transporters associated with antigen processing (TAP1/2), and to specifically knock out (KO) these genes in order to create a tool kit useful for studying peptide interactions with putatively classical feline and canine MHCI molecules. Having such a tool kit will allow for studies to detect CD8+ T-cell responses restricted by pathogen-derived epitopes presented by newly defined, classical MHCI allomorphs in these species. Herein, we determined the coding sequences of the canine TAP1/2 genes, and also confirmed the TAP2 locus in the cat by targeted KO using a biotechnological scissor-like mechanism, called transcription activator-like effector nucleases (TALENs). Furthermore, we created two novel feline cell lines (CRFK-PoBoy1 and 1A3-PoBoy2) that possess TALEN-mediated genomic modifications at the putative feline TAP2 locus, which resulted in reduced MHCI expression that is restored by exogenous TAP2 gene complementation. Future studies will determine the capability

of these cells to stabilize feline leukocyte antigen class I (FLAI) complexes at the surface following exposure to peptides that match the feline MHCI-E*02001 allelic peptide-binding motif, and to bulk peptides eluted from FLAI complexes on parental cells.

We further utilized TALEN technology in our second objective; the intentional downregulation of classical MHCI protein on murine cell lines. For this objective, we selectively targeted the heavy chain genes of MHCI and not other genes involved within the peptide loading complex, as other studies have shown that KO of non-heavy chain genes may still result in surface MHCI expression. Following transfection of a murine beta cell line (NIT-1) with TALENs and a green fluorescence protein (GFP) reporter, we enriched for GFP positive cells possessing high TALEN activity and characterized the resulting clones. By this technique, we created a novel MHCI-deficient insulinoma cell line, NIT-KG, which possess targeted mutations in both the classical murine H2 loci (H2-K1 and –D1), and determined the ability of these cells to escape recognition by H2-K^b-restricted, autoreactive CD8+ T cells. We show that preventing surface expression of murine MHCI by way of TALEN technologies results in protection of these insulin producing cells from transgenic, autoreactive CD8+ T cells, which are major effectors in type 1 diabetes onset and recurrence.

Overall, this body of work contributes to the understanding of antigen presentation in feline and canine species by providing new data on TAP genes in these species and by creating tool kits useful for studying CD8+ T-cell responses. It further provides data indicating the usefulness of TALEN technology in creating genetically engineered cell lines in multiple species. Finally, TALEN-mediated genetic engineering strategies that prevent surface MHCI expression may result in tissues that can evade anti-graft responses, providing for a possible new treatment option for type 1 diabetes patients.

Investigating and Manipulating Major Histocompatibility Complex (MHC) Class I-Restricted Peptide Epitopes and Cognate T-cell Responses

by
Gregory Steven Gojanovich

A dissertation submitted to the Graduate Faculty of
North Carolina State University
in partial fulfillment of the
requirements for the degree of
Doctor of Philosophy

Immunology

Raleigh, North Carolina

2014

APPROVED BY:

Paul R. Hess, DVM, Ph.D. Committee Chair	Susan L. Tonkonogy, Ph.D. Vice Chair
Scott M. Laster, Ph.D. Immunology Program Director	Barbara Sherry, Ph.D. Biotechnology Representative

DEDICATION

This dissertation is dedicated to the memory of Kay Jones Gojanovich, the woman who taught me the strength of spirit to be able to undertake such a grandiose challenge as a Ph.D. program. Her intelligence and wit were surely an appreciated inheritance to assist in attaining this degree.

BIOGRAPHY

Gregory Steven Gojanovich was born and raised in Melbourne FL by Kay Jones and Steven Gojanovich. His older and only sister, Britanna Fagan, married Matt Fagan and the couple happily gave birth to their first child, Cora Doreen Fagan, on September 7, 2013. Exactly one month later, Greg's mother, Kay, succumbed to her second bout with cancer; but only after getting to meet her most precious and first grandchild, which was her greatest wish. Kay and Steven taught their son to live by the principles of courtesy, integrity, perseverance, self control, and indomitable spirit.

Greg is an avid soccer fan, which he undoubtedly inherited from his British blood, and still tries to play today in order to keep in prime physical shape. When not in the lab, one can find him running onto the Fedex Field celebrating the victory of Manchester United over Barcelona, or playing hooky from teaching responsibilities to watch the USA play Italy in the FIFA World Cup. Greg played soccer throughout his years at Satellite High School and was recruited to play at a small Catholic college in Belmont NC, where he started his studies in the life sciences.

At the age of 15, Greg was diagnosed with type 1 diabetes with the assistance of the clever observations of a British Aunt, Anne Cheadle. Ironically, hypodermic needles were Greg's only true fear in life and were required to deliver the insulin he needed to counteract the hyperglycemia and downstream side effects. Thanks to more modern medicine, he has been on an insulin pump since his freshmen year in college, but his disease is what spurs on his career ambitions.

Greg believes he is indebted to the previous scientists that have elucidated the mechanisms of autoimmune-mediated diabetes, and feels it necessary to attempt to pay their good deeds forward onto other potential diabetics by performing research that he hopes will bring about an end to the disease. He first started his endeavors into immunology at Appalachian State University, where he study the effects of intensive exercise on immune functions.

Following completion of his Master degree, Greg attempted to study abroad in London, but it was not meant to be. Gratefully, Greg got to see his beloved Red Devils football team play for the first time during this trip abroad due to the generous assistance of his cousin, Mark Jones, who has been like an uncle to Greg. After this adventure, Greg returned home to Florida to situate his life goals and plan his next steps. It was during this time that Greg learned of North Carolina State University and the cutting edge diabetes research his future Ph.D. advisor, Dr. Paul Hess, was performing. Greg started his matriculation in the Immunology program at NCSU in 2009, where he performed research that focused on T-cell responses governed by classical major histocompatibility complex class I molecule.

Currently, Greg is residing in Raleigh, NC and starting a postdoctoral position at UNC, where he continues to research therapies and treatments for diabetes. His beloved lab/hound mixed dog, Po' Boy, is still laying on the couch/bed while his owner is away or is singing to his favorite musicians, Sublime and The Avett Brothers, to cheer Greg up.

TABLE OF CONTENTS

LIST OF TABLES

Chapter 2.

LIST OF FIGURES

Chapter 4.

Chapter 5.

Chapter 6.

CHAPTER 1: Role of classical class I MHC in regulating cellular immune responses

Introduction

This dissertation will be focused upon two broad topics, as depicted in Figure 1, relating to the intentional downregulation of classical class Ia major histocompatibility complex (MHCI) protein expression: 1) manipulating surface expression in order to elucidate cluster of differentiation (CD)8+ T-cell responses in the *Canis lupus familiaris* and *Felis catus* species, as this will contribute to the sparse data available in these companion animals; and 2) preventing surface expression in order to promote immune system evasion by graft tissues, as a potential therapy for type 1 diabetes (T1D) patients. In this chapter, I will provide a brief review of the current understanding of the mechanisms of MHCI expression as these molecules restrict CD8+ T-cell and inhibit natural killer (NK)-cell responses across species. Overall, we aim to 1) characterize and knock out the transporters associated with antigen processing (TAP) genes so as to create an invaluable tool kit for studying canine and feline T-cell responses; and to 2) use transcription activator-like effector nucleases (TALENs) to knock out (KO) the MHCI heavy chains in murine cell lines, resulting in the inability of CD8+ T cells to recognize these cells.

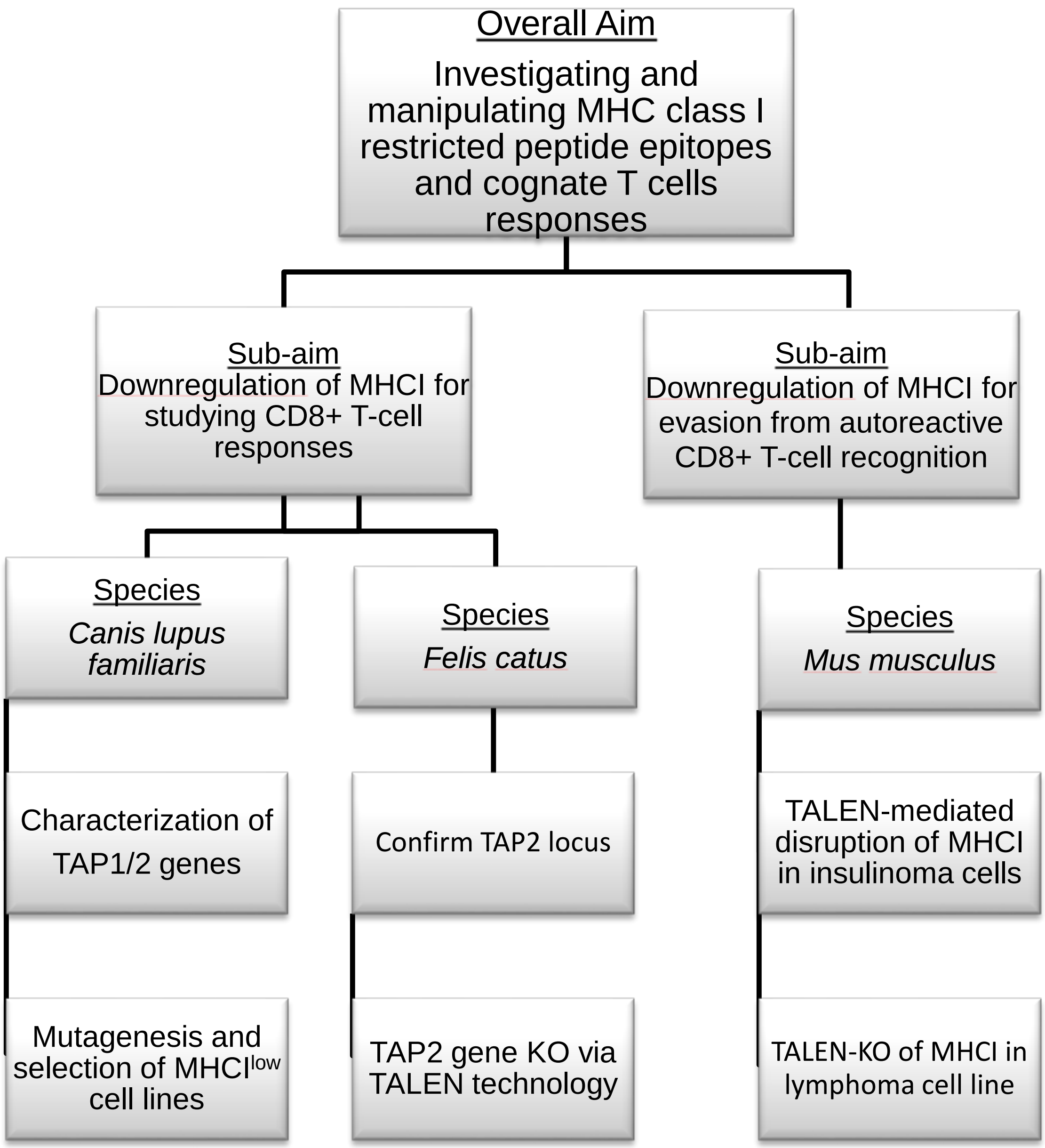

Figure 1. Schematic of dissertation organization depicting aims, species included in studies, and proposed outcomes. Chapters will be proceed as shown from left to right.

Regulation of immune cells by MHCI expression

The genomic region encoding a plethora of genes primarily involved in immune responses is called the major histocompatibility complex (MHC), and is thought to have co-evolved by way of duplication events and exon shuffling, while being conserved across Bilateria (Danchin et al., 2003, 2004). Genes important for immune function and antigen presentation, such as the classical and nonclassical class I MHC loci, the class II MHC genes, the TAP1/2 genes, and proteasome genes, are located within the MHC class 1 and 2 regions. The genes relevant to this dissertation are those that encode the heterodimeric TAP1 and 2 subunits and also the heavy chain units of the trimolecular peptide:MHCI complexes. For a detailed discussion of the organization and function of the TAP1/2 genes, see Chapter 2. The rest of this chapter will be dedicated to the function of the highly polymorphic MHCI genes as they restrict immune responses.

The classical heterotrimeric MHCI complex is comprised of the MHCI heavy chain, the beta-2-microglobulin (β2M) light chain, and a short peptide fragment that is derived from proteins within the cytosol, after degradation by the proteasome, and shuttled by the TAP heterodimer into the endoplasmic reticulum (ER), where these peptides can then interact with the multitude of molecules that create the peptide loading complex (Cresswell et al., 2006). The peptide-loaded MHCI (pMHCI) complex is transported to the extracellular surface via the golgi apparatus where receptors on NK- and CD8+ T-cells can interact with the complexes. Thus, MHCI antigen processing involves intricate molecular steps within the cell before it reaches the surface membrane, where it may then mediate multifaceted interactions with the immune system.

Numerous points along the above biochemical processes limit the breadth of peptides presented within the groove of the MHCI molecule, thereby restricting the ability of the T-cell receptor on the surface of CD8+ T cells to “see” all possible peptides presented by MHCI complexes [reviewed in (Yewdell, 2006)], resulting in certain antigen-specific clonotypes of CD8+ T cells to be more prevalent during infections. Peptides that have been fragmented from intracellular proteins by the proteasome and which are of sufficient affinity for MHCI peptide-binding residues, found within the highly variable regions within the alpha 1 and 2 domains of the MHC heavy chain (Bjorkman et al., 1987), may stabilize the MHCI complex to create a peptide-loaded mature state (Mage et al., 2013; Neefjes et al., 2011; Trombetta and Mellman, 2005). The constitutive proteasome and its interferon gamma (IFNγ)-induced altered state, known as the immunoproteasome, have been shown to result in differential peptide presentation (Toes et al., 2001) and influence CD8+ T-cell responses (Chen et al., 2001), though the overall reduction of possible epitopes presented following these antigen-editing pathways does not contribute significantly to the restriction of T-cell responses (Yewdell, 2006). Instead, it has been shown that allelic polymorphisms at the MHCI residues responsible for peptide-binding are what ultimately influence the repertoire of peptides displayed at the cell surface (Bleek and Nathenson, 1991), and thereby result in immunodominant CD8+ T-cell responses (Messaoudi et al., 2002). This discrimination in the abilities of MHCI allomorphs to bind peptides (often of variable lengths) is a result of conformational differences created during folding of the MHCI peptide-binding groove (Madden et al., 1991; Collins et al., 1994). MHCI folding results in the formation of pockets within the alpha 1 and 2 domains that allow for interactions with residues at specific positions of the peptide, thereby resulting in so-called peptide-binding motifs, which are useful for predicting the ability of any peptide to bind to an MHCI allele (Lundegaard et al., 2008). An example of such a peptide-binding motif is the preferential binding of the canine MHCI allele, DLA-88*50801, with peptide fragments possessing hydrophobic residues at positions 2 and 3, and either an arginine or lysine at position 9 [(Ross et al., 2012); manuscript in submission]. Furthermore, some allomorphs of MHCI also possess the characteristic of binding peptides with submotif-matching sequences (Fremont et al., 1995), thereby making peptide binding predictions more complicated. Other steps that also restrict the ability of pMHCI complexes from being recognized by CD8+ T cells include the inability of TAP to transport all degraded protein fragments into the ER and the availability of T-cell receptors (TCRs) capable of interacting with presented peptides in the MHCI complex, but these are purported to have minimal influence (Yewdell, 2006). Thus, the steps that reduce the pool of presented pMHCI complexes, antigen editing and MHCI binding primarily, result in a hierarchical distribution of CD8+ T cells capable of responding to specific intracellular infections or self peptides.

As mentioned above, the ability to predict peptides derived from pathogens that will bind MHCI, the rate limiting step in CD8+ T-cell recognition, is an extremely useful tool and numerous databases are available to assist in these predictions (Nielsen et al., 2007; Rammensee et al., 1999; Meydan et al., 2013). By applying “reverse immunology” strategies, researchers are able to derive peptides from the proteome of a pathogen, which can include some 135,000 proteins as in the poxvirus (Yewdell, 2006), that have a high likelihood of binding the MHCI allomorph of interest and stimulate cognate T-cell responses, which may ultimately provide vaccination strategies or tools for disease diagnoses (van Endert et al., 2006). The confirmation of a T-cell response to a putative MHCI-binding peptide can be achieved by detecting T-cell effector responses, which will be discussed later, including measurement of cytokine release, calcium flux, surface protein up- or downregulation, or proliferation, to name a few (Tobery et al., 2006; Abu-Khader and Krause, 2013). Yet, while pathogen-specific CD8+ T-cell responses have been described in the canine and feline species (Hartley et al., 2014; Miller et al., 2013), data regarding the precise roles of the MHCI loci responsible for restricting these responses is lacking for companion animals.

In order to derive such peptide prediction databases for canid and felid responses, the motifs of peptides bound by these species classical MHCI allomorphs must first be empirically determined; one of our primary. Such MHCI peptide motif characterization requires proper tool kits for 1) the collection of naturally processed and presented peptides by MHCI allomorphs for the purposes of creating binding motif hypotheses, and 2) the empirical testing of peptide-binding motif hypotheses by way of MHCI stabilization assays. We have recently described a tool kit for analyzing the peptide motif of the classical canine DLAI-88*50801 allomorph (Ross et al., 2012), and in this dissertation I will discuss efforts to create a similar tool for analyzing feline MHCI peptide-binding. The next subsections will briefly describe the functions of MHCI complexes in restricting immune responses of specific cellular subsets.

MHCI and T cells

Following the loading of edited peptides into the groove of the MHCI heavy chain associated with β2M, pMHCI is displayed at the cellular membrane, where the complex may interact with the TCRs on CD8+ T cells to create an immunological synapse. The CD8 co-receptor on αβ TCR-possessing T cells is comprised of a heterodimeric αβ glycoprotein complex that interacts with an invariant region of the alpha 3 domain of MHCI (Salter et al., 1990) to stabilize the pMHCI-TCR interaction and to enhance antigen sensitivity [reviewed in (Cole et al., 2012)]. Furthermore, the co-localization of CD8 co-receptor and TCR at the cell surface has been shown to relate to antigen sensitivity of T cells, possibly explaining the mechanism of functional avidity maturation that occurs during ongoing infection (Borger et al., 2014). The multidimensional pMHCI-TCR synapse [reviewed in (Zhu et al., 2013)] is often considered signal one of the processes that orchestrate a T-cell response. This synapse formation, which is not a binary type of interaction (Krummel et al., 2000), induces protein-tyrosine kinase signaling cascades by the TCR/CD3 complexes to ensue (Weiss, 1993), resulting in myriad downstream effects such as calcium flux and gene transcription depending on the maturation state of the T cell. Data are available, however, to indicate that only this signal may be required for T-cell responses to occur (Wang et al., 2000). Yet, it is widely accepted that further signaling cascades are associated with the initial synapse formation to enhance or prevent T-cell responses. Signal two is governed by co-receptors, such as activating CD28 or inhibitory PD-1 complexes (Okazaki et al., 2002), on the CD8+ T cell that provide further feedback signals to mediate responses by the T cell. Finally, the local cytokine milieu, produced by antigen-presenting cells and/or CD4+ T cells in close proximity to synapse formation, further enhances the regulatory feedback within CD8+ T cells following TCR-MHCI ligation (Leung et al., 2010). Thus, the production of an effective T-cell response is a complexly regulated pathway that starts with the interaction of pMHCI-TCR complexes.

The accumulation of stimulatory and inhibitory signals in T cells ultimately results in the activation of transcriptional regulatory factors that alter gene expression to allow for effector function acquisition [reviewed in (Taniuchi, 2009)]. The relatively new understanding of the plasticity in the spectrum of T-cell lineage differentiation has further highlighted the importance of the presence and qualitative differences of secondary and tertiary signals (Arens and Schoenberger, 2010; Murphy and Stockinger, 2010; Crispín and Tsokos, 2009). Thus, recent data reaffirm the long-held conception that CD8+ T cells are not only capable of cytotoxic activity, but also suppressor functions (Shafer-Weaver et al., 2009), though this concept will be addressed later in chapter 5. Also described more thoroughly in chapter 5 are the cytotoxic effector functions of CD8+ T cells in the realm of diabetes, but here I will briefly highlight general functions. Specifically, interferon-gamma (IFNγ) is one of the primary cytokines produced by CD8+ T cells and functions to amplify T-cell responses early after synapse formation (Teixeira et al., 2005), and to enhance CD8+ T-cell cytotoxicity against malignant or infected cells, and also specifically against the insulin producing beta (β) cells in type 1 diabetes (Chong et al., 2011). The release of tumor necrosis factor-alpha (TNFα) cytokine, the release of cytotoxic granules containing perforin and granzyme B onto target cells, and the presence of apoptosis-inducing Fas ligands at the cell surface are also well-described effector mechanisms utilized by CD8+ T cells (Janeway et al., 2001). Thus, the differentiation of CD8+ T-cell effector functions is a plastic spectrum involving transcriptional differences regulated epigenetically, which may result in the capacity to acquire cytotoxic capability, one of the primary means by which these cells induce immunity or tolerance.

The primary role of CD8+ T cells is to utilize effector functions to contain the spread of the intracellular pathogen and to create an inhospitable environment for pathogen replication [reviewed in (Demers et al., 2013)]. This is achieved by using cytotoxic functions (e.g. Fas ligand and granzyme) to induce apoptosis in cells displaying cognate peptides derived from intracellular pathogens by MHCI complexes, in order to directly destroy cells infected by pathogen. During differentiation, cytotoxic cells accumulate lytic molecules within granules (Sanchez-Ruiz et al., 2011). CD8+ T-cells (and NK cells) can then rapidly perform serial killing of target cells by way of polarization of granules towards the area of pMHCI synapses [reviewed in (Galandrini et al., 2013)], thereby limiting the directional release of cytotoxic molecules towards the infected cells. Furthermore, CD8+ T cells can release non-cytotoxic beta-chemokines or lymphokines that may inhibit viral entrance into the cell or viral replication within the cell (Demers et al., 2013). Cytotoxic effectors are therefore primed by activation signals and respond rapidly to intracellular pathogen to prevent spread of the infection.

Before circulating in the periphery where CD8+ T cells may perform the above functions, they are first “educated” in the thymus. Here, thymocytes are exposed to two primary types of processes, called positive and negative selection, mediated by cortical and medullary antigen-presenting thymic epithelial cells, respectively (Holländer and Peterson, 2009). These processes are responsible for producing CD8 single positive T cells that have TCR with affinity for self MHCI complexes, but have only low affinity for self peptides presented by MHCI complexes. Such TCR selection is thought to occur based on the zipper model of pMHCI-TCR interaction that correlates dwell time with activation thresholds that result in cell survival or apoptosis [reviewed in (Palmer and Naeher, 2009)]. A recent study quantified thymic selection processes in the mouse and determined that six times more thymocytes undergo apoptosis in negative selection than survive positive selection, and that the TCR signaling that induces cell death is only slightly stronger than signals that induce survival (Stritesky et al., 2013). The thymic education, and routine peripheral maintenance, of TCR signaling in CD4+ T-cell clonotypes has been recently described to have a profound effect on the magnitude and type of response elicited by these cells during infection (Persaud et al., 2014). The signaling cascades that influence activation thresholds involve TCR-proximal adaptor proteins, such as ZAP-70. Autoreactive T cells may possess mutations in ZAP-70 (Hsu et al., 2009) and therefore do not become anergic. Furthermore, inducible expression of a negative regulator of TCR signaling, CD5, on T cells during the negative selection process helps to fine tune TCR signaling, and CD5 expression correlates with the affinity of TCR for antigen (Azzam et al., 2001). When transgenic TCR with relatively high affinity for self-MHC are expressed in the absence of CD5 expression, these clonotypes undergo negative selection, likely due to strong TCR-mediated signal transduction levels being too high. As a counter-balancing regulatory mechanism, thymic processes can trigger survival, also a result of TCR affinity-based survival (Lee et al., 2012), of regulatory T cells with higher affinity for self pMHCI that assist in preventing autoreactivity by secreting immunosuppressive cytokines or expressing membrane-bound effector molecules [reviewed in (Josefowicz et al., 2012)]. Thus, the thymus produces CD8+ T cells displaying TCR with sufficient affinity for self MHCI complexes to allow for effector responses, but can also produce regulatory T cells that assist in preventing autoreactivity in the periphery.

As further discussed in chapter 5, T1D (and other autoimmune) patients possess CD8+ T cells in the periphery capable of recognizing self peptides at frequencies that overpower the regulatory T-cell effects (Tsai et al., 2010). While there are numerous types of peripheral tolerance mechanisms in place, such as extrathymic autoimmune regulator (Aire)-expressing cells (Bluestone and Bour-Jordan, 2012; Metzger and Anderson, 2011), autoreactive T cells in these patients somehow persist. There are numerous hypotheses regarding how such cells are not anergized during tolerization processes and how these cells become activated in peripheral circulation. Some hypotheses involve the peptide-centric model of TCR binding by autoreactive CD8+ T cells (Bulek et al., 2012) and the ability of a single TCR to recognize more than one peptide (Wooldridge et al., 2012). Furthermore, the concept of T cells displaying more than one rearranged TCR gene product at the cell membrane is also a possibility (Simpson et al., 1995; Fossati et al., 1999). The exact mechanisms by which these autoreactive cells are activated in the periphery to respond to self are still highly debatable. Two such hypotheses involve infection of islets by enteroviruses and the concept of viral mimicry (Laitinen et al., 2014; Enouz et al., 2012), resulting in release of cognate peptides to levels sufficient for CD8+ T-cell activation or viral peptides being displayed by MHCI on β cells that appear similar to those recognized by autoreactive TCR, respectively. Therefore, peripheral tolerance mechanisms are not always able to prevent autoreactivity to self peptides mediated by CD8+ T cells that escape central tolerance mechanisms.

CD4+ T cells interact with peptide:MHCII complexes and are also under the control of central and peripheral tolerance mechanisms, but will not be a focal point of this dissertation. Yet, CD4+ T-cell responses do play a large role in susceptibility to autoimmune diseases, as highlighted by the strong correlation between MHCII alleles and diabetes (Baker and Steck, 2011). Peptide binding preferences of MHCII allomorphs are believed to contribute heavily to disease progression in individuals possessing risk-associated alleles (Ettinger et al., 2006), and inadequate suppressor functions by CD4+ T cells are also believed to contribute to diabetes pathogenesis (Long et al., 2010). Normally, CD4+ T cells help to provide the necessary cues for mediating activation of CD8+ T cells against intracellular pathogens. Such cues including the cytokines interleukin (IL)-4, IL-10, or IFNγ (and many others), are involved in producing the milieu that results in an inflammatory or anti-inflammatory environment, and direct humoral- or cell-mediated responses. This environment can alter the activation statuses of antigen-presenting cells, e.g. upregulation of CD80 and CD86 on macrophages, and thereby enhance CD8+ T-cell activation by providing co-stimulation. CD4+ T-cells, therefore, help to propagate CD8+ T cell-responses, which are, normally, responsible for preventing the spread of intracellular infections.

In summary, this subsection highlights the function of pMHCI complexes to restrict CD8+ T-cell responses, which have been educated in the thymus to recognize primarily non-self antigens presented by self MHCI, and are assisted by CD4+ T cells [and other subsets (Lehuen et al., 2010)] that promote a cytokine milieu conducive to cell-mediated immunity. Furthermore, peripheral regulatory mechanisms, such as regulatory CD4+ and suppressor CD8+ T cells, assist in preventing autoreactive responses, but may be overwhelmed by genetic variations resulting in defective signaling within T cells of predisposed individuals. Thus, autoreactive CD8+ T cells may be activated by normal signaling cascades and utilize standard CD8+ T-cell cytotoxic capabilities, but are directed against self pMHCI complexes due to incomplete anergy induction.

MHCI and NK cells

Another immune cell subset that interacts directly with pMHCI complexes are natural killer (NK) cells, which are considered an intermediate between innate and adaptive immunity (Long et al., 2013). NK cells lack receptor diversity created by rearrangement of DNA, but do possess a wide array of receptors encoded in the germline, which use stimulatory (such as immunoreceptor tyrosine-based activation motifs; ITAM) and inhibitory (immunoreceptor tyrosine-based inhibitory motifs; ITIM) signaling cascades also present in other immune cell subsets. This section will only briefly describe the function of this cell type and provide insights into the importance of this cell type to our second major topic of this dissertation.

There are a plethora of NK cell receptors, but data regarding the function of each are not currently available. The broadest of categories can be considered the killer activation receptors (KAR) and killer inhibitory receptors (KIR) as based upon the motifs found in the cytoplasmic tails; these groups paradoxically contain some receptors that function antithetically to the group name (Orr and Lanier, 2011). Furthermore, the naming of identical, orthologous receptors across species are not consistent. However, the receptors primarily thought to be important for mediating NK-cell responses (Long et al., 2013) are CD16 (a receptor for the Fc portion of antibody), NKG2D (the natural killer group 2 isoform D receptor), and the MHCI-specific ITIM-bearing receptors (a broad group of inhibitory receptors that interact with classical and nonclassical MHCI complexes), which are of interest to our discussion. While NK cells are known to display a multitude of receptors and co-receptors that can propagate activation in synergistic and redundant manners, the receptors that interact with MHCI license NK cell activity.

The specific MHCI environment of the individual organism results in licensing of NK cells by interaction of inhibitory receptors on the NK cell with the individually expressed MHCI complexes (Kim et al., 2005). The precise mechanisms involved in NK cell licensing are debatable, as they may occur through a stimulatory or inhibitory model [reviewed in (Yokoyama and Kim, 2006)] but ligation of receptors on the NK cell with MHCI complexes is necessary for either. Such licensing corroborates the “missing self” hypothesis of NK cell function (Kärre et al., 1986; Ljunggren and Kirre, 1990), and indicates the importance of MHCI expression as a negative feedback mechanism that prevents NK cell cytotoxicity. The precise inhibitory signaling induced by the ligation of MHCI to KIR appears to be propagated by ITIM domains recruiting the Src homology region 2 domain-containing phosphatase-1 (SHP-1), thereby preventing signal propagation of ITAM-bearing receptors (Long et al., 2013) through dephosphorylation of a component in the activation pathway [possibly Vav1; (Long, 2008)]. The licensing of NK cells has been described to be revocable, in that NK cell hyporesponsiveness is found within hosts lacking MHCI expression, but may be re-initiated following certain infections (Sun and Lanier, 2008; Joncker et al., 2010), indicating that NK cell phenotypes are plastic, similar to other hematopoietic-derived cell subsets (Kawamoto and Katsura, 2009). NK cells, therefore, display a wide array of NK cell receptors, but the inhibitory receptors that recognize MHCI complexes as ligands are crucial for preventing NK cell-mediated killing of normal host cells and appear to be the dominant determinant of NK activation status.

Thus, MHCI complexes are critical for both NK- and CD8+ T-cell responses. NK and CD8+ T cells share cytotoxic capabilities [specifically, lytic granules (Galandrini et al., 2013)] and are very similar in their transcriptional profiles (Bezman et al., 2012). However, unlike CD8+ T cells, new data indicate that NK cells may be able to recognize viral infection due to the possession of pattern recognition receptors, a poorly studied realm of NK-cell function (Muntasell et al., 2013). Furthermore, NK cells require lower priming signals than CD8+ T cells in order to respond to virally infected, malignantly transformed, or allogeneic cells, which are the primary functions of NK cells. The capability of resting NK cells to rapidly respond also makes these cells dangerous to transplant survival (Liu et al., 2012), but also possibly helpful (Kroemer et al., 2008). Specifically, NK cells are not able to recognize allogeneic MHCI allomorphs, and thus destroy allographs due to “missing self”; but data also exist indicating that NK cells assist in destroying donor antigen-presenting cells (APC), thereby reducing recipient alloreactive CD4+ T-cell responses that are primed by donor APC. NK-cell activity detected against bioengineered graft tissues that display reduced levels of MHCI indicate destruction of these grafts as a likelihood (de la Garza-Rodea et al., 2011), but the precise levels of MHCI expression, and which complexes specifically, required for such reactivity are ill defined. NK cells therefore function as cytotoxic mediators in the early stages of cancer protection, viral infection, and graft rejection by using similar effector functions as CD8+ T cells, and these responses are MHCI-dependent, although NK-cell restrictions involve both classical and nonclassical MHCI.

NK cells are regarded as a primary line of defense against viral infection and cancer, but situations do arise in which NK cell surveillance is evaded. Viruses may possess specifically adapted protein mimicry, such as the murine cytomegalovirus m157 protein (Orange et al., 2002), and cancers that have undergone the elimination phase of cancer cell immunoediting are able to escape attack by NK cells (Dunn et al., 2002). One example of viral immunevasin gene application in tissues for transplant was described in the paper by de la Garza-Rodea cited above, in which the cytomegalovirus US11 protein was used to reduce MHCI expression in xenogeneic stem cells. While this application required the depletion of recipient NK cells for graft survival, other virally derived proteins, such as MHCI homologs, may further assist in graft survival (Orange et al., 2002). These naturally occurring mechanisms for immune system evasion, therefore, offer insights into strategies by which insulin producing grafts may be engineered to escape recognition by both autoreactive CD8+ T cells and licensed NK cells in diabetic recipients. Chapter 6 contains a discussion of methods to address these issues with the assistance of genetic engineering.

Summary of objectives

This chapter contains a brief review of the class I antigen processing pathway and how MHCI presentation restricts CD8+ T-cell and NK-cell responses Results presented in this dissertation will add to the understanding of the companion animal MHCI-restricted T-cell responses by characterizing the canine TAP genes, and by confirming the feline TAP2 locus while also creating KO cell lines. Additional results demonstrate the use of biotechnological tools to create insulin producing tissues capable of avoiding autoreactive T-cell responses.

References

Arens, R., and S.P. Schoenberger. 2010. Plasticity in programming of effector and memory CD8 T-cell formation. *Immunol. Rev.* 235:190–205. doi:10.1111/j.0105-2896.2010.00899.x.

Azzam, H.S., J.B. DeJarnette, K. Huang, R. Emmons, C.-S. Park, C.L. Sommers, D. El-Khoury, E.W. Shores, and P.E. Love. 2001. Fine Tuning of TCR Signaling by CD5. *J. Immunol.* 166:5464–5472.

Baker, P.R., and A.K. Steck. 2011. The Past, Present, and Future of Genetic Associations in Type 1 Diabetes. *Curr. Diab. Rep.* 11:445–453. doi:10.1007/s11892-011-0212-0.

Bezman, N.A., C.C. Kim, J.C. Sun, G. Min-Oo, D.W. Hendricks, Y. Kamimura, J.A. Best, A.W. Goldrath, L.L. Lanier, and T.I.G.P. Consortium. 2012. Molecular definition of the identity and activation of natural killer cells. *Nat. Immunol.* 13:1000–1009. doi:10.1038/ni.2395.

Bjorkman, P.J., M.A. Saper, B. Samraoui, W.S. Bennett, J.L. Strominger, and D.C. Wiley. 1987. Structure of the human class I histocompatibility antigen, HLA-A2. *Nature*. 329:506–512. doi:10.1038/329506a0.

Bleek, G.M. van, and S.G. Nathenson. 1991. The structure of the antigen-binding groove of major histocompatibility complex class I molecules determines specific selection of self-peptides. *Proc. Natl. Acad. Sci.* 88:11032–11036.

Bluestone, J.A., and H. Bour-Jordan. 2012. Current and future immunomodulation strategies to restore tolerance in autoimmune diseases. *Cold Spring Harb. Perspect. Biol.* 4. doi:10.1101/cshperspect.a007542.

Borger, J.G., R. Zamoyska, and D.M. Gakamsky. 2014. Proximity of TCR and its CD8 coreceptor controls sensitivity of T cells. *Immunol. Lett.* 157:16–22. doi:10.1016/j.imlet.2013.11.005.

Bulek, A.M., D.K. Cole, A. Skowera, G. Dolton, S. Gras, F. Madura, A. Fuller, J.J. Miles, E. Gostick, D.A. Price, J.W. Drijfhout, R.R. Knight, G.C. Huang, N. Lissin, P.E. Molloy, L. Wooldridge, B.K. Jakobsen, J. Rossjohn, M. Peakman, P.J. Rizkallah, and A.K. Sewell. 2012. Structural basis for the killing of human beta cells by CD8(+) T cells in type 1 diabetes. *Nat. Immunol.* 13:283–289. doi:10.1038/ni.2206.

Chen, W., C.C. Norbury, Y. Cho, J.W. Yewdell, and J.R. Bennink. 2001. Immunoproteasomes Shape Immunodominance Hierarchies of Antiviral Cd8+

T Cells at the Levels of T Cell Repertoire and Presentation of Viral Antigens. *J. Exp. Med.* 193:1319–1326. doi:10.1084/jem.193.11.1319.

Chong, M.M.W., H.E. Thomas, and T.W.H. Kay. 2011. y-Interferon Signaling in Pancreatic beta-Cells Is Persistent but Can Be Terminated by Overexpression of Suppressor of Cytokine Signaling-1. *Diabetes*. 50.

Cole, D.K., B. Laugel, M. Clement, D.A. Price, L. Wooldridge, and A.K. Sewell. 2012. The molecular determinants of CD8 co-receptor function. *Immunology*. 137:139–148. doi:10.1111/j.1365-2567.2012.03625.x.

Collins, E.J., D.N. Garboczi, and D.C. Wiley. 1994. Three-dimensional structure of a peptide extending from one end of a class I MHC binding site. *Nature*. 371:626–629. doi:10.1038/371626a0.

Cresswell, P., N. Bangia, T. Dick, and and G. Diedrich. 2006. The nature of the MHC class I peptide loading complex. *Immunol. Rev.* 172:21–8.

Crispín, J.C., and G.C. Tsokos. 2009. Transcriptional regulation of IL-2 in health and autoimmunity. *Autoimmun. Rev.* 8:190–195. doi:10.1016/j.autrev.2008.07.042.

Danchin, E., V. Vitiello, A. Vienne, O. Richard, P. Gouret, M.F. McDermott, and P. Pontarotti. 2004. The major histocompatibility complex origin. *Immunol. Rev.* 198:216–232. doi:10.1111/j.0105-2896.2004.00132.x.

Danchin, E.G.J., L. Abi-Rached, A. Gilles, and P. Pontarotti. 2003. Conservation of the MHC-like region throughout evolution. *Immunogenetics*. 55:141–148. doi:10.1007/s00251-003-0562-0.

Demers, K.R., M.A. Reuter, and M.R. Betts. 2013. CD8+ T-cell effector function and transcriptional regulation during HIV pathogenesis. *Immunol. Rev.* 254:190–206. doi:10.1111/imr.12069.

Dunn, G.P., A.T. Bruce, H. Ikeda, L.J. Old, and R.D. Schreiber. 2002. Cancer immunoediting: from immunosurveillance to tumor escape. *Nat. Immunol.* 3:991–998. doi:10.1038/ni1102-991.

Van Endert, P., Y. Hassainya, V. Lindo, J.-M. Bach, P. Blancou, F. Lemonnier, and R. Mallone. 2006. HLA class I epitope discovery in type 1 diabetes. *Ann. N. Y. Acad. Sci.* 1079:190–197. doi:10.1196/annals.1375.030.

Enouz, S., L. Carrié, D. Merkler, M.J. Bevan, and D. Zehn. 2012. Autoreactive T cells bypass negative selection and respond to self-antigen stimulation during infection. *J. Exp. Med.* 209:1769–1779. doi:10.1084/jem.20120905.

Ettinger, R.A., G.K. Papadopoulos, A.K. Moustakas, G.T. Nepom, and W.W. Kwok. 2006. Allelic variation in key peptide-binding pockets discriminates between closely related diabetes-protective and diabetes-susceptible HLA-DQB1*06 alleles. *J. Immunol. Baltim. Md 1950*. 176:1988–1998.

Fossati, G., A. Cooke, R.Q. Papafio, K. Haskins, and B. Stockinger. 1999. Triggering a second T cell receptor on diabetogenic T cells can prevent induction of diabetes. *J. Exp. Med.* 190:577–583.

Fremont, D.H., E.A. Stura, M. Matsumura, P.A. Peterson, and I.A. Wilson. 1995. Crystal structure of an H-2Kb-ovalbumin peptide complex reveals the interplay of primary and secondary anchor positions in the major histocompatibility complex binding groove. *Proc. Natl. Acad. Sci. U. S. A.* 92:2479–2483.

Galandrini, R., C. Capuano, and A. Santoni. 2013. Activation of lymphocyte cytolytic machinery: where are we? *Front. NK Cell Biol.* 4:390. doi:10.3389/fimmu.2013.00390.

De la Garza-Rodea, A., M. Verweij, H. Boersma, I. van der Velde-van Dijke, A. de Vries, R. Hoeben, D. van Bekkum, E.J. Wiertz, S. Knaän-Shanzer, and D. Unutmaz. 2011. Exploitation of Herpesvirus Immune Evasion Strategies to Modify the Immunogenicity of Human Mesenchymal Stem Cell Transplants. *PLoS ONE*. 6:e14493. doi:10.1371/journal.pone.0014493.

Hartley, A.N., G. Cooley, S. Gwyn, M.M. Orozco, and R.L. Tarleton. 2014. Frequency of IFNγ-producing T cells correlates with seroreactivity and activated T cells during canine Trypanosoma cruzi infection. *Vet. Res.* 45:6. doi:10.1186/1297-9716-45-6.

Holländer, G.A., and P. Peterson. 2009. Learning to be tolerant: how T cells keep out of trouble. *J. Intern. Med.* 265:541–561. doi:10.1111/j.1365-2796.2009.02093.x.

Hsu, L.-Y., Y.X. Tan, Z. Xiao, M. Malissen, and A. Weiss. 2009. A hypomorphic allele of ZAP-70 reveals a distinct thymic threshold for autoimmune disease versus autoimmune reactivity. *J. Exp. Med.* 206:2527–2541. doi:10.1084/jem.20082902.

Janeway, J.C., P.J. Travers, and M. walport. 2001. T cell-mediated cytotoxicity. *In* Immunobiology: The Immune System in Health and Disease. Garland Science.

Joncker, N., N. Shifrin, F. Delebecque, and D. Raulet. 2010. Mature natural killer cells reset their responsiveness when exposed to an altered MHC environment. *J. Exp. Med.* 207:2065–2072. doi:10.1084/jem.20100570.

Josefowicz, S.Z., L.-F. Lu, and A.Y. Rudensky. 2012. Regulatory T Cells: Mechanisms of Differentiation and Function. *Annu. Rev. Immunol.* 30:531–564. doi:10.1146/annurev.immunol.25.022106.141623.

Kärre, K., H.G. Ljunggren, G. Piontek, and R. Kiessling. 1986. Selective rejection of H-2-deficient lymphoma variants suggests alternative immune defence strategy. *Nature*. 319:675–678. doi:10.1038/319675a0.

Kawamoto, H., and Y. Katsura. 2009. A new paradigm for hematopoietic cell lineages: revision of the classical concept of the myeloid–lymphoid dichotomy. *Trends Immunol.* 30:193–200. doi:10.1016/j.it.2009.03.001.

Abu-Khader, A., and S. Krause. 2013. Rapid monitoring of immune reconstitution after allogeneic stem cell transplantation--a comparison of different assays for the detection of cytomegalovirus-specific T cells. *Eur. J. Haematol.* 91:534–545. doi:10.1111/ejh.12187.

Kim, S., J. Poursine-Laurent, S.M. Truscott, L. Lybarger, Y.-J. Song, L. Yang, A.R. French, J.B. Sunwoo, S. Lemieux, T.H. Hansen, and W.M. Yokoyama. 2005. Licensing of natural killer cells by host major histocompatibility complex class I molecules. *Nature*. 436:709–713. doi:10.1038/nature03847.

Kroemer, A., K. Edtinger, and X.C. Li. 2008. The innate natural killer cells in transplant rejection and tolerance induction: *Curr. Opin. Organ Transplant.* 13:339–343. doi:10.1097/MOT.0b013e3283061115.

Krummel, M., C. Wülfing, C. Sumen, and M.M. Davis. 2000. Thirty–six views of T–cell recognition. *Philos. Trans. R. Soc. Lond. B. Biol. Sci.* 355:1071–1076. doi:10.1098/rstb.2000.0644.

Laitinen, O.H., H. Honkanen, O. Pakkanen, S. Oikarinen, M.M. Hankaniemi, H. Huhtala, T. Ruokoranta, V. Lecouturier, P. André, R. Harju, S.M. Virtanen, J. Lehtonen, J.W. Almond, T. Simell, O. Simell, J. Ilonen, R. Veijola, M. Knip, and H. Hyöty. 2014. Coxsackievirus B1 Is Associated With Induction of β-Cell Autoimmunity That Portends Type 1 Diabetes. *Diabetes*. 63:446–455. doi:10.2337/db13-0619.

Lee, H.-M., J.L. Bautista, J. Scott-Browne, J.F. Mohan, and C.-S. Hsieh. 2012. A broad range of self-reactivity drives thymic regulatory T cell selection to limit responses to self. *Immunity*. 37:475–486. doi:10.1016/j.immuni.2012.07.009.

Lehuen, A., J. Diana, P. Zaccone, and A. Cooke. 2010. Immune cell crosstalk in type 1 diabetes. *Nat. Rev. Immunol.* 10:501–513. doi:10.1038/nri2787.

Leung, S., X. Liu, L. Fang, X. Chen, T. Guo, and J. Zhang. 2010. The cytokine milieu in the interplay of pathogenic Th1/Th17 cells and regulatory T cells in autoimmune disease. *Cell. Mol. Immunol.* 7:182–189. doi:10.1038/cmi.2010.22.

Liu, W., X. Xiao, G. Demirci, J. Madsen, and X.C. Li. 2012. Innate NK cells and macrophages recognize and reject allogeneic nonself in vivo via different mechanisms. *J. Immunol. Baltim. Md 1950*. 188:2703–2711. doi:10.4049/jimmunol.1102997.

Ljunggren, H., and K. Kirre. 1990. In search of the “missing self”: MHC molecules and NK cell recognition. *Immunol. Today*. 11:237–44.

Long, E.O. 2008. Negative signalling by inhibitory receptors: the NK cell paradigm. *Immunol. Rev.* 224:70–84. doi:10.1111/j.1600-065X.2008.00660.x.

Long, E.O., H. Sik Kim, D. Liu, M.E. Peterson, and S. Rajagopalan. 2013. Controlling Natural Killer Cell Responses: Integration of Signals for Activation and Inhibition. *Annu. Rev. Immunol.* 31:227–258. doi:10.1146/annurev-immunol-020711-075005.

Long, S.A., K. Cerosaletti, P.L. Bollyky, M. Tatum, H. Shilling, S. Zhang, Z.-Y. Zhang, C. Pihoker, S. Sanda, C. Greenbaum, and J.H. Buckner. 2010. Defects in IL-2R signaling contribute to diminished maintenance of FOXP3 expression in CD4(+)CD25(+) regulatory T-cells of type 1 diabetic subjects. *Diabetes*. 59:407–415. doi:10.2337/db09-0694.

Lundegaard, C., K. Lamberth, M. Harndahl, S. Buus, O. Lund, and M. Nielsen. 2008. NetMHC-3.0: accurate web accessible predictions of human, mouse and monkey MHC class I affinities for peptides of length 8-11. *Nucleic Acids Res.* 36:W509–512. doi:10.1093/nar/gkn202.

Madden, D.R., J.C. Gorga, J.L. Strominger, and D.C. Wiley. 1991. The structure of HLA-B27 reveals nonamer self-peptides bound in an extended conformation. *Nature*. 353:321–325. doi:10.1038/353321a0.

Mage, M.G., M.A. Dolan, R. Wang, L.F. Boyd, M.J. Revilleza, H. Robinson, K. Natarajan, N.B. Myers, T.H. Hansen, and D.H. Margulies. 2013. A structural and molecular dynamics approach to understanding the peptide-receptive transition state of MHC-I molecules. *Mol. Immunol.* 55:123–125. doi:10.1016/j.molimm.2012.10.021.

Messaoudi, I., J.A. Guevara Patiño, R. Dyall, J. LeMaoult, and J. Nikolich-Zugich. 2002. Direct link between mhc polymorphism, T cell avidity, and diversity in immune defense. *Science*. 298:1797–1800. doi:10.1126/science.1076064.

Metzger, T.C., and M.S. Anderson. 2011. Control of central and peripheral tolerance by Aire. *Immunol. Rev.* 241:89–103. doi:10.1111/j.1600-065X.2011.01008.x.

Meydan, C., H.H. Otu, and O.U. Sezerman. 2013. Prediction of peptides binding to MHC class I and II alleles by temporal motif mining. *BMC Bioinformatics*. 14 Suppl 2:S13. doi:10.1186/1471-2105-14-S2-S13.

Miller, M.M., E.M. Thompson, S.E. Suter, and J.E. Fogle. 2013. CD8+ clonality is associated with prolonged acute plasma viremia and altered mRNA cytokine profiles during the course of feline immunodeficiency virus infection. *Vet. Immunol. Immunopathol.* 152:200–208. doi:10.1016/j.vetimm.2012.12.005.

Muntasell, A., M. Costa-Garcia, A. Vera, N. Marina-Garcia, C.J. Kirschning, and M. López-Botet. 2013. Priming of NK cell anti-viral effector mechanisms by direct recognition of human cytomegalovirus. *Front. Immunol.* 4:40. doi:10.3389/fimmu.2013.00040.

Murphy, K.M., and B. Stockinger. 2010. Effector T cell plasticity: flexibility in the face of changing circumstances. *Nat. Immunol.* 11:674–680. doi:10.1038/ni.1899.

Neefjes, J., M.L.M. Jongsma, P. Paul, and O. Bakke. 2011. Towards a systems understanding of MHC class I and MHC class II antigen presentation. *Nat. Rev. Immunol.* 11:823–836. doi:10.1038/nri3084.

Nielsen, M., C. Lundegaard, T. Blicher, K. Lamberth, M. Harndahl, S. Justesen, G. Røder, B. Peters, A. Sette, O. Lund, and S. Buus. 2007. NetMHCpan, a method for quantitative predictions of peptide binding to any HLA-A and -B locus protein of known sequence. *PloS One*. 2:e796. doi:10.1371/journal.pone.0000796.

Okazaki, T., Y. Iwai, and T. Honjo. 2002. New regulatory co-receptors: inducible co-stimulator and PD-1. *Curr. Opin. Immunol.* 14:779–782. doi:10.1016/S0952-7915(02)00398-9.

Orange, J., M. Fassett, L. Koopman, J. Boyson, and and J. Strominger. 2002. Viral evasion of natural killer cells. *Nat. Immunol.* 3:1006–12.

Orr, M.T., and L.L. Lanier. 2011. Inhibitory Ly49 Receptors on Mouse Natural Killer Cells. *In* Negative Co-Receptors and Ligands. R. Ahmed and T. Honjo, editors. Springer Berlin Heidelberg. 67–87.

Palmer, E., and D. Naeher. 2009. Affinity threshold for thymic selection through a T-cell receptor–co-receptor zipper. *Nat. Rev. Immunol.* 9:207–213.

Persaud, S.P., C.R. Parker, W.-L. Lo, K.S. Weber, and P.M. Allen. 2014. Intrinsic CD4+ T cell sensitivity and response to a pathogen are set and sustained by avidity for thymic and peripheral complexes of self peptide and MHC. *Nat. Immunol.* 15:266–274. doi:10.1038/ni.2822.

Rammensee, H.-G., J. Bachmann, N.P.N. Emmerich, O.A. Bachor, and S. Stevanović. 1999. SYFPEITHI: database for MHC ligands and peptide motifs. *Immunogenetics*. 50:213–219. doi:10.1007/s002510050595.

Ross, P., J.C. Holmes, G.S. Gojanovich, and P.R. Hess. 2012. A cell-based MHC stabilization assay for the detection of peptide binding to the canine classical class I molecule, DLA-88. *Vet. Immunol. Immunopathol.* 150:206–212. doi:10.1016/j.vetimm.2012.08.012.

Salter, R.D., R.J. Benjamin, P.K. Wesley, S.E. Buxton, T.P.J. Garrett, C. Clayberger, A.M. Krensky, A.M. Norment, D.R. Littman, and P. Parham. 1990. A binding site for the T-cell co-receptor CD8 on the α3 domain of HLA-A2. *Nature*. 345:41–46. doi:10.1038/345041a0.

Sanchez-Ruiz, Y., S. Valitutti, and L. Dupre. 2011. Stepwise Maturation of Lytic Granules during Differentiation and Activation of Human CD8+ T Lymphocytes. *PLoS ONE*. 6:e27057. doi:10.1371/journal.pone.0027057.

Shafer-Weaver, K.A., M.J. Anderson, K. Stagliano, A. Malyguine, N.M. Greenberg, and A.A. Hurwitz. 2009. Cutting Edge: Tumor-Specific CD8+ T Cells Infiltrating Prostatic Tumors Are Induced to Become Suppressor Cells. *J. Immunol.* 183:4848–4852. doi:10.4049/jimmunol.0900848.

Simpson, E., P. Chandler, A. Sponaas, M. Millrain, and P.J. Dyson. 1995. T cells with dual antigen specificity in T cell receptor transgenic mice rejecting allografts. *Eur. J. Immunol.* 25:2813–2817. doi:10.1002/eji.1830251015.

Stritesky, G.L., Y. Xing, J.R. Erickson, L.A. Kalekar, X. Wang, D.L. Mueller, S.C. Jameson, and K.A. Hogquist. 2013. Murine thymic selection quantified using a unique method to capture deleted T cells. *Proc. Natl. Acad. Sci.* 110:4679–4684. doi:10.1073/pnas.1217532110.

Sun, J., and L. Lanier. 2008. Viral Infection Breaks NK Cell Tolerance to “Missing Self.” *J. Immunol.* 181:7453–7.

Taniuchi, I. 2009. Transcriptional regulation in helper versus cytotoxic-lineage decision. *Curr. Opin. Immunol.* 21:127–132. doi:10.1016/j.coi.2009.03.012.

Teixeira, L.K., B.P.F. Fonseca, A. Vieira-de-Abreu, B.A. Barboza, B.K. Robbs, P.T. Bozza, and J.P.B. Viola. 2005. IFN-gamma production by CD8+ T cells depends on NFAT1 transcription factor and regulates Th differentiation. *J. Immunol. Baltim. Md 1950*. 175:5931–5939.

Tobery, T.W., S.A. Dubey, K. Anderson, D.C. Freed, K.S. Cox, J. Lin, M.T. Prokop, K.J. Sykes, R. Mogg, D.V. Mehrotra, T.-M. Fu, D.R. Casimiro, and J.W. Shiver. 2006. A comparison of standard immunogenicity assays for monitoring HIV type 1 gag-specific T cell responses in Ad5 HIV Type 1 gag vaccinated human subjects. *AIDS Res. Hum. Retroviruses*. 22:1081–1090. doi:10.1089/aid.2006.22.1081.

Toes, R.E.M., A.K. Nussbaum, S. Degermann, M. Schirle, N.P.N. Emmerich, M. Kraft, C. Laplace, A. Zwinderman, T.P. Dick, J. Müller, B. Schönfisch, C. Schmid, H.-J. Fehling, S. Stevanovic, H.G. Rammensee, and H. Schild. 2001. Discrete Cleavage Motifs of Constitutive and Immunoproteasomes Revealed by Quantitative Analysis of Cleavage Products. *J. Exp. Med.* 194:1–12. doi:10.1084/jem.194.1.1.

Trombetta, E.S., and I. Mellman. 2005. Cell Biology of Antigen Processing in Vitro and in Vivo. *Annu. Rev. Immunol.* 23:975–1028. doi:10.1146/annurev.immunol.22.012703.104538.

Tsai, S., A. Shameli, J. Yamanouchi, X. Clemente-Casares, J. Wang, P. Serra, Y. Yang, Z. Medarova, A. Moore, and P. Santamaria. 2010. Reversal of Autoimmunity by Boosting Memory-like Autoregulatory T Cells. *Immunity*. 32:568–580. doi:10.1016/j.immuni.2010.03.015.

Wang, B., R. Maile, R. Greenwood, E. Collins, and J. Frelinger. 2000. Naive CD8+ T cells do not require costimulation for proliferation and differentiation into cytotoxic effector cells. *J. Immunol.* 164.

Weiss, A. 1993. T cell antigen receptor signal transduction: A tale of tails and cytoplasmic protein-tyrosine kinases. *Cell*. 73:209–212. doi:10.1016/0092-8674(93)90221-B.

Wooldridge, L., J. Ekeruche-Makinde, H.A. van den Berg, A. Skowera, J.J. Miles, M.P. Tan, G. Dolton, M. Clement, S. Llewellyn-Lacey, D.A. Price, M. Peakman, and A.K. Sewell. 2012. A single autoimmune T cell receptor recognizes more than a million different peptides. *J. Biol. Chem.* 287:1168–1177. doi:10.1074/jbc.M111.289488.

Yewdell, J.W. 2006. Confronting complexity: real-world immunodominance in antiviral CD8+ T cell responses. *Immunity*. 25:533–543. doi:10.1016/j.immuni.2006.09.005.

Yokoyama, W.M., and S. Kim. 2006. Licensing of natural killer cells by self-major histocompatibility complex class I. *Immunol. Rev.* 214:143–154. doi:10.1111/j.1600-065X.2006.00458.x.

Zhu, C., N. Jiang, J. Huang, V.I. Zarnitsyna, and B.D. Evavold. 2013. Insights from in situ analysis of TCR-pMHC recognition: response of an interaction network. *Immunol. Rev.* 251:49–64. doi:10.1111/imr.12016.

CHAPTER 2: TAP1/2 genes in the dog – sequence and function

Summary

This chapter contains our published article, highlighting the coding sequences and the promoter regions of the canine TAP1 and 2 genes, and also showing that the putative canine TAP2 gene is able to restore murine MHCI expression on the murine TAP2 negative cell line RMAS. As discussed in Chapter 3, the purpose for this survey of canine TAP gene polymorphism was to produce data that would be used to identify mutations in TAP genes of canine cells that express low levels of dog leukocyte antigen class I (DLAI) protein. These data can be used to design expression constructs used for transfection of mutated cell clones to confirm that supplementation with a functional TAP sequence results in rescue of DLAI expression. The results herein provide useful information regarding the canine class I antigen presentation pathway.

Developmental and Comparative Immunology 41 (2013) 578–586

Contents lists available at ScienceDirect

Developmental and Comparative Immunology

journal homepage: www.elsevier.com/locate/dci

Characterization and allelic variation of the transporters associated with antigen processing (TAP) genes in the domestic dog (*Canis lupus familiaris*)

Gregory S. Gojanovich, Peter Ross, Savannah G. Holmer, Jennifer C. Holmes, Paul R. Hess *

Immunology Program, Department of Clinical Sciences, College of Veterinary Medicine, North Carolina State University, Raleigh, NC 27607, USA

ARTICLE INFO

Article history:
Received 8 May 2013
Revised 15 July 2013
Accepted 21 July 2013
Available online 25 July 2013

Keywords:
Alleles
Canine
Immunology
Splice variants
Transporter associated with antigen processing

ABSTRACT

The function of the transporters associated with antigen processing (TAP) complex is to shuttle antigenic peptides from the cytosol to the endoplasmic reticulum to load MHC class I molecules for CD8+ T-cell immunosurveillance. Here we report the promoter and coding regions of the canine TAP1 and TAP2 genes, which encode the homologous subunits forming the TAP heterodimer. By sampling genetically divergent breeds, polymorphisms in both genes were identified, although there were few amino acid differences between alleles. Splice variants were also found. When aligned to TAP genes of other species, functional regions appeared conserved, and upon phylogenetic analysis, canine sequences segregated appropriately with their orthologs. Transfer of the canine TAP2 gene into a murine TAP2-defective cell line rescued surface MHC class I expression, confirming exporter function. This data should prove useful in investigating the association of specific TAP defects or alleles with immunity to intracellular pathogens and cancer in dogs.

1. Introduction

The development, homeostasis and function of $\alpha\beta$ CD8+ T cells depends on the interaction of the T cell receptor with MHC class I molecules presenting peptide epitopes derived from degraded intracellular proteins. An essential step in the antigen processing and presentation pathway is the shuttling of these cytosolic peptides across the ER membrane to ultimately access the extracellular compartment, a function performed with high efficiency by the transporters associated with antigen processing (TAP) complex. In a single mammalian cell under physiologic conditions, the TAP system can transport $>2 \times 10^4$ peptides per minute (Neefjes et al., 1993). While TAP-independent pathways for peptide loading have also been described (Henderson et al., 1992; Snyder et al., 1997), conventional TAP-mediated transport appears to be the dominant mechanism, as demonstrated by the almost complete loss of surface MHC class I expression in the absence of functional TAP (Gadola et al., 2000; Kelly et al., 1992; Powis et al., 1991; Van Kaer et al., 1992). An ATP-binding cassette (ABC) transporter superfamily member, TAP is a heterodimeric complex composed of TAP1 and TAP2 subunits, which are structurally homologous. Each half-transporter has a transmembrane domain (TMD) and a cytosolic nucleotide-binding domain (NBD). Together, the six C-terminal transmembrane helices of each TMD form the TAP core complex necessary for peptide translocation, which is powered by the binding and hydrolysis of ATP at the NBDs (Procko and Gaudet, 2009).

The TAP loci lie within the class II region of the MHC (Debenham et al., 2005). In humans, the genes encoding each half-transporter are modestly polymorphic, with official recognition of six TAP1 and five TAP2 (protein level) alleles (http://hla.alleles.org/classo.html). Additional subtypes and splice variants (SVs) of each subunit have been described. Only a few amino acid changes scattered throughout the protein sequences distinguish alleles of TAP1 and TAP2, unlike the polymorphisms of classical MHC molecules, where far more numerous allelic differences are observed, concentrated in hypervariable regions. Importantly, some TAP alleles in

Abbreviations: ABC, ATP-binding cassette; Ab, antibody; β2M, β2-microglobulin; CL, cytosolic loop; CDS, code determining sequence; DLA, dog leukocyte antigen; EST, expressed sequence tag; IFN, interferon; IFR, interferon regulatory factor; ISRE, IFN-stimulated response element; GAS, gamma activating sequence; GFP, green fluorescent protein; HLA, human leukocyte antigen; MED1, multiple start site element downstream1; NBD, nucleotide-binding domain; ORF, open reading frame; PBMC, peripheral blood mononuclear cells; PKR, protein kinase R; RLM-RACE, RNA ligase-mediated rapid amplification of cDNA ends; SNP, single nucleotide polymorphism; STAT, signal transducers and activators of transcription; SV, splice variant; TAP, transporter associated with antigen processing; TMD, transmembrane domain; TSS, transcription start site; UTR, untranslated region.

* Corresponding author. Address: Department of Clinical Sciences, College of Veterinary Medicine, North Carolina State University, Campus Box 8401, 1060 William Moore Drive, Raleigh, NC 27607, USA. Tel.: +1 919 513 6183; fax: +1 919 513 6336.

E-mail addresses: paul_hess@ncsu.edu, prhess1@gmail.com (P.R. Hess).

0145-305X/$ - see front matter © 2013 Elsevier Ltd. All rights reserved.
http://dx.doi.org/10.1016/j.dci.2013.07.011

humans have been correlated with increased susceptibility to immune-mediated (Barron et al., 1995; Gonzalez-Escribano et al., 1995; Ramos et al., 2009; Rau et al., 1997; Slomov et al., 2005) and infectious diseases (Rajalingam et al., 1997; Zhang et al., 2003), independent of linkage disequilibrium with class II genes. Whether these associations reflect altered CD8+ T-cell immunosurveillance is uncertain, as peptide selection and transport does not differ significantly between alleles (Daniel et al., 1997; Obst et al., 1995). Allelic variation of the TAP1 and TAP2 genes has also been described in the gorilla, rat, mouse, sea bass, and several avian species (Laud et al., 1996; Livingstone et al., 1991; Loflin et al., 1996; Marusina et al., 1997; Pinto et al., 2011; Sironi et al., 2008; Walker et al., 2011). The objectives of this study were to characterize the TAP genes of the domestic dog, and determine whether polymorphisms were present. Accordingly, we sequenced the coding regions of these genes obtained from dogs belonging to four genetically distinct breed clusters (Parker et al., 2004). Five TAP1 and four TAP2 alleles were found, discriminated by only a few amino acid substitutions. In several dogs, variants of both genes produced by alternative RNA splicing were also identified. The peptide exporter function of the canine TAP2 subunit was established by gene transfer into TAP2-defective murine RMA-S cells.

2. Materials and methods

2.1. Preparation of RNA and DNA samples

The canine histiocytic cell line DH82 (ATCC CRL-10389) was grown in Dulbecco's Modified Eagle Medium supplemented with 15% fetal bovine serum and 1% penicillin–streptomycin (cellgro). For passage or harvest, cells were detached with 0.05% trypsin–EDTA. Venous blood anticoagulated with EDTA was obtained with owner consent from samples collected from unrelated adult dogs ($n = 10$) undergoing evaluation at the North Carolina State University Veterinary Teaching Hospital. Peripheral blood mononuclear cells (PBMCs) were isolated by density gradient centrifugation (400g × 30 min at 22 °C) over Histopaque 1.077 (Sigma–Aldrich). From PBMC or DH82 cell lysates, RNA was extracted using Qiashredder columns and the RNeasy Plus Mini kit (Qiagen). Complementary DNA was generated by reverse transcription (Omniscript RT kit, Qiagen) using an oligo(dT)$_{15}$ primer.

2.2. Amplification and cloning of TAP genes

For PCR, exonic TAP1- and TAP2-specific primers (Supplementary Table 1) were generated using canine genomic and expressed sequence tag data, and homologous TAP gene sequences available through the National Center for Biotechnology Information (NCBI) HomoloGene database (http://www.ncbi.nlm.nih.gov/homologene), and were synthesized by Invitrogen. The upstream primers were designed to anneal to the most highly conserved 5′ regions of TAP1 and TAP2 across mammalian orthologs. Template cDNA was amplified with a HotStar HiFidelity Polymerase kit (Qiagen), using Q solution, on a Mastercycler Pro thermocycler (Eppendorf), programmed with the following cycling parameters: initial denaturation of 5 min at 95 °C, followed by 35 cycles of 15 s at 94 °C, 1 min at 65.1 °C, and 3 min at 72 °C, and a final elongation step for 10 min at 72 °C. Amplification products were electrophoresed on a 1% agarose gel, and ~2.5 kb bands for each TAP gene were excised and purified. Amplimers were TA cloned with pGEM-T Easy Vector (Promega), and colonies were screened by blue/white analysis and EcoRI digestion.

2.3. Sequencing and analyses of TAP1 and TAP2 alleles

Sanger DNA sequencing of insert-containing plasmids was performed by Eurofins MWG Operon, using standard primers (T7 and Sp6), as well as four internal primers for each gene, generating six total sequences per colony. Assembly of overlapping reads and alignment of concatenated sequences with the predicted TAP1-001 and TAP2-001 sequences obtained from the canine BAC clone 58o15 (GenBank ID: AJ630364.1) were performed using Geneious v.5.1 software (Drummond et al., 2010). For each dog, a minimum of six colonies were sequenced per gene in order to demonstrate homozygosity with >96% ($[1 - (0.5^{n-1})] \times 100$) confidence. The amino acid sequences for canine TAP1 and TAP2 genes were deduced using Geneious. Alleles were defined as sequences containing non-synonymous nucleotide substitutions found in three or more colonies, typically corroborated by a second, independent PCR amplification. Alleles were named following the nomenclature convention for MHC genes in dogs, i.e., *001, *002, *003, with the allele number *001 arbitrarily assigned to previously predicted sequences (Debenham et al., 2005). Sequences validated by ⩾3 colonies containing synonymous nucleotide changes were designated as subtypes, which was indicated by appending a letter to the allele number, e.g., *001B. A tree of TAP alleles was constructed on the basis of genetic distances (Tamura and Nei, 1993) using the neighbor-joining method (Saitou and Nei, 1987).

2.4. Determination of the 5′ untranslated regions (UTRs) of TAP1 and TAP2 genes

RNA Ligase-Mediated Rapid Amplification of cDNA Ends (RLM-RACE, FirstChoice®, Ambion) was performed on the 5′ ends of TAP1 and TAP2 mRNA per the manufacturer's protocol. Briefly, RNA was isolated from DH82 cells that had been cultured for 16 h with ~600 units/mL recombinant human interferon (IFN)-γ (Peprotech) to increase TAP gene transcript levels (Ma et al., 1997), and treated sequentially with calf intestinal alkaline phosphatase and tobacco acid pyrophosphatase, ligated to a 5′ adaptor, and reverse transcribed. Amplification was performed by nested PCR, using 5′ adaptor-specific primers and 3′ gene-specific primers (Supplementary Table 1) and the HotStar HiFidelity Polymerase kit. Cycling conditions were as follows: initial denaturation of 5 min at 95 °C, followed by 35 cycles of 15 s at 94 °C, 30 s at 60 °C, and 1 min at 72 °C, with a final elongation step for 7 min at 72 °C. After TA cloning of PCR products, plasmids were sequenced for each TAP gene.

2.5. Cloning and expression of the canine TAP2 gene in a TAP-defective murine cell line

The canine TAP2*001 allele was amplified from cDNA of IFN-γ-treated DH82 cells using the thermocycler conditions described in Section 2.2; primers are listed in Supplementary Table 1. The gel-purified PCR product was ligated into a pEgfp-C2 expression vector at the BamHI and NotI restriction sites to create an N-terminal green fluorescent protein (GFP) fusion protein. The murine lymphoma RMA-S cell line, which was grown in RPMI-1640 medium supplemented to 10% FBS, 2 mM L-glutamine and 1% penicillin/streptomycin, was transfected with the pEgfp-TAP2 and parental pEgfp-C2 constructs using the Amaxa Nucleofector Kit T solution and the A-030 program. Twenty-four hours later, cells were placed in medium containing G418 (1 mg/ml; Invitrogen). Following 2 weeks of selection, surface expression of MHC class I molecules was determined by staining cells cultured at 37 °C with anti-H2-D^b (28-12-8, BioLegend) and anti-H2-K$^{b/d}$ (34-1-2S, eBioscience) antibodies (Abs). An Alexa Fluor 647-labeled donkey anti-mouse IgG Ab (Jackson ImmunoResearch) was used for detection;

background fluorescence was established by omitting the primary Ab. Cell viability was discriminated on the basis of forward and side scatter. Flow cytometric list mode data were acquired with a FACSCalibur flow cytometer (BD Biosciences) and analyzed with Summit software v5.2 (Beckman Coulter).

3. Results and discussion

3.1. Polymorphisms of TAP1 and TAP2 sequences in the dog

Using PBMCs from a mixed-breed dog, we first determined the coding sequences of each of the TAP subunit genes, which have not been previously reported. Alignment of these sequences showed >99% identity with the predicted TAP1 and TAP2 sequences generated from a genomic BAC clone of the Dog Leukocyte Antigen (DLA) class II region (GenBank ID: AJ630364.1) (Debenham et al., 2005). For TAP1, expressed sequence tag (EST) representation of all 11 exons was found (20 ESTs with ⩾97% identity); for TAP2, 11 ESTs with ⩾97% identity to our sequences covered all exons, except for exons 5–8 (bp 877–1289).

While polymorphisms have been described in the TAP genes of other species, the number of alleles is generally few, and consequently, it was uncertain whether any variants would be found in dogs unless a large number of individuals were sampled. Moreover, diversity at canine MHC loci is relatively restricted, with low levels of heterozygosity and allelic variation, as a result of population bottlenecks that occurred with domestication. For example, at the DLA-DRB1 locus, only 100 alleles have been described (Kennedy et al., 2007), in contrast to the >1050 known Human Leukocyte Antigen (HLA)-DRB1 alleles (http://www.ebi.ac.uk/imgt/hla/stats.html). Accordingly, to increase the likelihood of TAP allele discovery, we obtained samples from two or more representative dogs from four divergent breed clusters: Ancient-Asian (Akita; Chow Chow; Shar-Pei), Herding-Sighthound (Greyhound; Shetland Sheepdog), Mastiff-like (Mastiff; Rottweiler), and Hunting (Airedale Terrier; Doberman Pinscher) (Parker et al., 2004). In humans, TAP allele usage has been shown to vary between ethnic populations (Faucz et al., 2000). Non-synonymous single nucleotide polymorphisms (SNPs) were found in the sequences of both canine TAP genes. Alignments of the amino acid sequences of these alleles are shown in Fig. 1A (TAP1) and 1B (TAP2). As in humans, the number of amino acid changes between variants is very low and distributed across exons. In addition to these alleles, SNPs that resulted in synonymous mutations were also found in our dogs, which were designated as allele subtypes (Table 1).

A list of alleles and the corresponding dog breed from which they were obtained is provided in Table 2. Consistent with limited diversity, only two heterozygotes were noted; interestingly, both individuals were in the Ancient-Asian group. Members of this

Fig. 1. Alignment of the amino acid translations of the TAP1 and TAP2 sequences recovered from dogs in this study with predicted GenBank sequences reveals limited polymorphisms in canine alleles. (A) Translated TAP1 sequences show four residue changes (letters; dots signify identities). The absent TAP1*002 designation was reserved for a TAP1-002 splice variant predicted by the data of Debenham et al. (2005) and was not found in this study. (B) Translated TAP2 sequences also display substitutions at four positions. The *001 alleles that we obtained for both genes match their reference sequences and are not shown. GenBank accession numbers are indicated in parentheses.

Table 1
Sites of synonymous SNPs in allele subtypes.

Gene	Subtype	CDS		3′ UTR		GenBank ID
TAP1	*001B	C597T[a]	T765C	C2271T	G2306A	JN656392
	*004B	G129C	C597T			JN656395
TAP2	*001B	G243C				JN656401
	*004B	T1566C	T1719C	A2189T	C2211T	JN656404

[a] Nucleotide substitutions are numbered relative to the start codon.

Table 2
Alleles carried by dogs in this study.

Gene	Cluster[a]	Breed	Alleles	
TAP1	Ancient Asian	Akita	*003	*004
		Shar-Pei	*001	*005
	Herding-Sighthound	Greyhound	*001B	
		Shetland Sheepdog	*001	
	Hunting	Airedale Terrier	*001	
		Doberman Pinscher	*006	
	Mastiff-like	Mastiff	*001B	
		Rottweiler	*001	
TAP2	Ancient Asian	Akita	*002	*003
		Chow Chow	*004B	
	Herding-Sighthound	Greyhound	*001	
		Shetland Sheepdog	*001	
	Hunting	Airedale Terrier	*001	
		Doberman Pinscher	*004	
	Mastiff-like	Mastiff	*001B	
		Rottweiler	*001	

[a] Genetic clusters were defined by Parker et al. (2004).

cluster (Akita; Chow Chow; Basenji) appear to have lower homozygosity across several MHC class II loci than other breeds (Angles et al., 2005), and are considered representatives of the ancestral gene pool of dogs (Parker et al., 2004). The *001 allele was the most prevalent variant of each gene: six of eight dogs carried TAP1*001/*001B and five of eight dogs carried TAP2*001/*001B. The TAP*001 sequences were originally identified from the RCPI-81 canine BAC library, prepared from a Doberman Pinscher. Hence, we included the same breed in this analysis; interestingly, our dog varied at both loci, bearing the TAP1*006 and TAP2*004 alleles.

3.2. Splice variants of canine TAP1 and TAP2 genes

Variants of both canine TAP genes resulting from alternative splicing were observed occasionally. Splice variants of TAP genes have been found in humans, pigs and sea bass (Furukawa et al., 1999; Garcia-Borges et al., 2006; Pinto et al., 2011; Yan et al., 1999). The most common variant, TAP2*001 SV1, was identified in two dogs (five colonies) and is depicted in Fig. 2A. The large deleted region in TAP2*001 SV1 appears to be a genuine product of alternative splicing, rather than an artifact caused by template switching during reverse transcription, as the exonic donor and acceptor sequences within the SV match 5′ and 3′ splice site consensus sequences (Mount, 1982). Several other TAP1 and TAP2 SVs were also found that appeared to be generated by exonic skipping or retention of intronic sequences, but were represented by only 1 or 2 colonies, and were not pursued further.

In humans, TAP gene SVs can have demonstrable functional consequences. The peptide selectivity of a TAP2 SV was shown to be qualitatively different than that of the standard allele (Yan et al., 1999). In a more dramatic example, a point mutation in the acceptor site at the 3′ end of intron 1 of TAP1 generated an SV with a frameshift and premature stop, resulting in the virtual lack of cell surface MHC class I expression, a condition known as Bare Lymphocyte Syndrome (Furukawa et al., 1999). The two TAP1 SVs that we found had small changes that lay outside of conserved functional regions and did not alter the reading frame. On the other hand, the TAP2*001 SV1 had deletions in sites important for peptide binding (residues 414–433) and interaction with ATP (residues 503–510), as well as a premature stop (Fig. 2A). Nonetheless, TAP2*001 SV1 presumably held no deleterious consequences for the dogs carrying this variant, as the wild-type allele was also amplified from these individuals.

3.3. Comparative analysis of 5′ UTR and flanking regions of canine TAP genes

We next wished to compare canine TAP genes with their counterparts from other species. To verify the predicted sequence of the 5′ UTR, we performed 5′ RACE, using RNA isolated from a canine histiocytic cell line, which expresses normal amounts of MHC class I molecules on the cell surface (not shown) and is heterozygous at both TAP loci (TAP1*001, *006; TAP2*001, *004 [DH82 cells are derived from a Golden Retriever (Wellman et al., 1988), a breed in the Hunting cluster]). The inner amplification product appeared as a single band (Fig. 2B), which was TA cloned. From a minimum of six colonies from each PCR, identical sequences of 631 bp (TAP1) and 516 bp (TAP2) were obtained, indicating a single transcription start site (TSS) for both, which differed from predicted sites. Typical of genes whose promoters lack a TATA box, transcription of TAP1 and TAP2 is usually initiated from multiple sites (Arons et al., 2001; Kishi et al., 1993; Wright et al., 1995). The finding of a single TSS may represent an idiosyncrasy of the DH82 cells, the effect of IFN-γ, or both; for example, Arons et al. (2001) found multiple TSSs in murine TAP2 using a T-cell leukemia line, but similarly, observed only one TSS in transcripts from IFN-γ-treated transformed fibroblasts. Multiple start site element downstream (MED)1 sequences (GCTCCC/G) were found in both TAP1 and TAP 2, which are common elements in TATA-less promoters that have multiple initiation sites, so presumably other TSSs are used in canine TAP genes, but 5′-RACE analysis of other canine cell lines will be needed to confirm this supposition.

For TAP1, 5′ RACE data from our transcripts showed a UTR of 202 bp, with the first exon 147 bp shorter than predicted in the annotated genomic sequence, as depicted in Fig. 2B (lower left panel). The TAP2 gene has a 5′ UTR of 39 bp. The 3′ end of exon 1 is 86 bp shorter than predicted (Fig. 2B, lower right panel), and similar to TAP2 of other species (Arons et al., 2001), there is a short 5′ stretch of 8 nucleotides (7–8 in rodents; 5 in humans) in exon 2 before the translation initiation codon.

We then examined the 5′ UTR (RACE data) and upstream flanking regions (GenBank genomic data) for promoter elements (in addition to MED1) that have been identified previously in murine and human TAP genes, using the search function in Geneious, and allowing for interpretations of ambiguities within query and sequence. Most notable among these *cis* elements are those related to responsiveness to IFN-γ. This inflammatory cytokine is an important bridge between innate and adaptive immune responses, possessing the well-established effects of increasing the expression of surface MHC class I molecules and several components of antigen processing pathway, including the TAP subunits, to enhance cytotoxic CD8[+] T-cell activity. Interferon-γ signaling can modulate gene expression by generating phosphorylated Signal Transducer and Activator of Transcription (STAT)1 homodimers that bind the Gamma Activating Sequence (GAS) (Saha et al., 2010). Such responses are subsequently amplified by GAS-regulated transcription of Interferon Regulatory Factors (IRFs), which can bind the Interferon-stimulated response elements (ISRE) to promote expression of additional immune genes. Additionally, IFN-γ can regulate gene expression by indirectly activating NF-κB though protein kinase R (PKR) (Deb et al., 2001). All three of the target

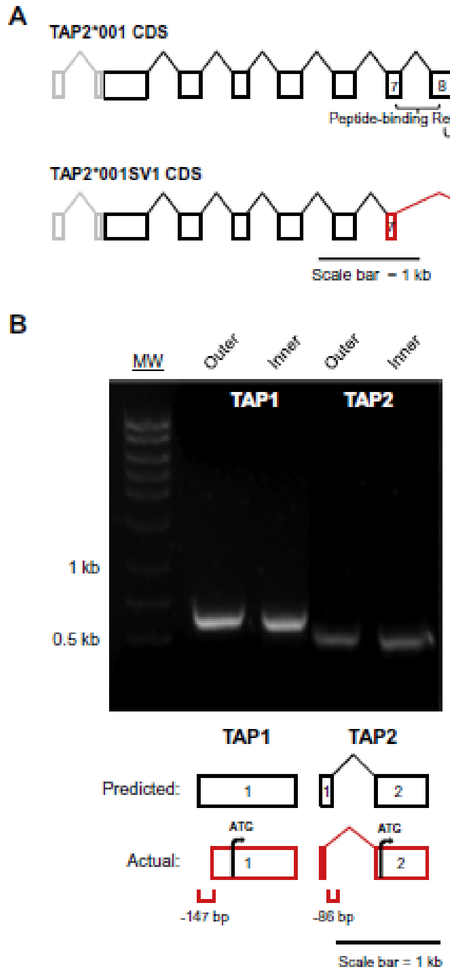

Fig. 2. (A) Schematic representation of the code determining sequence (CDS) for the TAP2*001 SV1 (GenBank ID: JN656405). Exons are depicted by boxes; the gray areas constitute the 5′ untranslated region. The SV1 transcript contains a 53 bp deletion at the 3′ end of exon 7 through exon 8 (red). Transcription is resumed at the beginning of exon 9, resulting in a frame shift and creation of a premature stop codon (symbol). The functional domains affected by splicing are shown above in the full-length TAP2*001 (GenBank ID: AJ630364.1). Introns (connecting lines) are placed for clarity and are not drawn to scale. (B) The 5′ UTR of canine TAP1 and TAP2 as determined by RLM-RACE. Electrophoresis of nested PCR products revealed a single band per reaction, which was TA cloned and sequenced; all colonies from each gene returned the same nucleotide sequence (GenBank ID: JN656391 [TAP1]; JN656400 [TAP2]). MW – molecular weight ladder. Lower panels: schematic alignment of the 5′ RACE products (shown in red) with the corresponding predicted TAP1 and TAP2 sequences (GenBank ID: AJ630364.1; shown in black). The translation start sites are indicated by the black arrows and ATG codon.

elements potentially responsive to IFN-γ – GAS, ISRE and the NF-κB element – were identified in both canine TAP sequences; a comparison to mouse and human TAP promoters is shown in Table 3.

In TAP1, a presumptive GC box (GCCCCGCCCCGCT) was found 315 bp upstream of the TSS; in human TAP1, there are two such elements (GCCCCGCCCCT) that bind the transcription factor Specificity Protein (SP)1 and are important for regulating basal expression of the gene (Wright et al., 1995). On the other hand, the cAMP response element (TGAC/AGTCA) common to the 5′ UTR of human TAP2 and both murine TAP genes (Arons et al., 2001) was not identified in our canine sequences, nor did we find the CCAAT/enhancer binding protein transcription factor element (GATTTGCGCAATCTGC; consensus: A/GTTGCGC/TAAC/T) that had been observed in the TAP2 promoter sequence of rainbow trout (Castro et al., 2008).

3.4. Comparative analysis of structural and functional elements and polymorphisms of canine TAP genes

The genomic organization of the TAP genes of the dog is essentially identical to that of the mouse and human (Marusina et al., 1997). The canine TAP1 gene has an open reading frame (ORF) of 2253 bp, with 11 exons. The canine TAP2 gene has an ORF of 2112 bp, with 12 exons; the first is non-coding. The predicted amino acid sequences of canine TAP1*001 and TAP2*001 were aligned with the orthologous genes from four other mammalian species. As

Table 3
Cis elements in TAP promoters that are potentially responsive to IFN-γ.

Gene	Species	GAS[a]	ISRE[b]	NFκB-E	Refs.
TAP1	Mouse	+/–[c]	+	+/–	Arons et al. (2001), Kishi et al. (1993), Saha et al. (2010), White et al. (1996)
	Human	+	+	+	Min et al. (1996), Wright et al. (1995)
	Dog	+[d]	+[e]	+[d,e]	This study
TAP2	Mouse	+	+	–	Arons et al. (2001), Guo et al. (2002), Saha et al. (2010)
	Human	+	–	+	Saha et al. (2010)
	Dog	+	+	+	This study

[a] Gamma Activating Sequence (GAS): TTNCNNNAA; IFN-stimulated response element (ISRE): AGTTTCNNTTTC/TCC or NGAAANNGAAAG/CN; NFκB-Element (NFκB-E): GGGA/GNNC/TC/TCC. Sequences from Saha et al. (2010).

[b] Highly homologous to sequences reported as: IFN Regulatory Factor (IRF)1/IRF2 binding element, Arons et al. (2001); IRF-enhancer (IRF-E), White et al. (1996); IFN response factor binding element (IRFE), Guo et al. (2002); and IFN Consensus Sequence (ICS), Arons et al. (2001), Min et al. (1996).

[c] The +/– symbol is shown when in silico analyses disagree and no empirical data is available.

[d] Observed in our 5′-RACE sequences; the remainder of canine elements listed in the table were identified in the genomic sequence (GenBank ID: AJ630364.1) 5′ to the TSS.

[e] Two elements were found.

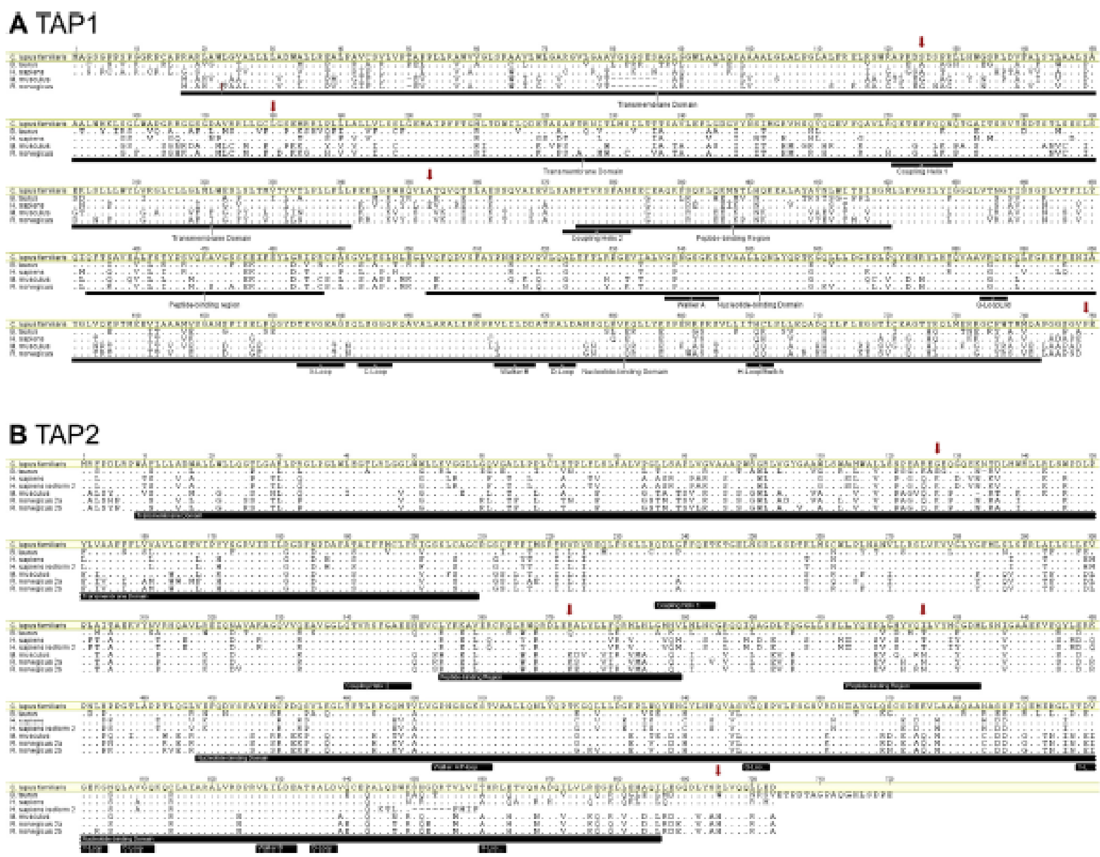

Fig. 3. Alignment of the deduced amino acid sequences of the TAP genes of the dog with orthologs from four mammalian species reveals strong conservation of all major functional elements. The most common canine allele at each locus (*001) was used for comparison; sites of polymorphisms are indicated by red arrows. For optimal alignment, the proline at position 23 of the rat TAP1 protein was omitted (red symbol); other gaps are shown as dashes. Dots signify identities; letters indicate substitutions. Annotations of functional regions, shown in the black bars below the sequences, are based on descriptions for human TAP proteins (Parcej and Tampe, 2010). Excluding the transmembrane domain, the greatest percentage differences between the canine and human sequences were observed in the H-Loop of TAP1, and in the peptide-binding regions of TAP2. (A) Canine TAP1 exhibits 72.8%, 72.8%, 72.8%, and 74.7% pairwise identity with the human, rat, mouse and cow genes, respectively. (B) Canine TAP2 exhibits 78.7%, 72%, 73.5%, and 78.9% pairwise identity with the human, rat, mouse and cow genes, respectively. The accession numbers for these sequences are listed in Supplementary Table 2. (For interpretation of the references to colour in this figure legend, the reader is referred to the web version of this article.)

expected, the major functional TAP elements were identified, as shown in the annotations of Fig. 3, with varying degrees of homology across domains. For example, when compared to murine TAP1, the canine protein shares 62.8% overall identity in the TMD, 74.6% in the NBD, 70.4% in the peptide-binding regions, and 100% identity in the C- and D-Loops and Coupling Helix 2. A comparable analysis for TAP2 reveals 100% identity in the Coupling Helices, Walker A and B motifs, and the C- and D-Loops, but differences in the peptide-binding regions (62.5% identity), X-Loop and H-Switch.

While the major peptide-binding regions of both TAP subunits reside both in the Cytosolic Loop (CL)2 domains and a stretch of 15 amino acids immediately following the last C-terminal transmembrane helix of the TMD (Nijenhuis and Hammerling, 1996), four residues recently have been identified in the CL1 of human TAP1 that are involved in the sensing of bound peptides (V288) and inter-domain transmission of this signal (G282; I284; R287) (Herget et al., 2007). These residues are conserved in all alleles of the canine ortholog (Fig. 3). While an analogous sensor has not been reported for human TAP2, a cysteine at position 213 (beginning of CL2) has been shown to be important for orientation of peptides in the binding pocket, thereby influencing peptide selectivity (Baldauf et al., 2010). The residue C213 is also present in the dog, but interestingly, neither in rodents nor cattle (Fig. 3). Other TAP2 residues that have been shown to alter transporter specificity by controlling the rate of peptide export, based primarily on side-chain properties (hydrophobicity and polarity/charge) of the C-terminal amino acid, have been mapped to the CLs at positions 217/218 and 374/380 (Armandola et al., 1996; Momburg et al., 1996). As seen in Fig. 3, dogs share M218 and A374 with humans, and have an R380Q substitution, identical to rat 2a. The rat alleles 2a (also designated 2^{a}) and 2b (2^{u}) have different peptide specificities (Momburg et al., 1994). Similar to the 2b variant, mouse TAP has a strong preference for hydrophobic residues and an aversion to positively charged amino acids at the C-terminus. In contrast, the human TAP transporter resembles the less stringent selectivity of the rat 2a allele, accepting C-terminal hydrophobic and basic residues (Momburg et al., 1996). Based on these key TAP2 residues alone, canine TAP might be expected to show affinities similar to human TAP. However, a more recent study has emphasized the important added contribution of the three N-terminal amino acids of the peptide substrate towards human TAP specificity (Burgevin et al., 2008). As the particular TAP sites that interact with these residues have not been identified, a comparison between human and dog sequences is precluded, and consequently, it is difficult to predict the selectivity of the canine transporter. Moreover, dogs uniquely have an isoleucine at position 217 (most orthologs use a threonine). Finally, the TAP1 subunit also contributes to peptide selectivity (Armandola et al., 1996), so the exporter preferences of canine TAP ultimately will require empirical determination.

Five polymorphisms, S125C, L180P, A353S and P749T/L, differentiate the five canine TAP1 alleles (Figs. 1 and 3), but all these positions are invariant across the six known human alleles (http://hla.alleles.org/data/txt/tap1_prot.txt). Conversely, none of the human TAP1 polymorphic sites (V80G, L131P, I333V, A370V, V458L, V518I, D637G and R648Q) were observed to vary in the deduced sequences from our dogs. All of the canine TAP2 sequences

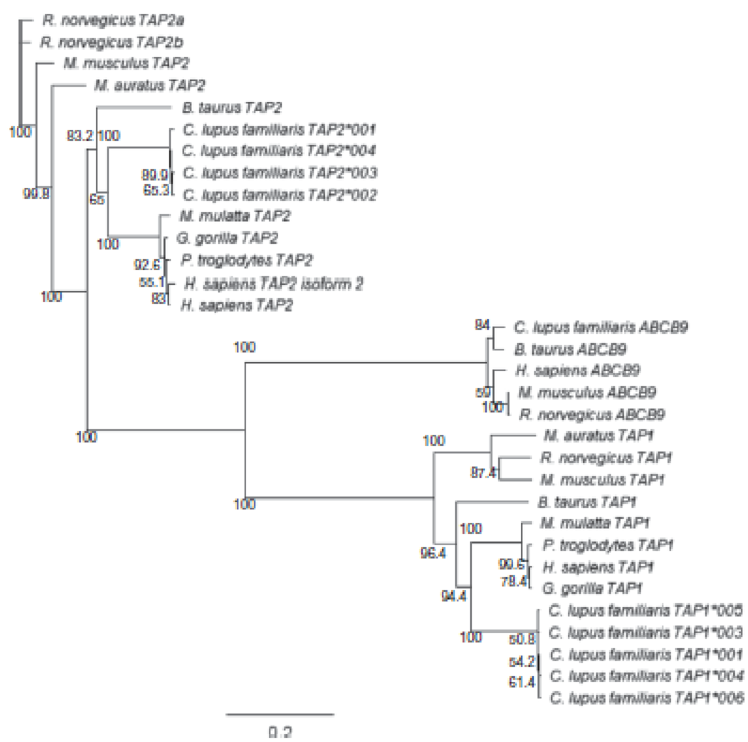

Fig. 4. Phylogenetic relationships of TAP1, TAP2 and TAPL (ABCB9) transporter proteins from various mammalian species. Predicted and actual protein sequences from public databases (see Supplementary Table 2 for accession numbers) were aligned and trimmed to the deduced TAP1 and TAP2 amino acid sequences from dogs in this study. An unrooted tree was built with Geneious 5.1, based on genetic distances, using the neighbor-joining method. Branch numbers are confidence values (%) based on bootstrap sampling (1000 replicates). Scale bar: number of substitutions per site.

encoded the C-terminal stretch of amino acids 688 – 703 present in human *02 alleles but absent in *01 group members. However, there was no overlap between canine (G127R, R373C, I425T and R695H) and human (V379I, A565T, R651C and Q665A) polymorphisms (http://hla.alleles.org/data/txt/tap2_prot.txt). Similarly, examination of the five TAP1 and six TAP2 alleles in mice (Marusina et al., 1997) revealed that only one TAP2 polymorphic site (N425S) was shared with the dog (I425T).

A phylogenetic analysis of TAP sequences shows the expected clustering of the canine alleles with their orthologs from rodents, primates and the cow (Fig. 4).

3.5. Functional assessment of the canine TAP2 gene

With loss of function of either TAP subunit, the export of cytosolic peptides into the ER lumen for loading onto class I heavy chain-β2M light chain dimers is halted. Occupied instead by low-affinity self-peptides that readily dissociate from the binding groove (De Silva et al., 1999), or simply empty, the MHC class I molecules transported to the cell surface are structurally unstable and rapidly disappear (Kelly et al., 1992; Van Kaer et al., 1992). This phenomenon allows the function of either TAP molecule to be conveniently demonstrated by rescue of surface class I expression – as measured by flow cytometry – upon gene transfer into cells that have a defect in the corresponding subunit. Murine RMA-S cells, generated by chemical mutagenesis and negative selection (Ljunggren and Karre, 1985), have intact TAP1 but a truncated, defective TAP2 molecule (Yang et al., 1992), and are sometimes employed for this purpose. We therefore sought to use this system to test the function of canine TAP2. Because of the strong conservation of TAP functional elements across species (Fig. 3), hybrid partnering of orthologous subunits can generate a working heterodimer, as has been shown for various combinations of human, mouse and rat TAP1 and TAP2 molecules (Armandola et al., 1996; Powis et al., 1991; Yewdell et al., 1993). In analogous fashion, we cloned the TAP2 gene (*001 allele) into a GFP expression vector for transfection into RMA-S cells. As seen in Fig. 5, GFP+ cells containing the empty vector have low expression of H2-D^b (A) and -K^b (B), identical to unmanipulated RMA-S cells (not shown), while GFP+ cells complemented with canine TAP2 have markedly increased surface expression of both H-2 class I molecules, consistent with the restoration of peptide export into the ER. The canine TAP2 gene therefore encodes a functional transporter subunit capable of pairing with murine TAP1 to produce a competent TAP heterodimer.

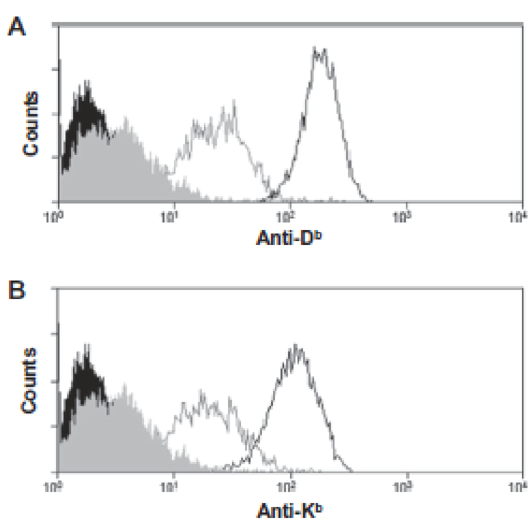

Fig. 5. Expression of surface MHC class I is restored in murine RMA-S cells by the canine TAP2 gene. Gray histograms show cells transfected with the empty GFP vector, and those in black represent cells that received the GFP vector encoding TAP2. Flow cytometric overlays are gated on live GFP+ cells. Filled histograms indicate staining with 2° Ab only. (A) H2-D^b; (B) H2-K^b. Histograms represent four independent analyses.

4. Conclusions

Here we provide the first description of the promoter regions and coding sequences for the canine TAP1 and TAP2 genes. All highly conserved functional elements common to ABC exporters were identified. As in other species, alleles and subtypes of both genes are observed. Whether these variants have functional significance will require additional investigation. In humans, the association of TAP alleles with some autoimmune and infectious diseases suggests that polymorphisms are functionally important, while studies of peptide selectivity (Daniel et al., 1997; Obst et al., 1995) and genotype distribution (Faucz et al., 2000) do not. In the dog, the very limited amino acid variations of TAP1 and TAP2 alleles imply that effects on immune function and disease susceptibility, if any, will be modest at best. TAP variants generated by alternative splicing, on the other hand, can have more profound consequences, such as altered peptide selectivity and enhanced susceptibility to bacterial and viral infections, as seen in humans (Furukawa et al., 1999; Yan et al., 1999). A canine TAP2 SV that contained a stop codon early in the NBD coding sequence was discovered; however, the coexistence of its full-length allelic counterpart (*001), which was capable of replacing a defective murine ortholog in RMA-S cells, suggested that peptide export and class I loading would be largely unimpaired by the presence of this variant transcript. Finally, the most significant clinical relevance of the TAP transporter is perhaps the acquired dysfunction of the TAP1 or TAP2 subunits that is observed in some human persistent viral infections and cancers, as a mechanism for avoiding detection by $CD8^+$ T cells (Ritz and Seliger, 2001). Investigating whether analogous processes of immunoevasion occur in canine malignant and virally infected cells should be assisted by the data from this study and will be important in fully understanding such disease processes in the dog.

Acknowledgments

We thank the Nordone, Tonkonogy and Yoder laboratories for helpful guidance and comments. We also thank Jeff Frelinger (University of Arizona) for the gift of RMA-S cells, and Farah Alayli (NCSU) for assistance with RLM-RACE. This study was supported by funding from the National Institutes of Health (K08 DK082264) and a NCSU Faculty Research and Professional Development Fund award (both to PRH). Gregory Gojanovich was supported by a fellowship from the US Department of Education Graduate Assistance in Areas of National Need (GAANN) Program.

Appendix A. Supplementary data

Supplementary data associated with this article can be found, in the online version, at http://dx.doi.org/10.1016/j.dci.2013.07.011.

References

Angles, J.M., Kennedy, L.J., Pedersen, N.C., 2005. Frequency and distribution of alleles of canine MHC-II DLA-DQB1, DLA-DQA1 and DLA-DRB1 in 25 representative American Kennel Club breeds. Tissue Antigens 66, 173–184.

Armandola, E.A., Momburg, F., Nijenhuis, M., Bulbuc, N., Fruh, K., Hammerling, G.J., 1996. A point mutation in the human transporter associated with antigen processing (TAP2) alters the peptide transport specificity. Eur. J. Immunol. 26, 1748–1755.

Arons, E., Kunin, V., Schechter, C., Ehrlich, R., 2001. Organization and functional analysis of the mouse transporter associated with antigen processing 2 promoter. J. Immunol. 166, 3942–3951.

Baldauf, C., Schrodt, S., Herget, M., Koch, J., Tampe, R., 2010. Single residue within the antigen translocation complex TAP controls the epitope repertoire by stabilizing a receptive conformation. Proc. Natl. Acad. Sci. USA 107, 9135–9140.

Barron, K.S., Reveille, J.D., Carrington, M., Mann, D.L., Robinson, M.A., 1995. Susceptibility to Reiter's syndrome is associated with alleles of TAP genes. Arthritis Rheum. 38, 684–689.

Burgevin, A., Saveanu, L., Kim, Y., Barilleau, E., Kotturi, M., Sette, A., van Endert, P., Peters, B., 2008. A detailed analysis of the murine TAP transporter substrate specificity. PLoS ONE 3, e2402.

Castro, R., Martin, S.A., Bird, S., Lamas, J., Secombes, C.J., 2008. Characterisation of gamma-interferon responsive promoters in fish. Mol. Immunol. 45, 3454–3462.

Daniel, S., Caillat-Zucman, S., Hammer, J., Bach, J.F., van Endert, P.M., 1997. Absence of functional relevance of human transporter associated with antigen processing polymorphism for peptide selection. J. Immunol. 159, 2350–2357.

De Silva, A.D., Boesteanu, A., Song, R., Nagy, N., Harhaj, E., Harding, C.V., Joyce, S., 1999. Thermolabile H-2Kb molecules expressed by transporter associated with antigen processing-deficient RMA-S cells are occupied by low-affinity peptides. J. Immunol. 163, 4413–4420.

Deb, A., Haque, S.J., Mogensen, T., Silverman, R.H., Williams, B.R., 2001. RNA-dependent protein kinase PKR is required for activation of NF-kappa B by IFN-gamma in a STAT1-independent pathway. J. Immunol. 166, 6170–6180.

Debenham, S.L., Hart, E.A., Ashurst, J.L., Howe, K.L., Quail, M.A., Ollier, W.E., Binns, M.M., 2005. Genomic sequence of the class II region of the canine MHC: comparison with the MHC of other mammalian species. Genomics 85, 48–59.

Drummond A.J., Ashton B., Buxton S., Cheung M., Cooper A., Heled J., Kearse M., Moir R., Stones-Havas S., Sturrock S., Thierer T., et al., 2010. Geneious, v. 5.04 ed.

Faucz, F.R., Probst, C.M., Petzl-Erler, M.L., 2000. Polymorphism of LMP2, TAP1, LMP7 and TAP2 in Brazilian Amerindians and Caucasoids: implications for the evolution of allelic and haplotypic diversity. Eur. J. Immunogenet. 27, 5–16.

Furukawa, H., Murata, S., Yabe, T., Shimbara, N., Keicho, N., Kashiwase, K., Watanabe, K., Ishikawa, Y., Akaza, T., Tadokoro, K., Tohma, S., et al., 1999. Splice acceptor site mutation of the transporter associated with antigen processing-1 gene in human bare lymphocyte syndrome. J. Clin. Invest. 103, 755–758.

Gadola, S.D., Moins-Teisserenc, H.T., Trowsdale, J., Gross, W.L., Cerundolo, V., 2000. TAP deficiency syndrome. Clin. Exp. Immunol. 121, 173–178.

Garcia-Borges, C.N., Phanavanh, B., Crew, M.D., 2006. Characterization of porcine TAP genes: alternative splicing of TAP1. Immunogenetics 58, 374–382.

Gonzalez-Escribano, M.F., Morales, J., Garcia-Lozano, J.R., Castillo, M.J., Sanchez-Roman, J., Nunez-Roldan, A., Sanchez, B., 1995. TAP polymorphism in patients with Behcet's disease. Ann. Rheum. Dis. 54, 386–388.

Henderson, R.A., Michel, H., Sakaguchi, K., Shabanowitz, J., Appella, E., Hunt, D.F., Engelhard, V.H., 1992. HLA-A2.1-associated peptides from a mutant cell line: a second pathway of antigen presentation. Science 255, 1264–1266.

Herget, M., Oancea, G., Schrodt, S., Karas, M., Tampe, R., Abele, R., 2007. Mechanism of substrate sensing and signal transmission within an ABC transporter: use of a Trojan horse strategy. J. Biol. Chem. 282, 3871–3880.

Kelly, A., Powis, S.H., Kerr, L.A., Mockridge, I., Elliott, T., Bastin, J., Uchanska-Ziegler, B., Ziegler, A., Trowsdale, J., Townsend, A., 1992. Assembly and function of the two ABC transporter proteins encoded in the human major histocompatibility complex. Nature 355, 641–644.

Kennedy, L.J., Barnes, A., Short, A., Brown, J.J., Lester, S., Seddon, J., Fleeman, L., Francino, O., Brkljacic, M., Knyazev, S., Happ, G.M., et al., 2007. Canine DLA diversity: 1 new alleles and haplotypes. Tissue Antigens 69 (Suppl 1), 272–288.

Kishi, F., Suminami, Y., Monaco, J.J., 1993. Genomic organization of the mouse Lmp-2 gene and characteristic structure of its promoter. Gene 133, 243–248.

Laud, P.R., Loflin, P.T., Jeevan, A., Lawlor, D.A., 1996. Transporter associated with antigen-processing-1 (TAP1) alleles in *Gorilla gorilla*: diversification of the locus postspeciation. Hum. Immunol. 50, 91–102.

Livingstone, A.M., Powis, S.J., Gunther, E., Cramer, D.V., Howard, J.C., Butcher, G.W., 1991. Cim: an MHC class II-linked allelism affecting the antigenicity of a classical class I molecule for T lymphocytes. Immunogenetics 34, 157–163.

Ljunggren, H.G., Karre, K., 1985. Host resistance directed selectively against H-2-deficient lymphoma variants. Analysis of the mechanism. J. Exp. Med. 162, 1745–1759.

Loflin, P.T., Laud, P.R., Watkins, D.I., Lawlor, D.A., 1996. Identification of new TAP2 alleles in gorilla: evolution of the locus within hominoids. Immunogenetics 44, 161–169.

Ma, W., Lehner, P.J., Cresswell, P., Pober, J.S., Johnson, D.R., 1997. Interferon-gamma rapidly increases peptide transporter (TAP) subunit expression and peptide transport capacity in endothelial cells. J. Biol. Chem. 272, 16585–16590.

Marusina, K., Iyer, M., Monaco, J.J., 1997. Allelic variation in the mouse Tap-1 and Tap-2 transporter genes. J. Immunol. 158, 5251–5256.

Momburg, F., Armandola, E.A., Post, M., Hammerling, G.J., 1996. Residues in TAP2 peptide transporters controlling substrate specificity. J. Immunol. 156, 1756–1763.

Momburg, F., Roelse, J., Howard, J.C., Butcher, G.W., Hammerling, G.J., Neefjes, J.J., 1994. Selectivity of MHC-encoded peptide transporters from human, mouse and rat. Nature 367, 648–651.

Mount, S.M., 1982. A catalogue of splice junction sequences. Nucleic Acids Res. 10, 459–472.

Neefjes, J.J., Momburg, F., Hammerling, G.J., 1993. Selective and ATP-dependent translocation of peptides by the MHC-encoded transporter. Science 261, 769–771.

Nijenhuis, M., Hammerling, G.J., 1996. Multiple regions of the transporter associated with antigen processing (TAP) contribute to its peptide binding site. J. Immunol. 157, 5467–5477.

Obst, R., Armandola, E.A., Nijenhuis, M., Momburg, F., Hammerling, G.J., 1995. TAP polymorphism does not influence transport of peptide variants in mice and humans. Eur. J. Immunol. 25, 2170–2176.

Parker, H.G., Kim, L.V., Sutter, N.B., Carlson, S., Lorentzen, T.D., Malek, T.B., Johnson, G.S., DeFrance, H.B., Ostrander, E.A., Kruglyak, L., 2004. Genetic structure of the purebred domestic dog. Science 304, 1160–1164.

Pinto, R.D., Pereira, P.J., dos Santos, N.M., 2011. Transporters associated with antigen processing (TAP) in sea bass (*Dicentrarchus labrax* L.): molecular cloning and characterization of TAP1 and TAP2. Dev. Comp. Immunol. 35, 1173–1181.

Powis, S.J., Townsend, A.R., Deverson, E.V., Bastin, J., Butcher, G.W., Howard, J.C., 1991. Restoration of antigen presentation to the mutant cell line RMA-S by an MHC-linked transporter. Nature 354, 528–531.

Procko, E., Gaudet, R., 2009. Antigen processing and presentation: tapping into ABC transporters. Curr. Opin. Immunol. 21, 84–91.

Rajalingam, R., Singal, D.P., Mehra, N.K., 1997. Transporter associated with antigen-processing (TAP) genes and susceptibility to tuberculoid leprosy and pulmonary tuberculosis. Tissue Antigens 49, 168–172.

Ramos, P.S., Langefeld, C.D., Bera, L.A., Gaffney, P.M., Noble, J.A., Moser, K.L., 2009. Variation in the ATP-binding cassette transporter 2 gene is a separate risk factor for systemic lupus erythematosus within the MHC. Genes Immun. 10, 350–355.

Rau, H., Nicolay, A., Usadel, K.H., Finke, R., Donner, H., Walfish, P.G., Badenhoop, K., 1997. Polymorphisms of TAP1 and TAP2 genes in Graves' disease. Tissue Antigens 49, 16–22.

Ritz, U., Seliger, B., 2001. The transporter associated with antigen processing (TAP): structural integrity, expression, function, and its clinical relevance. Mol. Med. 7, 149–158.

Saha, B., Jyothi, P.S., Chandrasekar, B., Nandi, D., 2010. Gene modulation and immunoregulatory roles of interferon gamma. Cytokine 50, 1–14.

Saitou, N., Nei, M., 1987. The neighbor-joining method: a new method for reconstructing phylogenetic trees. Mol. Biol. Evol. 4, 406–425.

Sironi, L., Lazzari, B., Ramelli, P., Stella, A., Mariani, P., 2008. Avian TAP genes: detection of nucleotide polymorphisms and comparative analysis across species. Genet. Mol. Res. 7, 1267–1281.

Slomov, E., Loewenthal, R., Korostishevsky, M., Goldberg, I., Brenner, S., Gazit, E., 2005. Pemphigus vulgaris is associated with the transporter associated with antigen processing (TAP) system. Hum. Immunol. 66, 1213–1222.

Snyder, H.L., Bacik, I., Bennink, J.R., Kearns, G., Behrens, T.W., Bachi, T., Orlowski, M., Yewdell, J.W., 1997. Two novel routes of transporter associated with antigen processing (TAP)-independent major histocompatibility complex class I antigen processing. J. Exp. Med. 186, 1087–1098.

Tamura, K., Nei, M., 1993. Estimation of the number of nucleotide substitutions in the control region of mitochondrial DNA in humans and chimpanzees. Mol. Biol. Evol. 10, 512–526.

Van Kaer, L., Ashton-Rickardt, P.G., Ploegh, H.L., Tonegawa, S., 1992. TAP1 mutant mice are deficient in antigen presentation, surface class I molecules, and CD4-8+ T cells. Cell 71, 1205–1214.

Walker, B.A., Hunt, L.G., Sowa, A.K., Skjodt, K., Gobel, T.W., Lehner, P.J., Kaufman, J., 2011. The dominantly expressed class I molecule of the chicken MHC is explained by coevolution with the polymorphic peptide transporter (TAP) genes. Proc. Natl. Acad. Sci. USA 108, 8396–8401.

Wellman, M.L., Krakowka, S., Jacobs, R.M., Kociba, G.J., 1988. A macrophage-monocyte cell line from a dog with malignant histiocytosis in vitro cell. Dev. Biol. 24, 223–229.

White, L.C., Wright, K.L., Felix, N.J., Ruffner, H., Reis, L.F., Pine, R., Ting, J.P., 1996. Regulation of LMP2 and TAP1 genes by IRF-1 explains the paucity of CD8+ T cells in IRF-1-/- mice. Immunity 5, 365–376.

Wright, K.L., White, L.C., Kelly, A., Beck, S., Trowsdale, J., Ting, J.P., 1995. Coordinate regulation of the human TAP1 and LMP2 genes from a shared bidirectional promoter. J. Exp. Med. 181, 1459–1471.

Yan, G., Shi, L., Faustman, D., 1999. Novel splicing of the human MHC-encoded peptide transporter confers unique properties. J. Immunol. 162, 852–859.

Yang, Y., Fruh, K., Chambers, J., Waters, J.B., Wu, L., Spies, T., Peterson, P.A., 1992. Major histocompatibility complex (MHC)-encoded HAM2 is necessary for antigenic peptide loading onto class I MHC molecules. J. Biol. Chem. 267, 11669–11672.

Yewdell, J.W., Esquivel, F., Arnold, D., Spies, T., Eisenlohr, L.C., Bennink, J.R., 1993. Presentation of numerous viral peptides to mouse major histocompatibility complex (MHC) class I-restricted T lymphocytes is mediated by the human MHC-encoded transporter or by a hybrid mouse-human transporter. J. Exp. Med. 177, 1785–1790.

Zhang, S., Penfornis, A., Harraga, S., Chabod, J., Beurton, I., Bresson-Hadni, S., Tiberghien, P., Kern, P., Vuitton, D.A., 2003. Polymorphisms of the TAP1 and TAP2 genes in human alveolar echinococcosis. Eur. J. Immunogenet. 30, 133–139.

Supplemental Data

Supplemental Table 1

Primers used in this study.

Gene			Sequence (5'- 3')
TAP1	PCR	Forward	GCTGCTGCTTCTCGCCGACT
		Reverse	AGCCGATCTTCCCTTCTCTGTACC
	5' RACE[a]	3' Outer	CCCGAGACTGGAGAGAACCA
		3' Inner	ACTGAGGGCGAACACATCCA
TAP2	PCR	Forward	TCCAGGCCTGTGGCTGGAGG
		Reverse	ACCTGCTCTACCCCTCCATACCTTAG
	5' RACE[a]	3' Outer	AAGATGGCGGTGGCAAAGGCGT
		3' Inner	GAAGAAGAAGGCTGCGACGA
	pEGFP-TAP2	Forward	TAATaagcttAGATAACACCATGCGGTTCCCTGA[b]
		Reverse	TAATgtcgacTCAGTCCTCCAGTAGCTGCTG

[a] For performing RLM-RACE, 5’ outer and inner primers supplied by the manufacturer that annealed to the 5’ RACE adapter sequence were used.
[b] Lower case letters designate restriction enzyme recognition sites.

Supplemental Table 2

Transporter sequences used in comparative analyses.

Gene	Species	Scientific name	Database accession number[a]
ABCB9	Cow	Bos taurus	DAA20670
	Dog	Canis lupus familiaris	XP_858668
	Human	Homo sapiens	Q9NP78
	Mouse	Mus musculus	Q9JJ59
	Rat	Rattus norvegicus	Q9QYJ4
TAP1	Cow	Bos taurus	DAA16696
	Dog	Canis lupus familiaris	AJ630364
	Gorilla	Gorilla gorilla	AAA91200
	Human	Homo sapiens	Q03518
	Monkey	Macaca mulatta	XP_001115506
	Hamster	Mesocricetus auratus	AAB58721
	Mouse	Mus musculus	P21958
	Chimpanzee	Pan troglodytes	XP_001166911
	Rat	Rattus norvegicus	NP_114444
TAP2	Cow	Bos taurus	DAA16704
	Dog	Canis lupus familiaris	AJ630364
	Gorilla	Gorilla gorilla	AAA36588
	Human	Homo sapiens	NP_000535; NP061313 (isoform 2)
	Monkey	Macaca mulatta	XP_002808427
	Hamster	Mesocricetus auratus	AAB58724
	Mouse	Mus musculus	NP_035660
	Chimpanzee	Pan troglodytes	XP_003311251
	Rat	Rattus norvegicus	P36372 (2a);NP_114445 (2b)

[a]NCBI GenBank or RefSeq;UniProtKB/Swiss-Prot

CHAPTER 3: Knocking out genes in the classical MHCI pathway to disrupt surface protein expression

Introduction

The primary objectives in this dissertation involve the disruption of surface MHCI protein expression; numerous strategies could be utilized to achieve this outcome, but here we will discuss the rational for use of genetic engineering techniques targeting the TAP2 and the class I MHC heavy chain loci (Chapters 4 and 6, respectively). In this chapter, we will also briefly cover our early efforts at knocking out TAP genes in canine cells, and describe the genome editing technique, transcription activator-like effector nucleases (TALENs), that we ultimately used to produce TAP2- and MHCI-KO cell lines.

Alternative target genes for prevention of surface MHCI expression would be any of those involved in the complex antigen processing pathway (see Chapter 1), such as chaperones involved in the peptide loading complex or the β2M gene. For the purpose of detecting stabilization of MHCI complexes following exposure to media containing putative MHCI-binding peptides, targeting the β2M gene would be a poor choice as it is also required for optimal MHCI stabilization (Elliott et al., 1991). Furthermore, this protein may be present in the cell culture medium (Pollack et al., 1988), which would result in false identification of MHCI protein on feline cells, though it is unknown whether these proteins would assist in stabilizing canine MHCI complexes. The tapasin or peptidase genes involved in receptive-state MHCI formation and antigen editing, respectively, are also known to enhance expression of pMHCI complexes, but some MHCI allomorphs are presented independent of these genes (Hulpke and Tampé, 2013). Therefore, we elected to target the TAP2 gene because two other TAP-deficient cell lines are available and useful in MHCI stabilization assays (Townsend et al., 1989; Powis et al., 1991). We also targeted the classical MHCI heavy chain loci for immune evasion strategies, and the rational for targeting these loci will be expanded upon in Chapter 6.

Canine TAP2-KO efforts

In Chapter 2, we show sequences and further characterization of the canine TAP1/2 genes. These data were used as reference in genetic screening of mutagenized canine cell clones, derived from MHCI^{low} cells (evaluated by flow cytometry) to identify substitutions in the coding sequences of the TAP genes that would render the gene dysfunctional. Though we performed both random and targeted mutagenesis, along with simultaneous cell sorting techniques, and created numerous cell clones, we were unsuccessful in detecting a clonal population that was useful for peptide:MHCI stabilization assays. Herein, I will briefly describe the strategies employed and the pitfalls discovered through our efforts.

For a non-specific TAP gene KO strategy, we utilized mutagenic ethyl methanesulfonate (EMS) treatments on DH82 cells, a canine malignant histiocytic immortal cell line, at a dose determined to induce 50% cell viability (data not shown). EMS-exposed canine cells were then labeled with a monoclonal antibody (H58a), which is cross-reactive with MHCI complexes from different species, and monitored for reduced DLAI expression via flow cytometry analysis. Multiple rounds of mutagenesis and cell sorting resulted in a population with reduced DLAI expression, see Figure 1. We then used fluorescent-activated cell sorting (FACS) to select DLAI^{low} cells and performed limiting dilution of cells into multiple 96-well plates, which were allowed to expand and then screened for the expected phenotype.

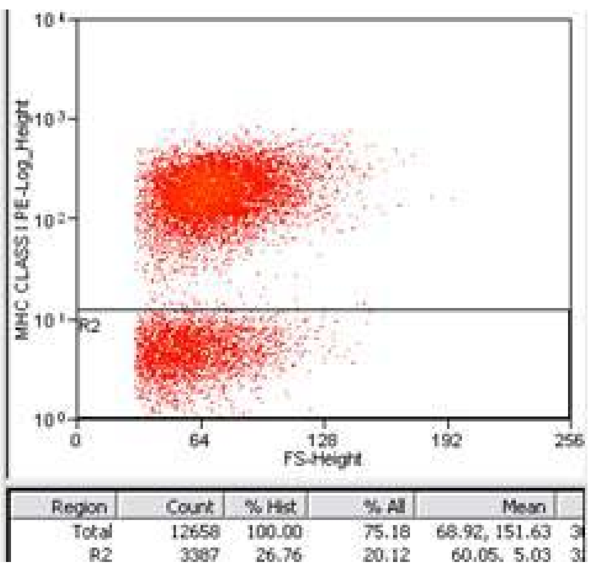

Figure 1. DH82 cell DLAI expression following five rounds of mutagenesis and cell sorting. Cells indicated in the R2 region were sorted and cloned for future analyses.

To limit the number of clones of interest prior to sequencing each of the >2500bp TAP genes (an expensive endeavor), we first performed flow cytometry analyses again to confirm that cells retained the DLAI^{low} phenotype (example clone shown in Figure 2), and attempted peptide pulsing experiments using antigens eluted from parental cells to detect the capability of cloned cells to stabilize MHCI. Prior to performing peptide pulsing assays, I acid-eluted bulk peptides from EL4 cells, a murine lymphoma line related to the RMAS line (Frances Gays et al., 2000), and detected MHCI stabilization on RMAS cells following culture with media containing purified bulk peptides, Figure 3. While this strategy showed success using the murine RMAS cells, we did not observe rescued DLAI expression on any of the mutated DH82 clones following pulsing with bulk peptide eluted from parental cells (>50 clones screened; data not shown).

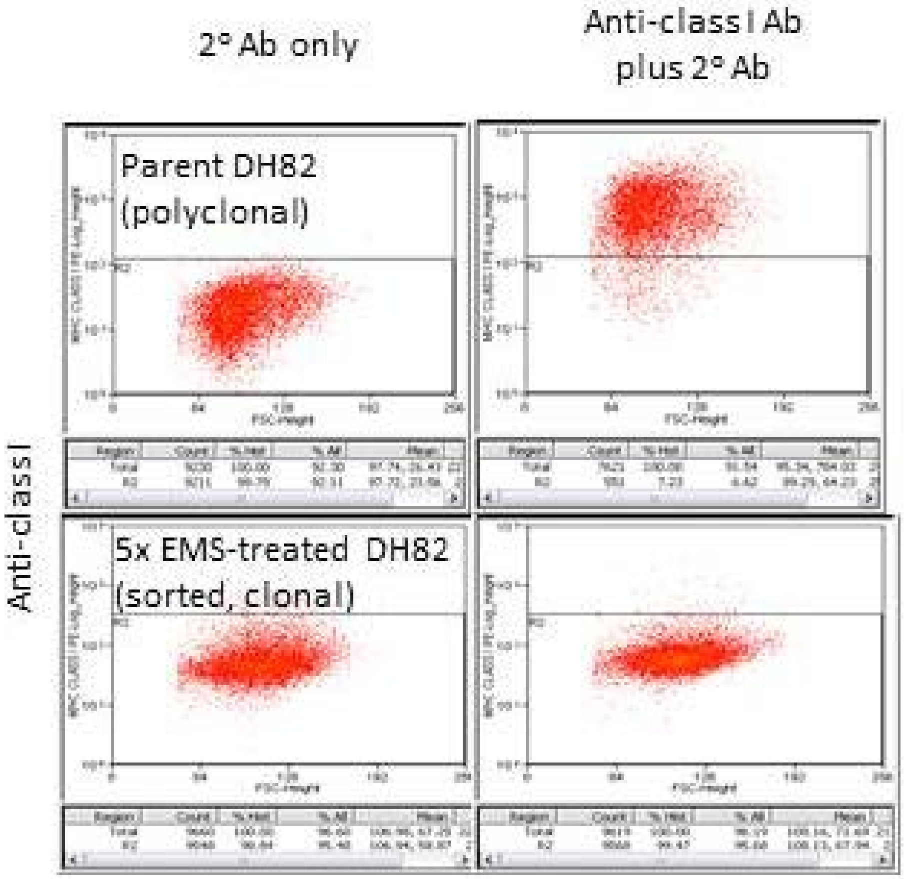

Figure 2. Example of a mutated DH82-derived cell clone displaying reduced DLAI expression. Labeling of a mutagenized cell clone with the H58a antibody and fluorescently-conjugated secondary antibody shows no DLAI expression compared to parental cells.

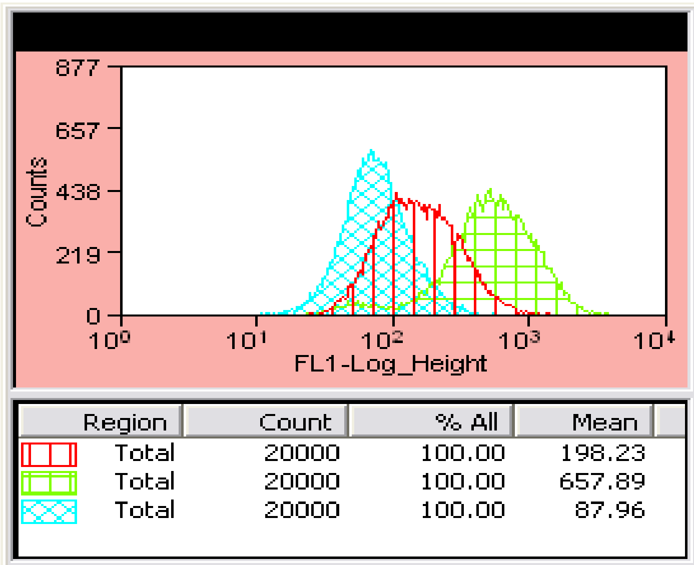

Figure 3. Overlay of flow cytometry histograms indicates RMAS cells display increased MHCI expression following bulk peptide pulse protocols. RMAS cells cultured with media containing no peptides (blue) display low MHCI expression, while cells pulsed with bulk peptides (red) show higher MHCI expression levels. The green histogram represents a control peptide (UTY) pulsed at a concentration known to stabilize the D^b molecule.

It is possible that we successfully mutated the TAP genes but our assay is not robust enough to detect corresponding MHCI stabilization because 1) the anti-MHCI antibody might detect TAP-independent nonclassical DLAI expression resulting in high background staining, or 2) only minor increases in MHCI expression occur because the eluted antigen preparation contains weakly-binding peptides. To address these possibilities, we created expression vectors encoding either of the canine TAP genes, transfected the cell clones with constructs, and monitored for restoration of DLAI expression. Again, none of the clones displayed restored DLAI expression (data not shown). We further employed the strategy of pulsing peptides known to bind the DLAI-88*50801 allele (manuscript in preparation; data not shown), with no positive results. Therefore, the most likely cause for failure in detecting MHCI stabilization by these cells is that mutations in the TAP genes did not cause the low DLAI expression. Another possible explanation for not finding a clone with the intended MHCI-stabilizing phenotype is that the number of rounds of mutagen exposure and cell sorting resulted in mutations to multiple genes in the MHCI antigen processing pathway. This hypothesis seems unlikely however as the expected mutation rate using the EMS mutagenesis method is extremely low (Ohnishi, 1977), and would need to induce biallelic KO in more than one gene, but cannot be ruled out. In all, randomly mutated DH82 cell clones did not display the expected phenotype for use in pMHCI stabilization assays.

We therefore abandoned random mutagenesis techniques and employed zinc finger nucleases (ZFN), as this technology is capable of inducing targeted biallelic gene disruption at frequencies much higher (>1%) than random mutagenesis (Santiago et al., 2008). ZFN plasmids were designed to target both TAP1 and 2 genes, transfected into DH82 cells, and we performed similar cell sorting and cloning strategies as above. While sorting of ZFN-transfected cells did produce DLAI^{low} clones, this strategy was also unsuccessful in creating cell lines responsive to peptides in MHCI assays (data not shown). However, members of our lab performed concurrent experiments that employed the strategy of transfecting the characterized, DLAI-88*50801 allele into RMAS cells. Transfection of the canine DLAI allele into TAP2-KO RMAS cells resulted in the ability to confirm the peptide binding motif for this allele (Ross et al., 2012; and manuscript in submission). Thus, while our mutagenesis strategies described above failed to produce a novel canine cell line for use in peptide MHCI stabilization assays, we have been able to create feline cells, described in the next chapter, that indeed possess mutated TAP2 genes.

TALEN technology

Ever evolving biotechnological tools are being created for genetic engineering purposes, with increasing targeting accuracy and efficiency (Gaj et al., 2013). One such technology uses transcription activator-like effectors (TALEs), which are protein complexes found in the bacterial plant pathogen *Xanthomonas* and used by this pathogen to hijack the transcriptional activity within the host (Boch and Bonas, 2010). The TALEs possess DNA-binding domains that recognize specific nucleotide sequences within the genome and are able to recruit transcription factors to the targeted site to induce either gene repression or activation. By amending an endonuclease-encoding sequence onto the 3` coding region in place of the transcription factor-recruiting domain (now deemed a TALEN) and targeting two such TALENs within close genomic proximity, researchers have shown the capacity of these modified tools to induce double-strand breaks (DSBs) within the gene of interest (Miller et al., 2010).

Data are available that describe the numerous proteins involved in eukaryotic cell-intrinsic DNA repair mechanisms, which occur following random DSB formation [reviewed in (Daley and Sung, 2014)] and which are also employed following TALEN-mediated DSB induction (Pan et al., 2013). The DNA repair mechanisms, however, are not able to correctly fix the nucleotide sequence with 100% fidelity (Bétermier et al., 2014), thus allowing for potential gene disruption to occur following TALEN-mediated DSB induction, which has been performed in numerous species (Doyle et al., 2012). The situations in which each repair mechanism [non-homologous end-joining (NHEJ) or homology-directed recombination (HDR) being the broad categories] is utilized are not fully understood, but results indicate that cell cycle might be involved (Daley and Sung, 2014). This understanding has allowed investigators to manipulate the cell cycle-dependent utilization of HDR to direct gene correction following TALEN exposure (Strouse et al., 2014). Thus, manipulation of both NHEJ and HDR repair mechanisms following TALEN-mediated DSB induction have allowed researchers to disrupt, insert, and correct targeted loci in many different species (Pan et al., 2013), making this technology a useful approach in our goals of creating TAP2- and MHCI-KO feline and murine cells, respectively.

TALEN specificities have been determined to be reprogrammable, in that the repetitive domains found within the naturally occurring TALEs define interactions with specific nucleotides (Mussolino and Cathomen, 2012), while the nucleotide specificity of ZFN technology has been more difficult to predict (Beumer et al., 2013), a possible reason for failures in earlier experiments employing this technology. The repeating variable di-residues (RVD) in TALENS are the 12^{th} and 13^{th} residues of the 34 amino acids encoded in each repetitive, highly modular DNA-binding domain, and have been determined to be crucial for nucleotide recognition (Scholze and Boch, 2010). By specifically ordering these RVD-containing domains (normally 12-30 RVD per TALE) within linear constructs attached to a nuclease domain, and by targeting two such TALENs within 12-20 base pairs apart, researchers are able to stringently target almost any locus. Recently published protocols are available describing the step-by-step (and automatable) procedures to create these TALEN expression constructs (Miller et al., 2010; Sander et al., 2010; Reyon et al., 2012; Sanjana et al., 2012), resulting in an abundance of recent publications using TALEN technologies in diverse species (i.e. a PubMed database search for “TALEN” restricted to the 2013 year yields 105 publications). Thus, TALENs are a highly modular and easily manipulated technology capable of targeting almost any gene of interest, further indicating it as useful for our intended outcomes.

Researchers have also described advances in the delivery and architecture of genetic engineering technologies yielding even higher modification rates, and have shown the capacity for the rapid creation of transgenic animals. The TALEN backbone has been found to be adaptable to the species of interest (Bedell et al., 2012), thereby increasing the efficiency with which mutations may occur. Microinjections of TALEN-encoding messenger RNA into stem cells can result in the rapid generation of modified offspring following *in vitro* fertilization protocols (Panda et al., 2013). Another DNA-modifying tool kit has been recently described that reduces the total amount (mass and length) of nucleotide information that must be transfected/electroporated/injected into targeted cells called the Cas9/CRISPR system [described in (Pennisi, 2013)]. Thus, the realm of genetic engineering is progressing extremely rapidly, and current technologies are readily available that make genome modification increasingly accessible.

TALEN experiments using K562 cells

Due to the previously described efforts attempting mutagenesis that resulted in failure to produce canine cell clones of interest, I designed and executed the following pilot experiment using TALEN technology to disrupt a chemokine gene, CCR5, within the human K562 cell line (Miller et al., 2010).

Miller et al. provided TALEN plasmid designs, CCR5 locus-specific PCR primers, and instructions for the detection of modifications at the target site by using the Surveyor endonuclease assay (Guschin et al., 2010). I therefore acquired the human K562 cell line (kind gift from Hayley Dirscherl in Jeffrey Yoder's lab, NCSU), the plasmids to construct the TALENs (kind gift from Odessa Marks in Jorge Piedrahita's lab, NCSU), and ordered the PCR primers described by Miller et al. to amplify the CCR5 locus. As an alternative readout for TALEN activity, Odessa Marks provided a single-strand annealing (SSA) GFP reporter assay (see Chapters 4 and 6 for further description) that I was able to modify and rename pCCR5. Briefly, the CCR5 nucleotide sequence that is targeted by the TALEN pair is introduced into the SSA GFP reporter and when that sequence is cleaved by the TALENs, GFP expression may ensue.

I co-transfected the K562 cell line with the pCCR5 reporter and the left and right CCR5-targeting TALEN constructs (matching those described by Miller et al.), and monitored cells for the presence of GFP expression (Figure 4) or genomic modifications (Figure 5). As seen in the left panel of Figure 4, cells receiving only the pCCR5 reporter may randomly express GFP, but cells receiving the reporter and TALENs show a 2.5-fold higher percentage of cells expressing GFP (Figure 4, right panel; 1 representative shown of 3 experiments). Thus, TALENs can modify the CCR5 target nucleotide-possessing GFP reporter in K562 cells, resulting in GFP expression and indicating TALEN activity in the cytosol of recipient cells. However, we must next confirm TALEN activity within the nucleus, where the CCR5 locus resides. Detection of genomic modifications via the Surveyor assays involves the hybridization of PCR products from gDNA of untransfected (WT) cells with amplimers from cells receiving TALENs (TAL). Following hybridization, products are exposed to digestion by an endonuclease that recognizes base pair mismatches. Figure 5 shows that WT/TAL and TAL/TAL hybrid products are recognized and cleaved by the Surveyor enzyme, while the WT/WT product is not. Thus the TALEN pair that I created by following the design of the Miller et al. paper resulted in disruption of the CCR5 locus within K562 cells. K562 cells do not express the CCR5 protein at levels consistently high enough for confirming disruption at the protein level (data not shown).

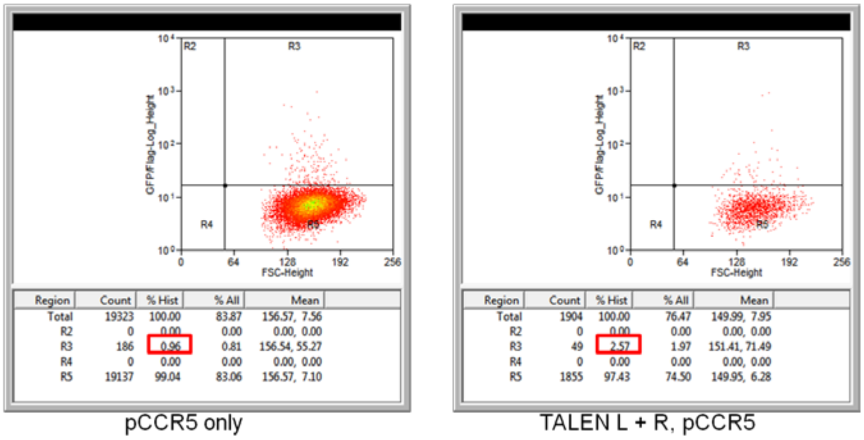

Figure 4. The transfection of K562 cells with pCCR5 and both TALEN plasmids results in GFP conversion, indicating TALEN activity.

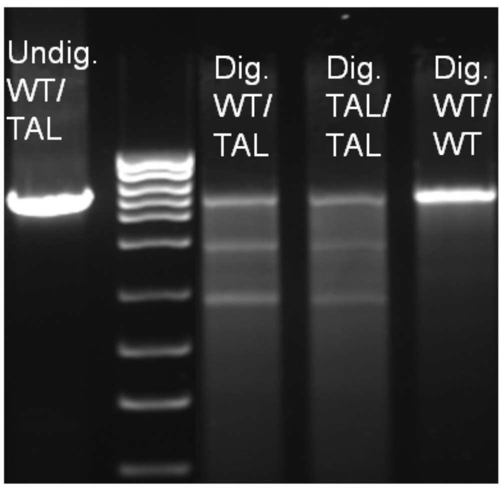

Figure 5. Surveyor assay indicates that the K562 TALEN-recipients (TAL) possess insertion/deletion events that result in cleavage by the endonuclease enzyme following PCR product hybridization, while control product hybrids are not cleaved.

Summary

The TAP loci are logical targets for gene disruption efforts aimed at creating a MHCI stabilization tool kit cell line, as the murine and human cell line equivalents also possess mutations in these genes. Random mutagenesis of canine cells resulted in DLAI^{low} cell clones, which were not responsive to bulk or allele-specific peptide pulsing. Similar results occurred using the ZFN strategy; however, the canine cell line was no longer needed because RMAS cells transfected with the DLAI-88*50801 allele were used to confirm its peptide-binding motif. TALENs provide a highly specific and modular biotechnological tool to be used for disrupting normal gene expression. I was able to use TALENs to modify genomic CCR5 loci within K562 cells, and I have shown that the SSA GFP reporter, in combination with TALENs, can act as a readout for TALEN activity in cells. In the next chapters, I will describe experiments that utilize this technology to derive cell lines that lack normal levels of MHCI expression for the purposes of studying MHCI-restricted CD8+ T-cell responses in the cat and also for evading immune responses against murine cell lines as a model for enhancing graft survival.

References

Bedell, V.M., Y. Wang, J.M. Campbell, T.L. Poshusta, C.G. Starker, R.G. Krug Ii, W. Tan, S.G. Penheiter, A.C. Ma, A.Y.H. Leung, S.C. Fahrenkrug, D.F. Carlson, D.F. Voytas, K.J. Clark, J.J. Essner, and S.C. Ekker. 2012. In vivo genome editing using a high-efficiency TALEN system. *Nature*. advance online publication. doi:10.1038/nature11537.

Bétermier, M., P. Bertrand, and B.S. Lopez. 2014. Is Non-Homologous End-Joining Really an Inherently Error-Prone Process? *PLoS Genet*. 10:e1004086. doi:10.1371/journal.pgen.1004086.

Beumer, K.J., J.K. Trautman, M. Christian, T.J. Dahlem, C.M. Lake, R.S. Hawley, D.J. Grunwald, D.F. Voytas, and D. Carroll. 2013. Comparing zinc finger nucleases and transcription activator-like effector nucleases for gene targeting in Drosophila. *G3 Bethesda Md*. 3:1717–1725. doi:10.1534/g3.113.007260.

Boch, J., and U. Bonas. 2010. Xanthomonas AvrBs3 Family-Type III Effectors: Discovery and Function. *Annu. Rev. Phytopathol.* 48:419–436. doi:10.1146/annurev-phyto-080508-081936.

Daley, J.M., and P. Sung. 2014. 53BP1, BRCA1 and the choice between recombination and end joining at DNA double-strand breaks. *Mol. Cell. Biol.* doi:10.1128/MCB.01639-13.

Doyle, E.L., N.J. Booher, D.S. Standage, D.F. Voytas, V.P. Brendel, J.K. Vandyk, and A.J. Bogdanove. 2012. TAL Effector-Nucleotide Targeter (TALE-NT) 2.0: tools for TAL effector design and target prediction. *Nucleic Acids Res.* 40:W117–122. doi:10.1093/nar/gks608.

Elliott, T., V. Cerundolo, J. Elvin, and A. Townsend. 1991. Peptide-induced conformational change of the class I heavy chain. *Nature*. 351:402–406. doi:10.1038/351402a0.

Frances Gays, Meera Unnikrishnan, Sunil Shrestha, Karen P. Fraser, Adam R. Brown, Colin M. G. Tristram, Z.M.A. Chrzanowska-Lightowlers, and and C.G. Brooks. 2000. The Mouse Tumor Cell Lines EL4 and RMA Display Mosaic Expression of NK-Related and Certain Other Surface Molecules and Appear to Have a Common Origin. *J. Immunol.* 164:5094–102.

Gaj, T., C.A. Gersbach, and C.F. Barbas III. 2013. ZFN, TALEN, and CRISPR/Cas-based methods for genome engineering. *Trends Biotechnol.* 31:397–405. doi:10.1016/j.tibtech.2013.04.004.

Guschin, D.Y., A.J. Waite, G.E. Katibah, J.C. Miller, M.C. Holmes, and E.J. Rebar. 2010. A rapid and general assay for monitoring endogenous gene modification. *Methods Mol. Biol. Clifton NJ*. 649:247–256. doi:10.1007/978-1-60761-753-2_15.

Hulpke, S., and R. Tampé. 2013. The MHC I loading complex: a multitasking machinery in adaptive immunity. *Trends Biochem. Sci.* 38:412–420. doi:10.1016/j.tibs.2013.06.003.

Miller, J.C., S. Tan, G. Qiao, K.A. Barlow, J. Wang, D.F. Xia, X. Meng, D.E. Paschon, E. Leung, S.J. Hinkley, G.P. Dulay, K.L. Hua, I. Ankoudinova, G.J. Cost, F.D. Urnov, H.S. Zhang, M.C. Holmes, L. Zhang, P.D. Gregory, and E.J. Rebar. 2010. A TALE nuclease architecture for efficient genome editing. *Nat. Biotechnol.* 29:143–148. doi:10.1038/nbt.1755.

Mussolino, C., and T. Cathomen. 2012. TALE nucleases: tailored genome engineering made easy. *Curr. Opin. Biotechnol.* 23:644–650. doi:10.1016/j.copbio.2012.01.013.

Ohnishi, O. 1977. Spontaneous and Ethyl Methanesulfonate-Induced Mutations Controlling Viability in DROSOPHILA MELANOGASTER. II. Homozygous Effect of Polygenic Mutations. *Genetics*. 87:529–545.

Pan, Y., L. Xiao, A.S.S. Li, X. Zhang, P. Sirois, J. Zhang, and K. Li. 2013. Biological and Biomedical Applications of Engineered Nucleases. *Mol. Biotechnol.* 55:54–62. doi:10.1007/s12033-012-9613-9.

Panda, S.K., B. Wefers, O. Ortiz, T. Floss, B. Schmid, C. Haass, W. Wurst, and R. Kühn. 2013. Highly efficient targeted mutagenesis in mice using TALENs. *Genetics*. 195:703–713. doi:10.1534/genetics.113.156570.

Pennisi, E. 2013. The CRISPR Craze. *Science*. 341:833–836. doi:10.1126/science.341.6148.833.

Pollack, M.S., A. Hayes, S. Mooney, N.C. Pedersen, and R.G. Cook. 1988. The detection of conventional class I and class II I-E homologue major histocompatibility complex molecules on feline cells. *Vet. Immunol. Immunopathol.* 19:79–91.

Powis, S.J., A.R.M. Townsend, E.V. Deverson, J. Bastin, G.W. Butcher, and J.C. Howard. 1991. Restoration of antigen presentation to the mutant cell line RMA-S by an MHC-linked transporter. *Nature*. 354:528–531.

Reyon, D., S.Q. Tsai, C. Khayter, J.A. Foden, J.D. Sander, and J.K. Joung. 2012. FLASH assembly of TALENs for high-throughput genome editing. *Nat. Biotechnol.* 30:460–465. doi:10.1038/nbt.2170.

Ross, P., J.C. Holmes, G.S. Gojanovich, and P.R. Hess. 2012. A cell-based MHC stabilization assay for the detection of peptide binding to the canine classical class I molecule, DLA-88. *Vet. Immunol. Immunopathol.* 150:206–212. doi:10.1016/j.vetimm.2012.08.012.

Sander, J.D., M.L. Maeder, D. Reyon, D.F. Voytas, J.K. Joung, and D. Dobbs. 2010. ZiFiT (Zinc Finger Targeter): an updated zinc finger engineering tool. *Nucleic Acids Res.* gkq319. doi:10.1093/nar/gkq319.

Sanjana, N.E., L. Cong, Y. Zhou, M.M. Cunniff, G. Feng, and F. Zhang. 2012. A transcription activator-like effector toolbox for genome engineering. *Nat. Protoc.* 7:171–192. doi:10.1038/nprot.2011.431.

Santiago, Y., E. Chan, P.-Q. Liu, S. Orlando, L. Zhang, F.D. Urnov, M.C. Holmes, D. Guschin, A. Waite, J.C. Miller, E.J. Rebar, P.D. Gregory, A. Klug, and T.N. Collingwood. 2008. Targeted gene knockout in mammalian cells by using engineered zinc-finger nucleases. *Proc. Natl. Acad. Sci.* 105:5809–5814. doi:10.1073/pnas.0800940105.

Scholze, H., and J. Boch. 2010. TAL effector-DNA specificity. *Virulence*. 1:428–432. doi:10.4161/viru.1.5.12863.

Strouse, B., P. Bialk, R.A. Niamat, N. Rivera-Torres, and E.B. Kmiec. 2014. Combinatorial gene editing in mammalian cells using ssODNs and TALENs. *Sci. Rep.* 4. doi:10.1038/srep03791.

Townsend, A., C. Öhlén, J. Bastin, H.-G. Ljunggren, L. Foster, and K. Kärre. 1989. Association of class I major histocompatibility heavy and light chains induced by viral peptides. *Nature*. 340:443–448. doi:10.1038/340443a0.

CHAPTER 4: Use of a TAP2-KO CRFK clone generated by TALEN-mediated gene disruption for detecting peptide binding to the classical MHCI molecule, FLAI-E

Introduction

As discussed in Chapter 3, transcription activator-like effector nucleases (TALENs) are able to be used to disrupt genomic loci, with the intention of preventing protein expression. Due to our penultimate objective of detecting classical feline leukocyte antigen class I (FLAI)-restricted CD8+ T-cell responses, we attempted to create a novel feline tool kit by TALEN-mediated disruption of the transporter associated with antigen processing 2 (TAP2) gene in the Crandall-Rees feline kidney (CRFK) cell line for use in FLAI stabilization assays. The failure of random mutagenesis and ZFN strategies for creation of canine TAP2-KO cells was circumvented by the use of a murine TAP2-KO RMAS cell line. We could attempt to transfect FLAI alleles into RMAS cells, however uncertainty of the capacity of FLAI complexes to interact with murine peptide loading complexes, the selection of which FLAI allele to use, and the overall lack of data regarding which FLAI loci actually present peptides at the cell surface to activate CD8+ T-cell responses are factors that promoted us to consider an alternate strategy. We will therefore attempt to recapitulate the TAP2-KO RMAS tool kit in CRFK cells, as the TAP2 gene is required for presentation of the majority of peptides by classical MHCI, see Chapter 2. Such a tool kit in the feline species will aid in confirming the peptide-binding motifs associated with allelic FLAI complexes, and be useful as peptide-pulsed targets for detection of FLAI-restricted CD8+ T-cell responses *in vitro*, which have not yet been shown in an allele-specific manner.

We recently demonstrated that the FLAI- E, -H, and –K loci of the feline genome are classical MHCI genes due to their wide tissue expression and the possession of hypervariable regions in the exons encoding the alpha 2 and 3 domains (Holmes et al., 2013), but the confirmation of the ability of these FLAI complexes to restrict αβ TCR expressing CD8+ T-cell responses is still lacking. While limited data are available regarding the requirements of FLAI-restrictions for CD8+ T-cell responses (Bucci et al., 1998), peptide-specific responses have been detected in felines against certain pathogens, with some responses being conserved between human and feline immunodeficiency virus infections (Cornelissen et al., 2007; Sanou et al., 2013; Song et al., 1992; Vermeulen et al., 2012). Thus, studies of specific peptide:FLAI-restricted CD8+ T-cell responses in the feline breeds will assist in confirming the classical class I status of the E, H, and K loci.

Concurrent studies by our group are attempting to elucidate peptide sequences presented by FLAI complexes in feline immunodeficiency virus (FIV)-infected CRFK cells. For such purposes, we screened cats used in FIV-infection studies for expression of FLAI alleles, cloned the FLAI-E*02001 allele, and transfected this FLAG-tagged allele into the CRFK cell line, designated 1A3. These cells have undergone FIV-infection procedures and were lysed for use in coimmunoprecipitation strategies in order to elute virus-derived peptides from the clefts of the FLAG-tagged allele-specific FLAI-E peptide-binding groove. The eluted peptide fragments can then be sequenced via mass spectroscopy (M/S) analyses, and a hypothetical peptide-binding motif may be constructed for the E*02001 allele. These data will allow us to produce recombinant peptides matching the putative binding motif to be confirmed via FLAI complex stabilization assays, such as by measuring radio-labeled competitive peptide binding assays (Maguire et al., 2012) or by measuring thermal denaturation via circular dichroism strategies (Morgan et al., 1997). However, such motif-confirming studies would benefit from availability of a tool kit similar to the one utilized in studies of the DLA-88*50801 complex (Ross et al., 2012), which took advantage of a TAP2-deficient murine cell line.

Thus, in this chapter I will describe the creation of two modified CRFK cell lines [wild type (WT) and a clone derived from the 1A3 lineage] that possess characteristics similar to the previously described TAP2-KO RMAS cell line (Ljunggren et al., 1990), for use in the confirmation of FLAI binding motifs and, eventually, as targets for detection of antigen-specific T-cell responses. We created a WT CRFK-derived clone during these experiments for the capability of transfecting in other FLAI genes of interest at later times for motif analyses. Herein, we confirm the predicted TAP2 locus in felines to be correct, the ability of TALENs to disrupt this locus resulting in downregulation of surface FLAI expression, but we have to this point been unable to confirm the ability of TALEN-modified cell clones to stabilize surface FLAI-expression following culture with peptides eluted from parental and FIV-infected CRFK cells.

Methods and Materials

Cell care

The Crandall-Rees feline kidney cell line, CRFK, was a kind gift from Gregg Dean (NCSU) and cultured in DMEM (CellGro) with 10% FBS and 1% P/S at 5% CO_2 in 37C. During some experiments, cells were cultured at 27C in 5% CO_2 overnight in order to decelerate reuptake of surface proteins. Following FACS-based isolation, cells underwent ring-cloning techniques and were expanded for two weeks prior to confirmation of genome modification. CRFK cells that are perpetually infected with the Petaluma strain of FIV were also obtained as a kind gift from Wayne and Mary Tompkins (NCSU). Supernatants were collected from the Petaluma-infected cell line for use in coordinating infection times in CRFK cells.

FLAI-E plasmid preparation and transfection

The 1A3 line of CRFK cells contains a vector encoding the FLAI-E*02001 allele fused with a FLAG tag (to be published elsewhere). This allele was selected for use due to its relatively wide expression within cats used for studies of FIV infection. Transfection was performed using Lipofectamine LTX and transfected cells were selected using the G418 antibiotic (Invitrogen) at 800 µg/ml and clones were maintained at 200 µg/ml.

CONFIRMATION OF FLAG EXPRESSION IN 1A3 CELL LINES

Intracellular detection of FLAG protein was performed following manufacturer protocols for the BD Cytofix/Cytoperm™ kit (BD Biosciences). Briefly, the M2 anti-FLAG antibody was used to label permeabilized cells of either WT or 1A3 origin. The secondary goat anti-mouse F(ab`)$_2$ conjugated to Alexa Fluor 647 (Jackson ImmunoResearch) was applied to cells receiving the primary antibody or unlabeled samples as controls. Flow cytometry data acquisition was performed on the FACSCalibur instrument (BD Biosciences) and analyzed using Summit software v5.2 (Beckman Coulter).

Primers used for PCR-based detection of the FLAG-tagged, FLAI-E plasmid were created to amplify a hybrid sequence that contained the 5` portion of the FLAI CDS and the 3` region of the FLAG-encoding nucleotides using Primer-BLAST (data not shown).

TAP2 GENE CONFIRMATION

Primers to the feline TAP2 gene (GenBank ID #101089770) were designed using Primer-BLAST: 468F= 5` CTTCCTTGGTGGTGCCGTAT; 479F= 5` GTGCCGTATGGGGTGAGTCA; 1211R= 5` AGATTGGGGCTGGGTGTAGA; 1382R= 5` ACTGCTGCTTGGAGCCTAGG. The 468F and 1382R primers were combined in PCR reactions with the HotStar HiFi (Qiagen) polymerase, using Q solution, in which annealing steps were performed at 62C following manufacturer's recommendations for other cycling parameters. Products from PCR reactions were gel electrophoresed and excised for purification using QIAquick gel extraction (Qiagen). Products were then ligated to pGEM vector for TA-cloning, blue/white screening, and subsequent DNA sequencing of insert-containing plasmids. The Geneious software (version 6.1.6 from Biomatters, available at http://www.geneious.com/) was utilized for comparison of collected TAP2 sequences to published data.

TALEN CONSTRUCTION AND TRANSFECTION

Exon 2 of the TAP2 gene was selected for TALEN targeting due to the presence of *BamHI* and *StyI* restriction enzyme recognition sites, which make for easier detection of gene modifications post TALEN transfection, and also due to the presence of multiple possible open reading frames within the gene upstream of this section. The ZiFiT targeter (Sander et al., 2010) was utilized to create TALEN pairs that flanked both the *BamHI* or *StyI* recognition sites, and these respective Bam and Sty TALEN pairs were constructed using the REAL method (Reyon et al., 2012) from plasmids kindly shared by Jorge Piedrahita (NCSU). The DNA sequences of the left and right, Bam and Sty TALEN plasmids were confirmed prior to transfection (data not shown). As a reporter assay for TALEN activity, the usage of single-strand annealing (SSA) plasmids was modified from a previous protocol (Perez-Pinera et al., 2012). Briefly, the pSSA GFP vector (kind gift from Odessa Marks, NCSU) was modified to contain the TALEN-targeted nucleotide sequence of TAP2 (Figure 1A & B), and renamed pTAP2. As a control for spontaneous GFP reporter plasmid conversion, the pSSA GFP reporter plasmid was transfected along with the left TALEN plasmid only into CRFK cells. Co-transfection of CRFK cells with either of the TALEN pair plasmids and reporter plasmids was performed for 4 hours (1:1:1 ratio, total 2.5 µg) and lipofectamine LTX (1:2 DNA to reagent ratio) with Plus reagent (Invitrogen) following manufacturer's protocols. Early experiments comparing the TALEN pairs determined the Bam TALEN to be more efficient and that pair was used for transfections, and clones of the transfected cells were derived.

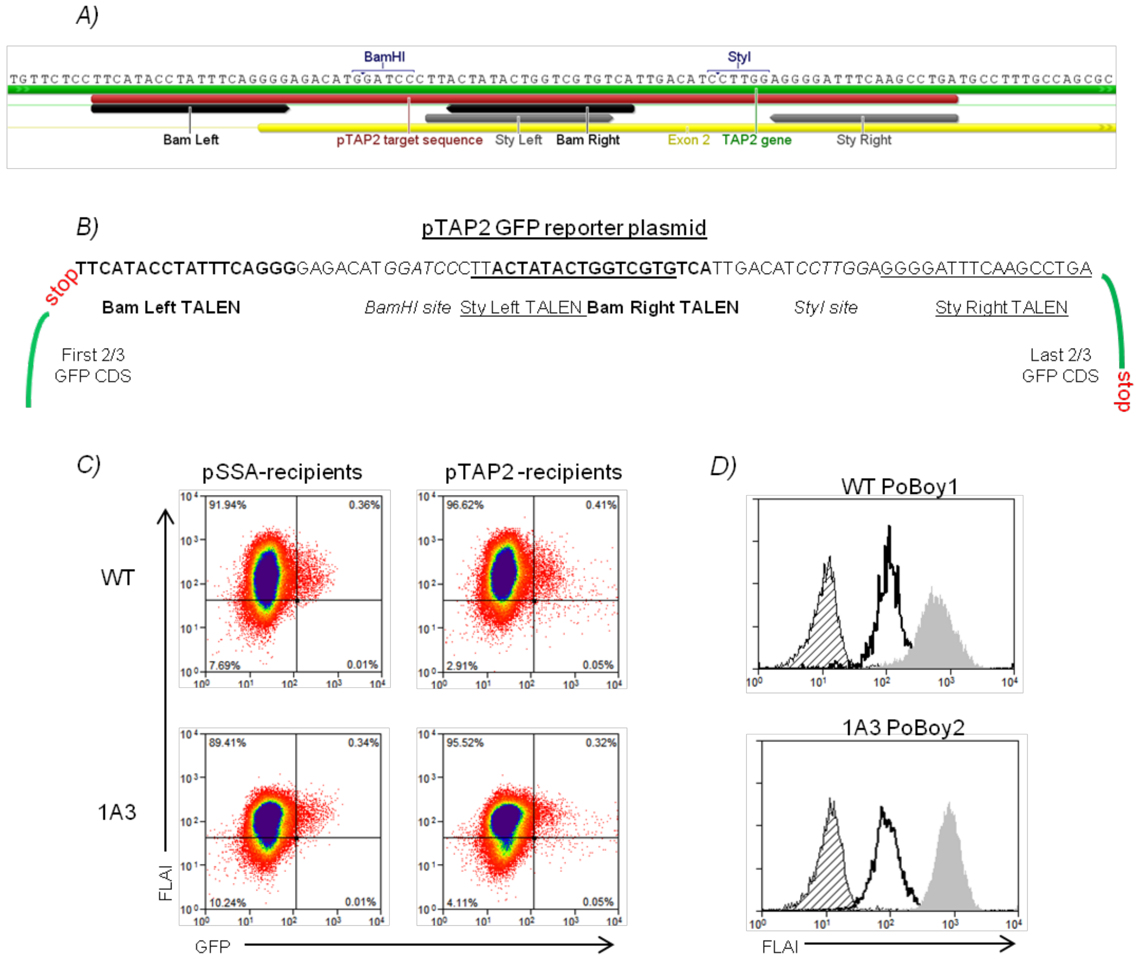

Figure 1. TALEN and GFP reporter co-transfection into CRFK cells increases GFP+ MHCI- population. *A)* TALENs were designed to flank restriction enzyme recognition sites found within exon 2 (yellow bar) of the feline TAP2 gene (GenBank ID: 101089770). Nucleotides underscored by red bar were ligated into the pSSA GFP plasmid to create pTAP2. *B)* The pSSA GFP plasmid reporter construct contains two partial coding sequences for GFP separated by a stop codon and restriction sites that allow for ligation of a nucleotide sequence between the GFP coding stretches. The pTAP2 plasmid is a modified version of the pSSA GFP reporter that includes the TAP2 target region. Cleavage of the pTAP2 target sequence by TALEN activity can result in repair mechanisms that produce full GFP coding sequences, causing cells that possess active TALENs to fluoresce. *C)* Co-transfection of CRFK cell lines (WT top row, 1A3 bottom) with both Bam TALENs and pTAP2 results in 5 fold more GFP+ MHCI^{low} cells compared to pSSA-recipients. Percentage of cells in quadrants labeled. *D)* FACSorted clones from WT (PoBoy1, above) and 1A3 (PoBoy2, below) TALEN-transfectant lines retain MHCI^{low} phenotype following expansion. Empty histograms depict cell clone surface FLAI expression compared to parental line (filled) and clones labeled with secondary antibody alone (striped).

GENOME MODIFICATION DETECTION

Following transfection of TALEN and reporter plasmids (see above section), cells were sorted based on high GFP fluorescence and simultaneous low surface FLAI expression, as detected by labeling with the 3F10 antibody (Ancell) followed by a goat anti-mouse $F(ab`)_2$ conjugated to Alexa Fluor 647 (Jackson ImmunoResearch). Following FACS selection, cells were seeded into 96-well plates for clonal expansion. Clones were selected that possessed similar growth kinetics to parental CRFK cells, screened for reduced FLAI expression, and then genomic DNA was extracted using the Quick-gDNA MiniPrep Kit (Zymo). As a control for any possible spontaneous accumulation of mutations in the TAP2 locus during cloning, cell clones from transfectants receiving the pSSA-GFP reporter and only one TALEN plasmid were also included in analyses, and named “SSA” clones. Amplification of the TAP2 locus from cell clones was performed as above, followed by restriction enzyme digestion for 2 hours using the high fidelity version of the BamHI enzyme (NEB). Digestion products were gel electrophoresed for visualization. TA clone plasmids were created using undigested PCR products for use in Sanger DNA sequencing (Eurofins MWG Operon), and the sequences were aligned to SSA clone data for analysis.

RESTORATION OF SURFACE FLAI EXPRESSION

Cold incubation of CRFK cells was performed similarly to previously described (De Silva 1999 JI), except at 27C, followed by 4 hours at 37C. To prevent new FLAI complexes being shuttled to the cell surface, brefeldin-A (BioLegend) was applied at 5 µg/ml for 4 hours prior to transfer to 37C and antibody labeling of FLAI. Three separate cold incubation experiments were performed with triplicate samples in each experiment, and data were compared by repeated measures one-way ANOVA, followed by Tukey's multiple comparisons test. Significance was set to P=0.05.

We have previously described a GFP-fused canine TAP2 CDS-containing expression construct (GFP-TAP2 vector; Chapter 2, Gojanovich et al 2013), which we used here to transfect into TALEN-mediated TAP2 knockout feline cell clones. Parental GFP plasmids not containing the TAP2 CDS were also transfected into KO clones and these cells were used as controls for FLAI expression during flow cytometry data analysis. Three days post plasmid transfection, cells were checked for FLAI expression. While GFP could not be monitored in KO clones due to retention of the previously transfected pTAP2 reporter plasmid, GFP expression in parental CRFK cells transfected with the GFP-TAP2 plasmid served as transfection efficiency controls. Three separate transfection experiments were performed and data were analyzed for statistical significance by *t* test.

Peptide isolation and pulsing

Cell surface proteins were acid-stripped using a protocol as described previously (Storkus et al., 1993). Briefly, adherent cells were incubated with 0.05% trypsin in HBSS (Caisson) for 10 minutes at 37C, washed in PBS two times, and then resuspended in 4 ml of pH3.3 citrate-phosphate buffer containing 1% BSA. Cells were gently mixed for 3 minutes on ice and centrifuged to remove the buffer. Peptide-containing buffer was stored at -80C until purification. Buffer was quick thawed and applied to a 4 ml capacity Amicon 3K centrifugal filter (Millipore) and spun for 1 hr at 4000g. Flow through was then applied to Oasis HLB 1 cc extraction cartridges (Waters), washed according to manufacturer's protocol, and serially eluted using increasing methanol solutions. Purified peptides were then dried using a speed-vacuum centrifuge and resuspended in PBS prior to cell application. Peptides were acid-eluted from uninfected WT cell pellets containing 1.9×10^8 and 0.9×10^8 cells, and from FIV-infected WT cell pellets containing 1.1×10^8 and 0.6×10^8 cells, and resuspended in PBS prior to addition to overnight culture conditions. RMAS cells were pulsed with the D^b-binding Lymphocytic Choriomeningitis virus (LCMV) nucleoprotein$_{396\text{-}404}$ peptide fragment as an assay control, which was also used as an unrelated peptide control treatment for pulses on CRFK cell lines.

VIRAL INFECTIONS

Confirmation of viral infection of CRFK cells was performed using RT-PCR analysis by Jenny Holmes, and duration of infections was standardized for maximal virus protein expression. Peptides were acid-eluted from infected cells as described above.

Results

TALENs targeting the feline TAP2 locus produce cell clones expressing reduced surface FLAI

The FLAG-tagged FLAI-E-expressing CRFK clone, 1A3, and the parental (WT) CRFK line were used here as recipients of TAP2-targeting TALENs. Using the predicted feline TAP2 sequence (GenBank ID# 101089770) within the chromosome B2 contig., (GenBank ID# NC_018727.1) we created two TALEN pairs targeting sequences that flank the *BamHI* and *StyI* restriction consensus sites within exon 2 (Figure 1A). Prior to design of TALEN pairs, the CRFK TAP2 genomic sequences were confirmed to match the published sequence (data not shown). The ZiFiT software program was used to define the TALEN plasmids to be constructed using the REAL method, and TALEN pairs were named according to the restriction site that is found within the spacer region between the two nucleotide-recognizing TALEN arms, i.e. the Bam TALEN pairs interact with nucleotides adjacent the *BamHI* consensus site, while the Sty TALENs flank the *StyI* consensus sequence. Initial comparisons of cells transfected with the Sty and Bam TALEN pairs showed higher proportions of FLAI^{low} cells and higher percentages of TALEN-modified PCR products in loss of restriction site assays in cells receiving the Bam TALEN pair (data not shown). The Bam TALENs were therefore used for creation of TALEN-modified TAP2 cell lines.

As a reporter of TALEN activity, we modified a single-strand annealing (SSA) GFP plasmid protocol (Perez-Pinera et al., 2012) to incorporate the TALEN-targeted nucleotide sequences of TAP2 within the pSSA plasmid, which we renamed pTAP2 (Figure 1B). When co-transfected with TALEN pair plasmids, the coding sequence-disrupted GFP reporter plasmids (pSSA and pTAP2) may be repaired by cell-intrinsic mechanisms to produce functional GFP coding sequences if TALEN-mediated nuclease activity cleaves the target site found within the plasmid. Alternatively, random repair and conversion of the reporter plasmids may also occur (Figure 1C, left panels). WT and 1A3 cells co-transfected with the control pSSA reporter plus a single TALEN plasmid (pSSA-recipients) showed lower mean fluorescence intensities for GFP expression than cells receiving the pTAP2 plasmid plus both TALEN arms (pTAP2-recipients), though the change was modest (data not shown). However, pTAP2-recipients showed a 5-fold higher proportion of GFP^{+} $FLAI^{low}$ cells (Figure 1C, bottom right quadrants of dot plots), which were cloned following fluorescent-activated cell sorting into 96-well plates.

Cloned GFP^{+} $FLAI^{low}$ pTAP2-recipients were screened (n=45) for FLAI expression and compared to GFP^{+} pSSA-recipient clones (n=11), which were found to express FLAI at similar levels to the parental lines and no clones were found to display a lack of FLAI expression (data not shown). A clone derived from the WT pSSA-recipient group, WT SSA, was used for all downstream comparisons to adjust for any possible mutations occurring during the transfection, sorting, and expansion protocols that might affect TAP gene function. Cloned pTAP2-recipients that were determined to be low for FLAI expression and high for GFP expression (20% of clones) were expanded and further characterized. Selection of clones with high GFP expression was used as an indicator for successful transfection, increasing the chances of low FLAI expression being the result of TALEN activity and not a result of random mutations accumulated during cell culture.

We selected one clone from each CRFK lineage and characterized FLAI expression compared to its parental line, Figure 1D. The WT CRFK-derived PoBoy1 clone expresses ~7-fold less FLAI than its parental line, and similar expression levels of FLAI were found on the 1A3-derived PoBoy2 clone. Interestingly, the 3F10 Ab used to label surface FLAI molecules was able to detect presence of surface protein on sorted clones as compared to control samples labeled with secondary Ab only, possibly indicating 3F10 Ab interactions with TAP-independent MHCI complexes. Thus, sorting of pTAP2-recipients for simultaneously increased GFP and reduced FLAI expression results in cell clones that maintain this phenotype.

TAP2 TALENs induced genomic modifications in 1A3- and WT-derived cell lines

To corroborate that lack of FLAI protein expression was a result of TALEN-mediated modifications, we employed a loss of restriction site assay, and concomitantly sequenced the genomic TAP2 loci within cell clones. A schematic depicting the design of primers for the amplification of the feline TAP2 locus is shown in Figure 2A. PCR amplification of gDNA from control samples (lane 2; Figure 2B) results in a band cleavable into two fragments by the high-fidelity *BamHI* enzyme (lane 3). However, when cellular DNA repair mechanisms have introduced insertions/deletions during correction of double-strand breaks induced by TALEN activity, then the *BamHI* restriction enzyme site may be lost, resulting in products that cannot be cleaved (lanes 5 and 7; Figure 2B). Thus, PoBoy1 and PoBoy2 clones possess TAP2 alleles that have been modified and no longer contain the *BamHI* recognition sequence.

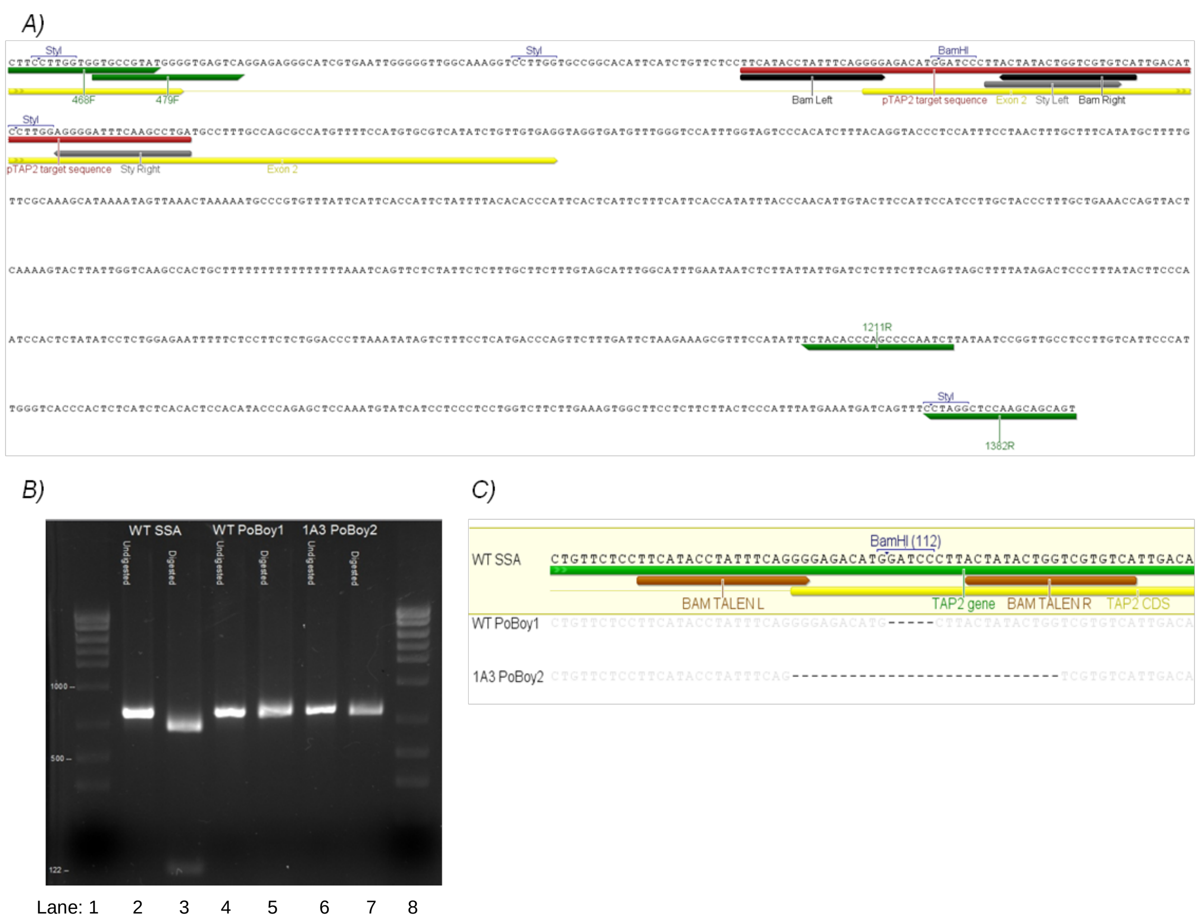

Figure 2. Cell clones of GFP+ MHCI- TALEN transfectants have modified genomic TAP2 sequences. *A)* The predicted DNA sequence of feline TAP2 (GenBank ID: 101089770) was used to design primers and TALEN target sites; the sequence was confirmed in the CRFK cell line. *B)* PCR amplification of the TAP2 locus from gDNA of MHCI^{low} clones returns products that cannot be digested by the *BamHI* restriction enzyme. WT amplimers are cleaved to produce a 122 base pair fragment if restriction site is intact. Lanes 2, 4, 6 are undigested PCR products, while lanes 3, 5, and 7 were exposed to digestion by the *BamHI*-HF enzyme for 2 hrs. *C)* Sequencing of 11 pGEM clones for each of the PCR products yields single modifications found at both alleles within each MHC^{low} clone, while the WT SSA clone returned the expected sequences.

To further characterize the modified TAP2 alleles within TALEN-recipients, PCR products from gDNA of each cell line were purified, TA-cloned, and sequenced. Data from ≥10 pGEM clones were identical within each cell line and are shown in Figure 2C; the PoBoy1 clone contains a 5bp deletion, while a 28bp deletion occurred in the PoBoy2 clone TAP2 locus. Both clones were found to possess a single modification shared at each chromosome, as determined by the number of pGEM clones screened. To reduce the possibility that TALEN-mediated modifications may have resulted in novel TAP2 alleles no longer able to be amplified by designed primer sets, we shifted the annealing location of the 3` primer 150bp downstream, as seen in Figure 2A. Sequencing efforts returned no other sequences, corroborating that both alleles within each clone indeed possess the same modification (data not shown). Analyses of translations from the modified TAP2 genes of each cell clone predicted the creation of novel stop codons within exon 2, and thus truncated products. The above data corroborate that the PoBoy1 and PoBoy2 cell lines display reduced surface FLAI expression due to KO of the TAP2 gene as a result of modifications induced by TALENs in CRFK cells.

TAP2 gene complementation restores surface FLAI expression on PoBoy cells

To confirm that the reduction in surface FLAI protein was directly due to KO of the TAP2 gene, we performed experiments that transfected a TAP2 ortholog into the PoBoy clones and monitored for restoration of surface FLAI expression. Previously, we described the sequence and functionality of a canine TAP2 gene fused to the C-terminus of a GFP expression vector (Gojanovich et al., 2013), which was used here to transfect the feline PoBoy clones. Data in Figure 3 are representative histogram overlays from three separate transfection experiments, and show that the Bam TALEN-transfected clones restore expression of surface FLAI following ortholog complementation (red histograms; panels A and B). Transfection of the canine GFP-TAP2 construct into the PoBoy1 line resulted in 18% of the population regaining surface FLAI expression, while cells receiving the GFP construct lacking the TAP2 coding sequence were unable to rescue surface FLAI (Figure 3A). Across three experiments, the increase in FLAI expression on GFP-TAP2-recipient cells was significantly higher than on the GFP only-recipients (P=0.001). Similar restoration of FLAI expression was seen for the PoBoy2 cell line (Figure 3B), although increases in proportion of cells expressing FLAI protein did not reach significance (P=0.0647). Due to the retention of the GFP reporter plasmids used in initial TALEN co-transfections, the detection of GFP fused to TAP2 proteins could not be directly measured. To validate that the modest percentage of FLAI restoration in TAP2-KO clones was due to low transfection efficiency of the GFP-TAP2 vector, we transfected WT CRFK cells with this construct and monitored for GFP expression. As seen in Figure 3C, the proportion of WT cells that expressed GFP following GFP-TAP2 transfection was similar to the percentages seen for FLAI restoration on TAP2-KO clones. Of note, our previous results with transfections of the TAP2-KO murine RMAS cell line also show poor transfection efficiencies, requiring gating on GFP positive cells for discrimination of MHCI restoration (Gojanovich et al., 2013).

Collectively, the above data confirm that TALEN-mediated KO of the TAP2 gene in CRFK clones is responsible for reduced expression of FLAI protein.

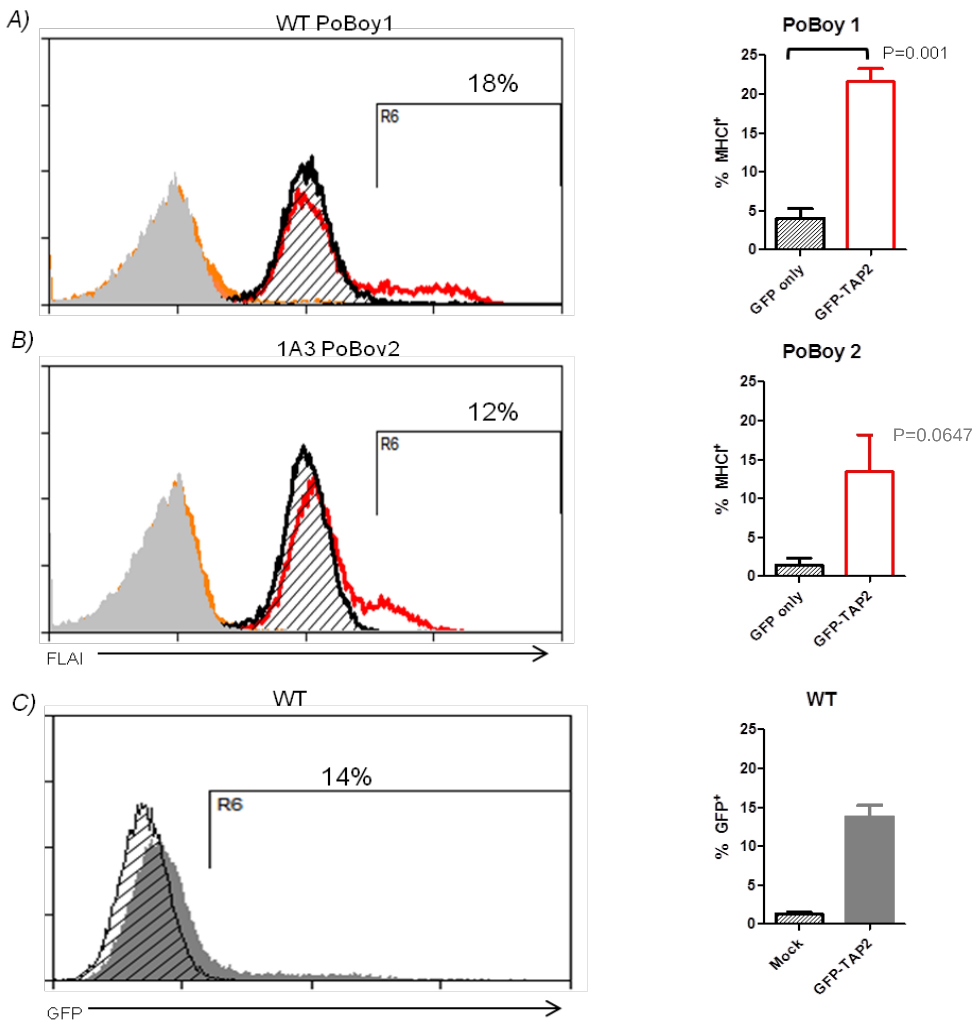

Figure 3. Exogenous TAP2 transfection into TAP2 KO clones restores surface FLAI expression. *A)* Left panel depicts an overlay of WT-derived PoBoy1 flow cytometry histograms from samples transfected with empty GFP vector or canine GFP-TAP2. Shaded histograms represent samples receiving secondary antibody only, while striped represent GFP only transfectants. The empty red histograms depict samples receiving canine GFP-TAP2 plasmids and show a higher proportion of cells positive for FLAI expression. Results from three separate transfections confirm MHCI expression by TAP2-recipients to be significantly different (P<0.001) from GFP-recipients, right panel. *B)* Similar flow cytometry histogram overlay for 1A3-derived PoBoy2 clone transfections, left panel. One representative shown of 3 separate transfections. Data from three experiments trended towards significance, but did not reach it (P=0.0647). *C)* Low FLAI restoration efficiency is a function of vector expression following transfection. GFP expression overlays for mock- (stripes) and GFP-TAP2-transfected (filled) WT cells. One representative flow cytometric overlay from 3 replicate transfections shown.

<u>POBOY2 CELLS RETAIN THE FLAI-E ALLELE POST TALEN-MEDIATED MODIFICATION</u>

In order to be useful to future studies of the FLAI allele-specific restriction of CD8+ T cells, the PoBoy2 clone would need to possess the FLAG-tagged FLAI-E*02001 allele. To confirm transgene expression in PoBoy2 cells, FLAG protein was monitored and compared to the parental 1A3 cell line, Figure 4A. Control cells receiving only secondary Ab were used to determine background fluorescence (striped histograms). FLAG protein expression was found in both the parental 1A3 (Figure 4A, top panel) and the PoBoy2 cell lines (figure 4A, bottom panel), but not in untransfected WT cells (identical to secondary Ab only; data not shown).

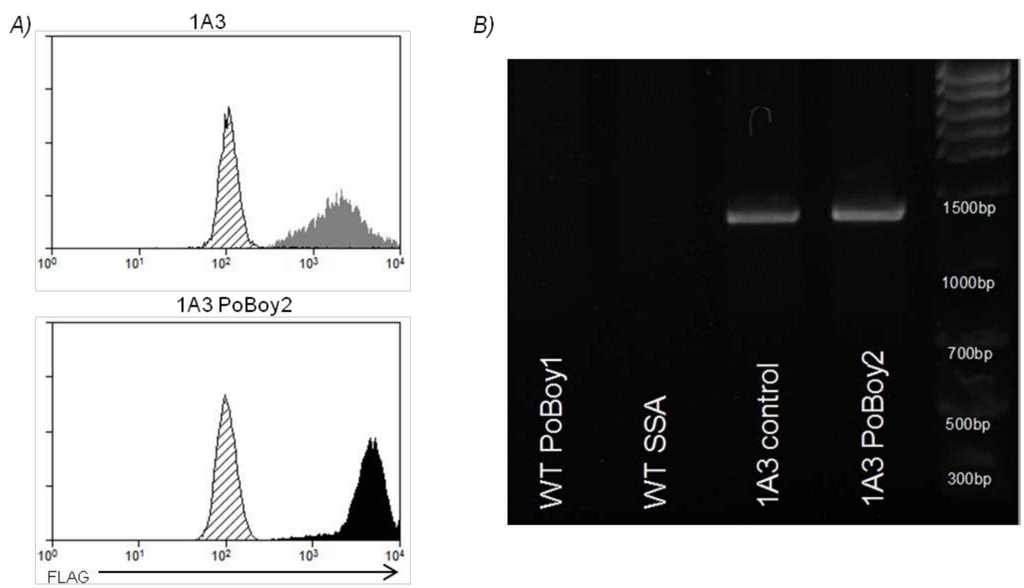

Figure 4. The1A3-derived PoBoy2 clone retains the FLAG-tagged FLAI allele. *A)* Intracellular staining for FLAG protein shows expression in the 1A3 PoBoy2 clone. Shown as a positive control for FLAG is the parental cell line (top, 1A3) from which the MHC^{low} clone (bottom panel) was derived. Histogram overlays of the secondary antibody alone samples (striped) compared to M2 anti-FLAG Ab-labeled samples (filled) . *B)* PCR amplification using FLAI allele- and FLAG-specific primers produces bands from gDNA of the 1A3 and 1A3 PoBoy2 clone, but not from WT cells.

To further confirm FLAG-tagged FLAI-E allele presence, DNA from parental and TALEN-modified clones was extracted and amplified using primers that anneal to the 5` portion of the E allele sequence and to the FLAG-specific nucleotide sequence. Figure 4B shows PCR amplification products only in the parental 1A3 and 1A3-derived PoBoy2 cell lines, thus confirming the presence of the FLAG-tagged FLAI-E allele coding sequence. The above data confirm that the PoBoy2 cell line possesses and expresses the FLAG-tagged FLAI-E construct.

Cold incubation of PoBoy clones transiently increases FLAI expression

As a characteristic of TAP deficiency, “empty” MHCI complexes, which lack peptides completely or present weakly binding peptides independent of TAP function, are transported to the cell surface where they quickly dissociate and are recycled by the cell at physiologic conditions (Silva et al., 1999). As a result of this characteristic, peptide-binding assays that utilize the TAP2-KO RMAS cell line usually include incubation at reduced temperatures in order to increase the amount of empty MHCI molecules at the surface, which quickly dissociate if peptides added to the culture medium do not stabilize the interaction with MHCI complexes at 37C (Ross et al., 2012). To determine whether PoBoy clones possess the characteristic of shuttling empty FLAI molecules to the surface, cells were incubated at 27C and monitored for surface FLAI expression. As seen in Figure 5, both the PoBoy1 (panel A) and PoBoy2 (panel B) TAP2-KO cell lines increased FLAI protein at the cell surface in cold conditions (filled histograms). The addition of a brefeldin-A solution and a four hour incubation at 37C following the end of overnight cold incubations (empty histograms) resulted in return of surface FLAI expression to levels displayed at constant 37C incubation (hashed histograms). Cold incubation significantly increased FLAI expression compared to both constant 37C expression and following brefeldin A exposure ($P<0.0001$) for both cell lines. These data indicate that FLAI complexes on the CRFK line are thermolabile, a useful characteristic in peptide-MHCI stabilization assays.

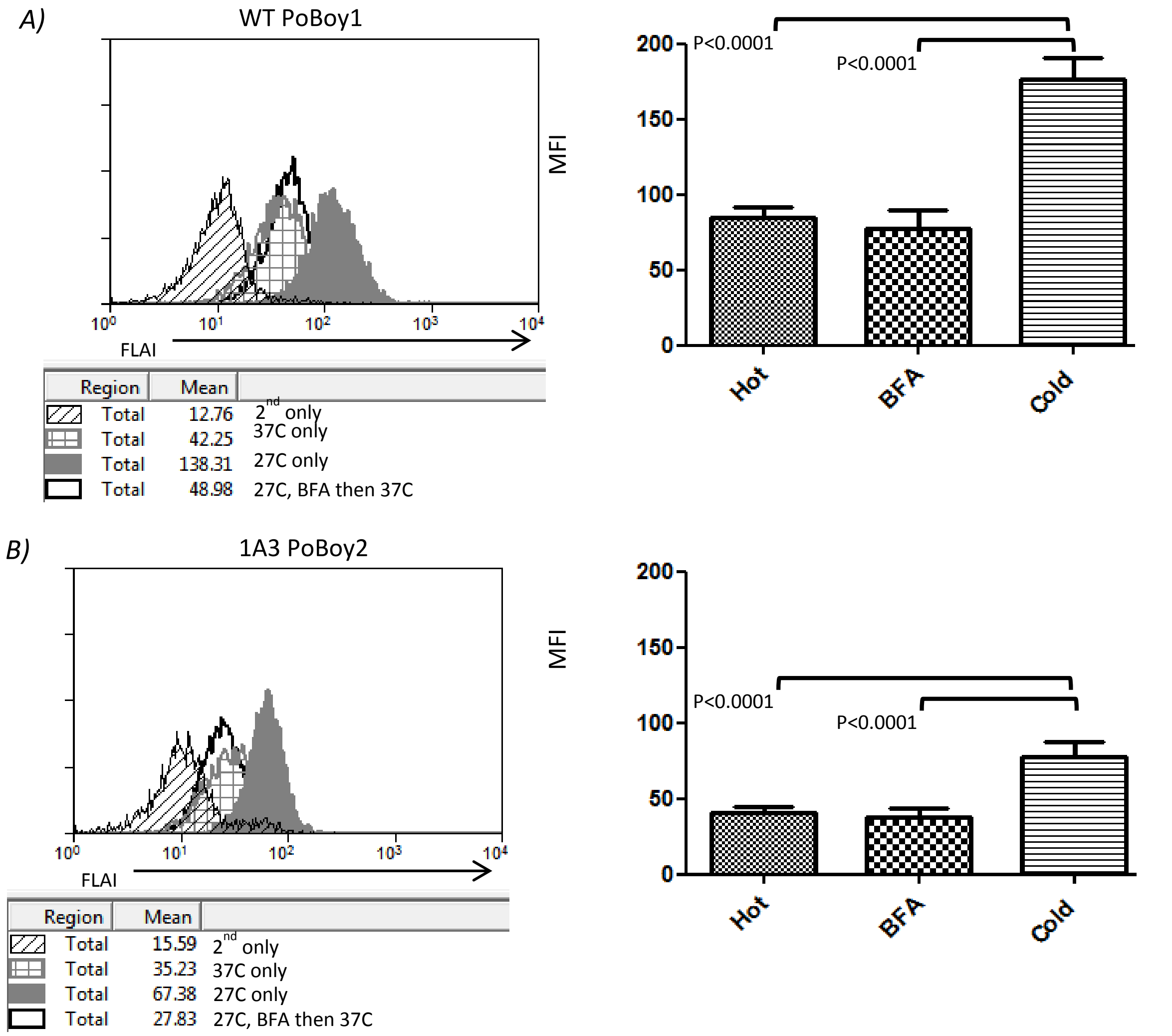

Figure 5. Cold incubation increases surface FLAI expression on TAP2 KO clones. Overnight incubation at 27C results in higher surface FLAI expression, while transfer back into 37C following overnight 27C and addition of brefeldin A (BFA) for 4 hours results in similar expression levels as seen in samples incubated at 37C overnight. *A)* Left panel depicts the overlay of WT PoBoy1 histograms from samples treated with secondary antibody only (striped), incubated at 37C only (hashed), 27C overnight plus BFA and transfer to 37C (empty), or 27C only (filled) prior to full antibody staining. Right panel indicates that across experiments, the incubation of PoBoy1 cells in the cold results in significantly higher FLAI expression (P<0.001). *B)* Similar histogram overlay for 1A3 PoBoy2 clone. One representative sample shown for 3 experiments performed in triplicates. Right panel highlights significance values for comparisons across experiments.

PEPTIDES STRIPPED FROM THE SURFACE OF PARENTAL WT CELLS FAIL TO STABILIZE FLAI COMPLEXES ON POBOY CLONES

Addition of citrate-phosphate buffers at pH3.3 has been used previously to elute peptides from the clefts of surface MHCI complexes (Storkus et al., 1993). To confirm the ability of acid to strip FLAI complexes from parental cells in our hands, we performed the acid elution protocol, then labeled cells for FLAI expression. The flow cytometry data in Figure 6A show that WT cells exposed to citrate-phosphate buffer have lower FLAI expression compared to untreated samples collected prior to acid treatment.

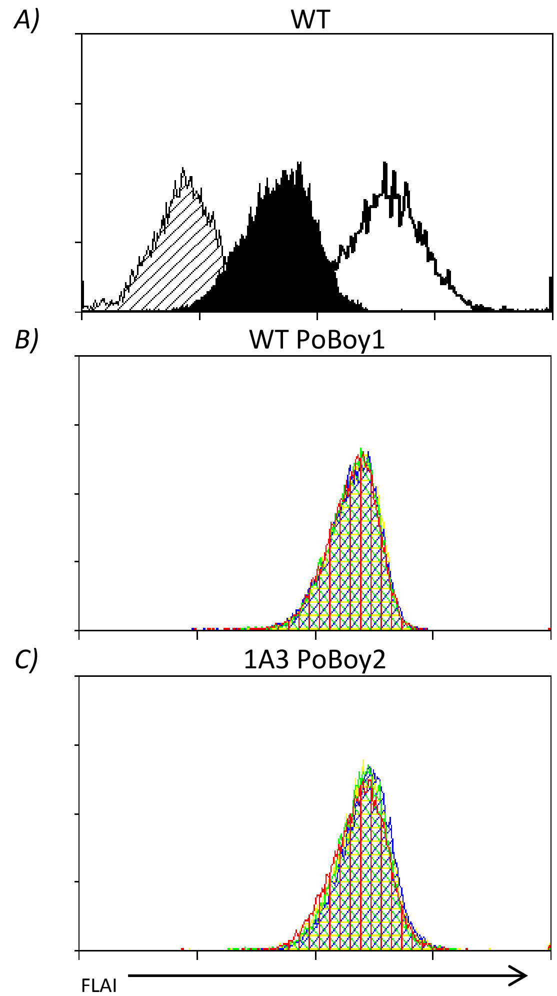

Figure 6. Peptides eluted from parental cell lines fail to stabilize surface FLAI complexes on PoBoy clones**.** *A)* Resuspension of WT cells in the mildly acidic citrate-phosphate buffer reduces surface FLAI expression. Histogram overlays depict cell staining with secondary only (striped) or with 3F10 antibodies prior to acid treatment (empty) and following acid reconstitution (filled). *B)* Pulsing of the WT-PoBoy1 clone with no peptide (red histogram), unrelated peptide ($NP_{396\text{-}404}$; green), peptides from FIV-infected parental cells (blue), and peptides from WT parental cells (yellow) displays no FLAI stabilization. *C)* Similar results are found for 1A3-PoBoy2 cells during similar peptide conditions as described in panel B. Three separate peptide strips were performed from parental cells and increasing cell equivalencies were pulsed onto cell lines in triplicates. Shown are overlays from one representative experiment.

Next, we determined whether or not FLAI complexes could be stabilized on the surface of PoBoy clones following exposure to peptides eluted from parental cells. When we pulsed the PoBoy cells with peptides stripped from varying cell numbers of either uninfected or FIV-infected WT cells, we were unable to detect restoration of FLAI expression. However, simultaneous pulse experiments of RMAS cells using a known D^b-binding control peptide did yield MHCI stabilization (data not shown), indicating an issue with our purification of peptides from CRFK cells.

Discussion and Future Directions

The results of this study is the first to show that the proposed feline TAP2 locus (Gene ID# 101089770) is functional and necessary for optimal expression of classical class I FLA complexes on the surface of CRFK cells, as has been described for TAP2 gene function in other species. We show the ability of TALENs to modify genomic sequences and disrupt gene function for the first time in a feline cell line. TALEN-modifications to the TAP2 genes resulted in two feline cell lines with reduced FLAI expression, which will assist in confirming the peptide-binding motifs of FLAI complexes, further discussed in Chapter 7.

As the objective of this study was for the creation of a tool kit and not to determine the functional kinetics of TALENs created using the Joung architecture, as has been described elsewhere (Cade et al., 2012; Reyon et al., 2012), we did not extensively analyze the levels of TALEN efficiency in this study, but such issues will be addressed when using TALENs in the next chapter. Yet, we did produce cell lines with modifications directly at the site of TALEN targeting that display the expected phenotypes, such as higher FLAI expression following cold incubation. Enrichment of cells with disrupted TAP2 loci was achieved via GFP reporter constructs, modified from a previous study, and FACS selection, and further enrichment strategies are discussed in Chapter 6.

As shown in Figure 3, transfection of TAP2-KO CRFK cell lines with an exogenous, canine TAP2 expression construct resulted in modest, yet significant for the PoBoy1 line, restoration of FLAI expression. We showed this modest restoration to be a result of poor transfection/expression efficiency characteristic of the GFP-TAP2 vector, as introduction of this construct into WT parental cells yielded similar GFP expression efficiencies as those seen for FLAI restoration in PoBoy clones. Another possible explanation for this result is the inability of canine TAP2 protein to properly interact with the peptide loading complex (PLC) found within the feline cell ER, and this hypothesis is bolstered by our previous work in which this construct only minimally restored MHCI expression on murine cells, Chapter 2. Results of previous studies have shown that the tapasin protein, a part of the PLC that stabilizes empty MHCI complexes (Grandea and Van Kaer, 2001), interacts with TAP2 transmembrane domains in order to increase the efficiency with which peptides are loaded into receptive-state MHCI molecules (Koch et al., 2004; Procko et al., 2005). Thus, this tapasin-TAP2 interaction may not be highly conserved for trans-species stabilization of MHCI. However, we cannot currently compare the tapasin-binding domains of the canine and feline TAP2 proteins due to a lack of information of regarding the residues in these species. Yet, now that the TAP2 locus is confirmed in the feline species, future experiments can be designed to elucidate such functional domains. Furthermore, future studies will be able to determine the promoter elements, the transcription initiation sites, and whether feline TAP genes contain polymorphisms across cat breeds, as has been recently shown for the canine TAP genes (Chapter 2, Gojanovich et al., 2013).

While we do not show here the successful stabilization of FLAI complexes on TAP2-KO cell lines following peptide pulses, we expect this outcome to be achieved shortly. Possible reasons for the failure of purifying FLAI-binding peptides eluted from the parental cell lines include the inability of peptides to be removed from peptide-binding clefts of FLAI due to inadequate acid strength of the elution buffer, the inability to retain eluted peptides on the HLB column due to unexpected biochemical compositions, the inability to elute peptides from the HLB column due to chemical composition of our selected eluent, and improper reconstitution of peptides in solution prior to pulse experiments. It has been shown previously that the mild acid elution of peptides from MHCI clefts of different species can provide peptides suitable for MHCI stabilization assays (Hegde et al., 1999; Nakatsuka et al., 1999; Storkus et al., 1993), and I have verified this procedure using murine EL4 cells (Chapter 3, Figure 3), thus we do not believe this protocol to be a primary issue. Furthermore, we show in Figure 6A, that FLAI complexes are removed from the cellular surface following acid treatment. Therefore, we speculate that the removal of peptide from the stripped FLAI cleft and the purification of peptides from the columns are the likely points of concern. To address this issue, our lab has attempted two different approaches: the acid elution of ~1 x 10^{10} cell equivalents followed by peptide purification steps and double mass spectroscopy (M/S) analysis performed by the Duke proteomics core facility; and FLAG-affinity purification of the E*02001 allele from cell lysates, followed by elution of peptides directly from the affinity column using stronger acids, as in other studies (Haeri et al., 2005). Recent data indicate that our HLB column purification protocol was ineffective at isolating bulk FLAI-bound peptides from the acid solution, as the Duke proteomics facility obtained peptide sequences which will be pulsed onto the PoBoy clones. Furthermore, these recent data have allowed us to create a generic peptide-binding motif for bulk FLAI complexes expressed on CRFK cells that will be used to produce recombinant peptides for pulsing assays.

When allele-specific peptide motif data are available through the above FLAG-affinity purification assay, we will perform peptide pulsing experiments using the 1A3 PoBoy2 cell clone. If high concentrations of recombinant peptides, created based upon the M/S data, do not stabilize the FLAI-E*02001 complex on this cell clone, further peptide purifications may be performed utilizing much greater quantities of cells, which are now in the process of expansion. If it is determined that the described TAP2-KO cell lines created by TALEN-modifications do not stabilize FLAI following repeated pulses, then other clones, cryogenically stored, may be tested for function in the assay. If all of these clones fail in the peptide-binding assay, then we will question our conclusion that the predicted feline TAP2 sequence is correct would be untrue. However, gene complementation strategies, Figure 3, strongly argue against this supposition. Yet, in this worst case scenario, salvage of experiments aimed at confirming FLAI-E motifs would be possible by transfecting this (or other) FLAI-allele constructs into RMAS cells as has been done previously (Ross et al., 2012).

Thus, results in this chapter show successful modification of the locus predicted to be the feline TAP2 gene, creation of clonal lines that display reduced FLAI expression at physiological temperatures but which is increased in the cold and following gene complementation, and shows the successful removal of FLAI on the surface of parental lines by way of mild acid elution. Together, these results demonstrate progress towards the goal of creating a feline cell-based FLAI-stabilization assay, which will eventually allow confirmation of peptide-binding to specific FLAI complexes.

References

Bucci, J.G., R.V. English, H.L. Jordan, T.A. Childers, M.B. Tompkins, and W.A.F. Tompkins. 1998. Mucosally Transmitted Feline Immunodeficiency Virus Induces a CD8+ Antiviral Response that Correlates with Reduction of Cell-Associated Virus. *J. Infect. Dis.* 177:18–25. doi:10.1086/513822.

Cade, L., D. Reyon, W.Y. Hwang, S.Q. Tsai, S. Patel, C. Khayter, J.K. Joung, J.D. Sander, R.T. Peterson, and J.-R.J. Yeh. 2012. Highly efficient generation of heritable zebrafish gene mutations using homo- and heterodimeric TALENs. *Nucleic Acids Res.* 40:8001–8010. doi:10.1093/nar/gks518.

Cornelissen, E., H.L. Dewerchin, E. Van Hamme, and H.J. Nauwynck. 2007. Absence of surface expression of feline infectious peritonitis virus (FIPV) antigens on infected cells isolated from cats with FIP. *Vet. Microbiol.* 121:131–137. doi:10.1016/j.vetmic.2006.11.026.

Gojanovich, G.S., P. Ross, S.G. Holmer, J.C. Holmes, and P.R. Hess. 2013. Characterization and allelic variation of the transporters associated with antigen processing (TAP) genes in the domestic dog (Canis lupus familiaris). *Dev. Comp. Immunol.* 41:578–586. doi:10.1016/j.dci.2013.07.011.

Grandea, A.G., 3rd, and L. Van Kaer. 2001. Tapasin: an ER chaperone that controls MHC class I assembly with peptide. *Trends Immunol.* 22:194–199.

Haeri, M., L.R. Read, B.N. Wilkie, and S. Sharif. 2005. Identification of peptides associated with chicken major histocompatibility complex class II molecules of B21 and B19 haplotypes. *Immunogenetics*. 56:854–859. doi:10.1007/s00251-004-0760-4.

Hegde, N.R., M.S. Deshpande, D.L. Godson, L.A. Babiuk, and S. Srikumaran. 1999. Bovine Lymphocyte Antigen-A 11-Specific Peptide Motif as a Means to Identify Cytotoxic T-Lymphocyte Epitopes of Bovine Herpesvirus 1. *Viral Immunol.* 12:149–161. doi:10.1089/vim.1999.12.149.

Holmes, J.C., S.G. Holmer, P. Ross, A.S. Buntzman, J.A. Frelinger, and P.R. Hess. 2013. Polymorphisms and tissue expression of the feline leukocyte antigen class I loci FLAI-E, FLAI-H, and FLAI-K. *Immunogenetics*. 65:675–689. doi:10.1007/s00251-013-0711-z.

Koch, J., R. Guntrum, S. Heintke, C. Kyritsis, and R. Tampé. 2004. Functional Dissection of the Transmembrane Domains of the Transporter Associated with Antigen Processing (TAP). *J. Biol. Chem.* 279:10142–10147. doi:10.1074/jbc.M312816200.

Ljunggren, H.-G., N.J. Stam, C. Öhlén, J.J. Neefjes, P. Höglund, M.-T. Heemels, J. Bastin, T.N.M. Schumacher, A. Townsend, K. Kärre, and H.L. Ploegh. 1990. Empty MHC class I molecules come out in the cold. *Nature*. 346:476–480. doi:10.1038/346476a0.

Maguire, J.J., R.E. Kuc, and A.P. Davenport. 2012. Radioligand binding assays and their analysis. *Methods Mol. Biol. Clifton NJ*. 897:31–77. doi:10.1007/978-1-61779-909-9_3.

Morgan, C.S., J.M. Holton, B.D. Olafson, P.J. Bjorkman, and S.L. Mayo. 1997. Circular dichroism determination of class I MHC-peptide equilibrium dissociation constants. *Protein Sci. Publ. Protein Soc.* 6:1771–1773.

Nakatsuka, K., H. Sugiyama, Y. Nakagawa, and H. Takahashi. 1999. Purification of antigenic peptide from murine hepatoma cells recognized by Class-I major histocompatibility complex molecule-restricted cytotoxic T-lymphocytes induced with B7-1-gene-transfected hepatoma cells. *J. Hepatol.* 30:1119–1129. doi:10.1016/S0168-8278(99)80268-2.

Perez-Pinera, P., D.G. Ousterout, M.T. Brown, and C.A. Gersbach. 2012. Gene targeting to the ROSA26 locus directed by engineered zinc finger nucleases. *Nucleic Acids Res.* 40:3741–3752. doi:10.1093/nar/gkr1214.

Procko, E., G. Raghuraman, D.C. Wiley, M. Raghavan, and R. Gaudet. 2005. Identification of domain boundaries within the N-termini of TAP1 and TAP2 and their importance in tapasin binding and tapasin-mediated increase in peptide loading of MHC class I. *Immunol. Cell Biol.* 83:475–482. doi:10.1111/j.1440-1711.2005.01354.x.

Reyon, D., C. Khayter, M.R. Regan, J.K. Joung, and J.D. Sander. 2012. Engineering Designer Transcription Activator–Like Effector Nucleases (TALENs) by REAL or REAL-Fast Assembly. *In* Current Protocols in Molecular Biology. John Wiley & Sons, Inc.

Ross, P., J.C. Holmes, G.S. Gojanovich, and P.R. Hess. 2012. A cell-based MHC stabilization assay for the detection of peptide binding to the canine classical class I molecule, DLA-88. *Vet. Immunol. Immunopathol.* 150:206–212. doi:10.1016/j.vetimm.2012.08.012.

Sander, J.D., M.L. Maeder, D. Reyon, D.F. Voytas, J.K. Joung, and D. Dobbs. 2010. ZiFiT (Zinc Finger Targeter): an updated zinc finger engineering tool. *Nucleic Acids Res.* gkq319. doi:10.1093/nar/gkq319.

Sanou, M.P., S.R. Roff, A. Mennella, J.W. Sleasman, M.H. Rathore, J.K. Yamamoto, and J.A. Levy. 2013. Evolutionarily conserved epitopes on human immunodeficiency virus type 1 (HIV-1) and feline immunodeficiency virus reverse transcriptases detected by HIV-1-infected subjects. *J. Virol.* 87:10004–10015. doi:10.1128/JVI.00359-13.

Silva, A.D.D., A. Boesteanu, R. Song, N. Nagy, E. Harhaj, C.V. Harding, and S. Joyce. 1999. Thermolabile H-2Kb Molecules Expressed by Transporter Associated with Antigen Processing-Deficient RMA-S Cells Are Occupied by Low-Affinity Peptides. *J. Immunol.* 163:4413–4420.

Song, W., E.W. Collisson, P.M. Billingsley, and W.C. Brown. 1992. Induction of feline immunodeficiency virus-specific cytolytic T-cell responses from experimentally infected cats. *J. Virol.* 66:5409–5417.

Storkus, W.J., H.J.Z. III, R.D. Salter, and M.T. Lotze. 1993. Identification of T-cell epitopes: Rapid isolation of class I-presented peptides from viable cells by mild acid elution. *J. Immunother.* 14:94–103.

Vermeulen, B.L., S.E. Gleich, A. Dedeurwaerder, D.A. Olyslaegers, L.M. Desmarets, H.L. Dewerchin, and H.J. Nauwynck. 2012. In vitro assessment of the feline cell-mediated immune response against feline panleukopeniavirus, calicivirus and felid herpesvirus 1 using 5-bromo-2’-deoxyuridine labeling. *Vet. Immunol. Immunopathol.* 146:177–184. doi:10.1016/j.vetimm.2012.03.004.

CHAPTER 5: Type 1 diabetes mellitus: adaptive autoimmune mechanisms, pMHC multimer usage and advances in disease understanding, the 8.3-NOD mouse model, and islet cell transplantation

Type 1 diabetes (T1D) review, MHC multimer usage and advances in disease understanding; adapted from review articles (Gojanovich and Hess, 2012; Gojanovich et al., 2012)

INTRODUCTION

Due to antigen-specific assaults on the insulin producing beta (β) cells of the pancreas by diabetogenic T cells, insulin synthesis and secretion is lost, resulting in dysregulation of blood glucose homeostasis and aberrant lipid and protein metabolism in type 1 diabetic (T1D) patients. T1D is one of the most prevalent chronic autoimmune diseases in the United States and affects ~36 million individuals worldwide (National diabetes fact sheet: national estimates and general information on diabetes and prediabetes in the United States., 2011; Juvenile Diabetes Research Foundation). The incidence of T1D is predicted to increase worldwide by 3% annually (World Health Organization). With administration of exogenous sources of insulin via daily injections, continual pump therapy, or islet replacement transplants, diabetics can currently enjoy near normal life spans and reduced incidence of heart disease, kidney failure, blindness, and neuropathy (DeWitt and Hirsch, 2003). However, none of the currently available therapies can adequately quell the long-term risks of hypoglycemia or microvascular damage, or reduce the financial expense of treatment (National diabetes fact sheet: national estimates and general information on diabetes and prediabetes in the United States., 2011; DeWitt and Hirsch, 2003). In addition, the total direct and indirect costs associated with diabetes in 2007 were $174 billion dollars in the United States (National diabetes fact sheet: national estimates and general information on diabetes and prediabetes in the United States., 2011). Therefore, new therapies are needed to reduce the burden of this chronic disease on both the individual and society.

The aforementioned T1D therapies are directed only at the consequences of the disease rather than the causative agent(s). While the ultimate cause of T1D is not currently defined and is likely multifactorial (Polychronakos and Li, 2011), T cells specific for islet antigens are the proximate cause of β cell destruction. Diabetogenic T cells that have been inappropriately activated and allowed to escape central and peripheral tolerance mechanisms [possibly due to assistance from aberrant innate cells (Lehuen et al., 2010)] have been implicated in β cell damage in both the nonobese diabetic (NOD) mouse and the human form of disease. In peripheral lymphoid organs and in circulation, CD4+ T cells and CD8+ T cells interact with peptide-major histocompatibility complex class II or class I (pMHCII or pMHCI) molecules, respectively. MHCII molecules are externally displayed on the cell surface of professional antigen presenting cells (APCs) and contain peptide fragments primarily derived from extracellular proteins, while classical MHCI molecules are found on the surface of all nucleated cells and present peptides of cytosolic origin. In T1D, diabetogenic CD4+ T cells (TH) are responsible for providing the cytokine microenvironment in which islet-specific CD8+ T cells (CTL) destroy β cells. Furthermore, islet-specific TH activity may also be cytotoxic to islets at later disease stages, and CTL may not need prior costimulation before killing β cells (Katz et al., 1993; Di Lorenzo et al., 1998; Zekzer et al., 1998; Wang et al., 2000; Amrani et al., 2000b). Thus, both TH and CTL are contributors to diabetes pathogenesis and are suitable targets for strategies aimed at preventing T1D.

T CELLS IN TYPE 1 DIABETES MELLITUS

While multiple immune cell populations are involved in the development of T1D (Lehuen et al., 2010), T cells are indispensable for progression to overt diabetes (Katz et al., 1993; Sibley et al., 1985a; Yagi et al., 1992; Itoh et al., 1993). Other cell types infiltrating the islets—B cells, dendritic cells, and macrophages—serve as antigen-presenting cells (APCs), providing a combination of stimuli capable of activating autoreactive CD4+ and CD8+ T cells: pMHC (so-called signal one), co-stimulation (signal two), and an inflammatory cytokine microenvironment (signal three). Initially, this set of signals is delivered in the pancreatic lymph nodes, “priming” the naïve T cell for action; later, these stimuli are also provided in the islets (Figure 1), amplifying the responses of previously activated T cells. Signals inhibitory to T-cell activation may be given at the same time by certain APCs or T-regulatory cells, but in T1D-susceptible individuals, these “braking forces” usually are overwhelmed by positive stimuli, resulting in clinical autoimmunity.

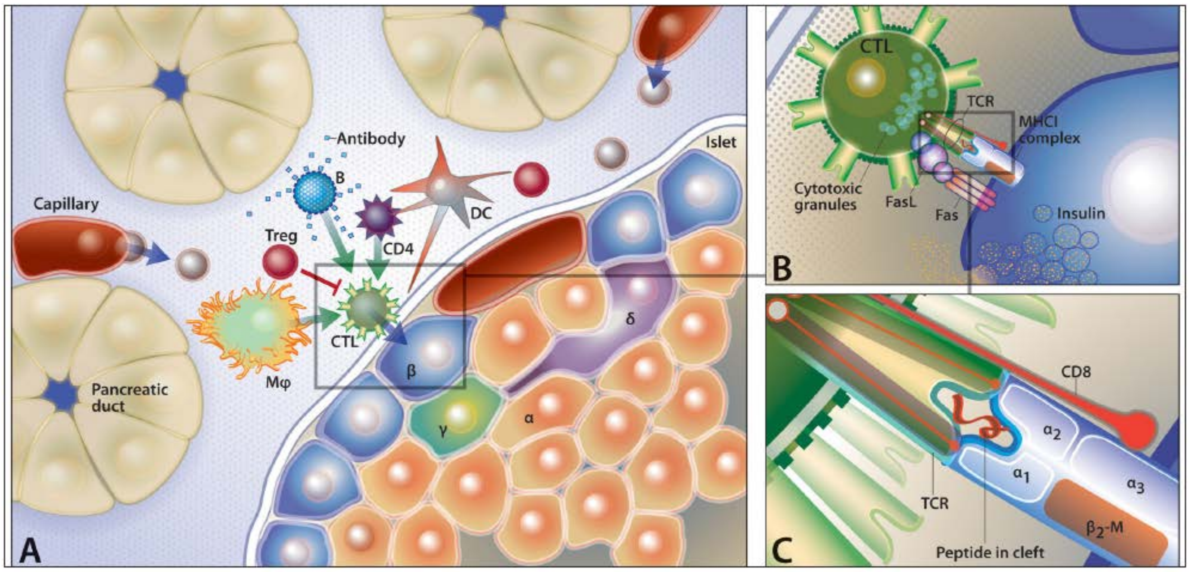

Figure 1. Immune cell interactions in T1DM. The pancreatic islets contain insulin-producing β cells, which are the targets of autoreactive T cells. Antigen-presenting cells (macrophages, dendritic cells, and β cells) stimulate diabetogenic CD-4+ and CD-8+ T cells, which infiltrate the islets and generate an inflammatory microenvironment in which β cells are destroyed. The inhibitory signals (red bar) given by T-regulatory cells to CTLs typically are overwhelmed by positive stimuli (green arrows). (**Zoom 1**) T-cell receptors of diabetogenic CTL bind to pMHC-I complexes on the surface of β cells, creating an immunological synapse, which triggers the release of cytotoxic granules and increased expression of Fas ligand, inducing apoptosis of target cells. (**Zoom 2**) The antigen that drives the proliferation and cytotoxic function of CTL through TCR signaling is a combination of a particular peptide and proper MHC-1 molecule, and it is this specific interaction that forms the basis of class I multimer technology. In analogous fashion, the TCR of CD-4+ T cells binds to surface MHC-II molecules, which are α and β chain heterodimers that present slightly longer peptides, 12–20 amino acids in length (not pictured). In both instances, the CD-4 and CD-8 co-receptors also bind to their respective MHC molecules, supplying added stability to these trimolecular interactions. Mϕ, macrophages; DC, dendritic cells; Treg, T-regulatory cells.

Activated CD4+ T cells characteristically function as T-helper (TH) cells, secreting specific cytokines that direct the immune response. In T1D, islet-reactive TH cells—primarily those that produce IFNγ and IL-2—infiltrate the endocrine pancreas, where they interact with APCs via MHCII. This interaction results in cytokine production that supports CD8+ T-cell proliferation and reinforces TH pro-inflammatory activity via a positive feedback loop (IFNγ induces IL-12 secretion from APCs, which, in turn, promotes IFNγ production by TH cells). Therefore, TH cells mainly help to stimulate and perpetuate autoreactive T-cell responses in the islets during diabetogenesis, although, in later stages of the disease, CD4+ T cells have also been shown to exert direct cytotoxic activity (Di Lorenzo et al., 1998).

Primed CD8+ T cells (CTLs) enter and are retained within insulitic lesions in significant numbers only if they are helped by CD4+ T cells and recognize islet antigens (Yagi et al., 1992; Wang et al., 2010). After infiltration, the TCR of the autoreactive CTL binds to its corresponding pMHCI on β cells, creating an “immunologic synapse” (Figures 1B and 1C). The formation and stabilization of multiple immunological synapses triggers the CTL to release IFNγ, perforin, and granzyme B, ultimately killing the β cell. Some diabetogenic CTL also express Fas ligand, which turns on the Fas-mediated apoptosis pathway within β cells after the synapse has formed (Moriwaki et al., 1999). Through these mechanisms, islet-specific CTLs mediate destruction of native β cells (Wong et al., 1996) as well as transplanted islet tissues (Sibley et al., 1985; Prange et al., 2001).

It seems clear that both subsets of T cells are involved in the pathogenesis of T1D in largely nonoverlapping roles: TH cells help prime and potentiate CTLs, which kill β cells. Which one of these populations would be best to disable in order to halt or reverse diabetes is likely an empirical question, and it should not be surprising if the most effective treatment ultimately targets both helper and cytotoxic T cells.

MHC MULTIMER USAGE AND RELATED ADVANCES IN DISEASE UNDERSTANDING

The ability to modulate the behavior of T cells is therefore an approach for novel treatments in T1D and other T-cell-mediated diseases (e.g., multiple sclerosis, transplant rejection). Most T-cell-targeting strategies have utilized nonspecific or blanket therapies, such as Thymoglobulin or anti-CD3 monoclonal antibodies, that target all T cells. Therefore, these treatments may also prevent protective immunity by the adaptive immune system, resulting in susceptibility to new infections, viral reactivation, or increased risk of cancer (Herold et al., 2009; Keymeulen et al., 2009). Thus, researchers have pursued various means of exclusively modulating the autoreactive T cells with antigen, which can be delivered covalently linked to tolerizing cells, within viral vectors, or as whole proteins or soluble peptide fragments (Ludvigsson, 2009; Culina et al., 2011). Many studies have addressed the identity of cognate antigens for diabetogenic T cells in mouse and human T1D (Di Lorenzo et al., 2007), but the relative importance of each peptide is still unknown for human disease (Mallone et al., 2011). While the repertoire of diabetogenic T-cell epitopes has been investigated extensively, the molecular form of antigen (e.g., whole protein versus peptide fragments), the route of delivery, or modifications such as carrier proteins or adjuvant combinations still need to be more clearly defined in order to produce efficient therapeutic strategies (Culina et al., 2011; Waldron-Lynch and Herold, 2011).

One major obstacle to the use of soluble peptides to target antigen-specific T cells is the relatively short half-life of these molecules once administered. To remedy this, researchers have designed vehicles that mimic the natural setting in which a peptide is presented to T cells; that is, peptides are combined *in vitro* with purified or recombinant MHC molecules to create soluble, stable complexes (Altman et al., 1996; Wooldridge et al., 2009). These pMHC complexes are then able to bind to cognate TCR on antigen-specific T cells. The binding affinity of the TCR to a single pMHC molecule is in the weak micromolar range but can be increased by producing pMHC multimers. The multimeric form allows for numerous pMHC-TCR interactions to occur simultaneously on the surface of a cognate T cell to synergistically increase the binding avidity into the nanomolar range (Dal Porto et al., 1993). This advancement has allowed for identification and enumeration of T-cell populations that are found at frequencies of less than 10^{-5}. The most common form of pMHC multimer currently used is the tetramer, which is produced by linking four biotinylated pMHC complexes via streptavidin. In most forms, pMHC multimers can be labeled for use in flow cytometry, magnetic resonance imaging, or modulation of antigen-specific T-cell activity. The following subsections will cover how pMHC multimers have been used to unravel T1D pathogenesis and how these agents may be applied to treat the disease.

Peptide-major histocompatibility complex multimers in T1D

Our understanding of islet-specific T cells in the pathogenesis of T1D has been greatly enhanced following the elucidation of major β cell autoantigens and the creation of pMHC multimers specific for diabetogenic T-cell subsets. In fact, the use of these tools may allow for more accurate prognoses than the currently used predictions based on islet autoantibody titers. For example, researchers can collect blood samples from at-risk individuals and evaluate TH and CTL specific for islet antigens using fluorochrome-labeled pMHC tetramers. While earlier studies of autoreactive T cells in peripheral circulation required *ex vivo* peptide stimulation in order to detect antigen-specific TH cells via multimer labeling (Liu et al., 2000; Reijonen et al., 2002), advances in pMHCII technology have allowed for direct detection of diabetogenic T cells in lymph nodes of NOD mice (Crawford et al., 2011), indicating that pMHC technology may eventually allow for enumeration of autoreactive TH clonotypes in peripheral circulation. Alternatively, the use of ELISPOT techniques, while still requiring a stimulatory incubation period, also allows for enumeration of islet-reactive T cells in diabetics (Kotani et al., 2002) though the differences between pMHC multimer and ELISPOT assays in detecting islet-specific T cells that physiologically function as diabetogenic clonotypes remain to be clarified (Roep and Peakman, 2012). Utilizing pMHCI multimers to label the blood cells of young NOD mice, elevated numbers of CTL specific for the NRP mimotope, a synthetic analog of the islet antigen $IGRP_{206-214}$, were found to strongly correlate with the degree of insulitis (Trudeau et al., 2003). Importantly, this correlation predicted the onset of overt diabetes prior to detection of hyperglycemia. In a similar fashion, investigators detected pMHCI-specific autoreactive CTL in the blood of recent onset diabetics that were not present in control subjects (Velthuis et al., 2010). The presence of islet-reactive CTL in peripheral blood also correlated with impending insulin dependence in islet transplant recipients. Thus, pMHC multimers offer clinically relevant tools for T1D that may surpass current diagnostic protocols.

In addition to the value of pMHC multimers as diagnostic tools for blood specimens, this technology has led to demonstrations of the presence and expansion of diabetogenic T cells within secondary and tertiary immune compartments. Liu et al*.* were the first to describe the presence of glutamic acid decarboxylase (GAD)65-reactive TH cells in the lymphoid tissues of NOD mice by utilizing tetramers composed of murine MHCII molecules that were in complex with GAD65-derived peptides (Liu et al., 2000). Similar protocols and results were described in recent-onset human T1D patients (Reijonen et al., 2002). Wong et al*.* utilized pMHCI tetramers loaded with an insulin-derived peptide epitope (determined via cDNA screening libraries) to demonstrate CTL infiltration into islets of young NOD mice, finding that insulin $B_{15–23}$-reactive CTL comprised a large proportion of islet infiltrating T cells and that this population decreased over time (Wong et al., 1999). Studies by Amrani et al*.* indicated that NRP-A7-specific CTLs predominate as animals age (Amrani et al., 2000a) and that this phenomenon occurs due to a process deemed “avidity maturation,” in which higher-avidity, more aggressive IGRP-reactive CTL clonotypes expand within the islets over time, likely due to a lack of tolerance mechanisms that restrict the clones as disease progresses (Han et al., 2005).

Such insights could indicate that there is a primary clonotype responsible for T1D initiation—but which one? Krishnamurthy et al. demonstrated that NOD mice tolerized to proinsulin do not develop IGRP-specific CTL infiltration into islets and, importantly, do not become diabetic, while those tolerized to IGRP still developed proinsulin-reactive CTL, resulting in T1D (Krishnamurthy et al., 2006). These results support the idea of a driver clonotype (proinsulin-reactive) and the recruitment of secondary effectors (IGRP-reactive) through the phenomenon of “epitope spreading.” Thus, it may be difficult to determine which specificity to target with antigen-specific therapy, particularly in light of the variability of diabetogenic CTL populations found in both mice and humans. For example, Lieberman et al*.* compared CTL specificities in age-matched NOD mouse islets at different time points and found different antigen-specific clonotypes predominating in each animal (Lieberman et al., 2004). Similarly, research involving recent onset human diabetics also found no immunodominant CTL reactivity across individuals (Martinuzzi et al., 2008). Again, such variability could arise from epitope spreading; alternatively, these data could signify that there is no universal, underlying epitope responsible for T1D induction in either species. Even this worst case scenario—where private T-cell specificities initiate diabetogenesis—does not automatically doom antigen-specific-based treatment as a practical therapy for T1D, because of immunodominance, which likely restricts these specificities to one or a few epitopes per MHC haplotype. Thus, a limited number of antigen-specific agents presumably would cover a large percentage of the diabetic patient population. This restriction is reinforced by the relative dominance of some class I (HLA-A*0201,B*3906, or C*0501) and class II

(DPA1*0103-DPB1*0202 or DRB1*0405-DQA1*0301-DQB1*0302) alleles in T1D (Baker and Steck, 2011).

Whether there is a primum movens diabetogenic T-cell specificity is debatable; however, T-cell trafficking to the islets clearly occurs prior to overt diabetes. Tetramers labeled with magnetic nanoparticles have allowed real-time magnetic resonance imaging of NRP-specific CTL infiltrating NOD islets (Moore et al., 2004; Medarova et al., 2008). Such a noninvasive procedure could be invaluable for the detection of insulitis in at-risk patients, further supporting the use of multimerized pMHC as diagnostic measurements of T1D onset. In addition to the use of pMHC multimers described previously, these constructs can also be employed to manipulate both TH and CTL subsets *in vivo.* The strategy of pMHC therapy in T1D is based on TCR-pMHC binding in the absence of costimulatory or cytokine signals, thereby inducing anergic or regulatory T-cell phenotypes. Numerous studies have described the possible outcomes, such as full priming, partial activation, unresponsiveness, or induction of apoptosis, following administration of pMHCI to CTL *in vitro* and *in vivo* (Wang et al., 2000; Cebecauer et al., 2005; Maile et al., 2006; Samanta et al., 2011). Similar results have been detected in human TH treated with pMHCII multimers (Mallone, 2005; Mallone et al., 2004). Such varying effects of pMHC administration upon modulation of diabetogenic T cells will be highlighted later, but are likely due to pMHC multimer avidity, functional plasticity of the clonotype targeted, and the molecule conjugated to the pMHC multimer. Specifically, shortened linkage length between the pMHCI monomers in multimeric complex correlated with induction of CTL apoptosis (Cebecauer et al., 2005), and the numbers, or valence, of pMHCII monomers in complex was determined to affect TH fate (Preda-Pais et al., 2005). Alternatively, if the goal is to delete specific T-cell subsets, pMHC multimers may be used to deliver toxic moieties to cognate T cells (Clark et al., 1994; Casares et al., 2001; Yuan, 2004; Penaloza-MacMaster et al., 2009).

Advantages of pMHC multimer therapies over “blanket” or mAb-based treatments include the capacity to rapidly create “designer” pMHC multimers that directly target diabetogenic T cells. Specifically, pMHCI folding protocols can incorporate photocleavable peptides into the MHCI binding groove that can be rapidly replaced by peptides of interest following exposure to UV light, while still maintaining the MHCI complex (Toebes et al., 2009). This technique was recently applied to human T1D patients and led to the discovery of new preproinsulin epitopes against which T-cell frequencies were found to correlate with islet transplant rejection outcomes (Unger et al., 2011). Unlike in toxic mAb therapies, diabetogenic T cells cannot be selected to escape targeting by toxic multimers because the pMHC is the ligand for the TCR, which is necessary for recognizing and killing β cells. However, certain issues will need to be addressed before pMHC become clinically acceptable treatments for T-cell-mediated diseases. Firstly, multimer therapy in its current form may be immunogenic, resulting in production of anti-multimer antibodies following repeated administration. Secondly, some studies have indicated that pMHC therapy may actually activate T cells and exacerbate disease due to the transfer of peptides from multimers to native MHC on host tissues (Ge et al., 2002). Yet, the first concern could be addressed by altering the structural design of the therapeutic pMHC to reduce immunogenicity, while covalent linkage of peptides to the multimer could obviate the second issue (Samanta et al., 2011). Lastly, pMHC administration may induce refractory periods during which T cells are transiently resistant to binding pMHC complexes (Drake et al., 2005). This issue could be addressed by determining the optimal dosing interval in order to avoid delivery during such periods. While unanticipated technical problems are likely to arise, the ability to manipulate T cells in an antigen-specific manner warrants further investigation into pMHC therapy for T1D.

CD8+ T-Cell-Directed Multimer Usage

Immunomodulation of CTL activity via pMHCI multimers was first described by Dal Porto et al., who created dimeric MHCI-Ig fusion proteins that were capable of inhibiting alloreactive CTL *in vitro* (Dal Porto et al., 1993). Subsequently, other studies confirmed that pMHCI multimers can inhibit CTL activity *in vivo* (O’Herrin et al., 2001; Angelov et al., 2006). The mechanisms by which pMHCI multimers modulate aggressive activity of CTL were addressed in a murine model of tissue rejection (Maile et al., 2006). This study utilized the male HY alloantigen to determine the capacity of pMHCI multimer treatment to prevent tissue rejection *in vivo*. Administration of pMHCI to naive female recipients of male skin grafts induced a $CD8^{lo}$ phenotype in allospecific CTL, which corresponded to antigen hyporesponsiveness and the production of TGFβ. Thus, pMHCI tetramer treatment induced immunosuppressive CTL in female mice that prevented other alloreactive CTL from rejecting male tissue grafts. Results of these studies indicate that immunomodulation of diabetogenic CTL clonotypes might also be feasible. However, when pMHCI multimers targeting IGRP-reactive CTL for immunomodulation were administered to NOD mice, diabetes was not prevented (unpublished observations). More recently, promising results for pMHCI multimers have been obtained in both WT and humanized (transgenic HLA-A*0201 expression) NOD mice (Tsai et al., 2010). Tsai et al. utilized iron-oxide nanoparticles coated with antigenic islet epitope-displaying MHCI molecules to determine the effects on diabetogenic CTL. Surprisingly, pMHCI-nanoparticle treatment boosted numbers of the antigen-specific CTL clonotype, but prevented or reversed diabetes in pre- and newly-diabetic NOD mice. This finding was attributed to the expansion of low avidity, autoregulatory (or suppressor) CTL that are capable of suppressing autoimmunity via IFNγ-, indoleamine-2, 3-dioxygenase-, and perforin-dependent mechanisms in a non-antigen-specific manner. Thus, pMHCI-based therapies may prevent and even counteract insulitis in T1D-susceptible individuals via enhancement of autoregulatory mechanisms.

While pMHCI-mediated expansion of islet-specific suppressor CTL appears to hold great promise for recent onset T1D treatment, it is plausible that such therapies would be ineffective for modulating all islet-specific CTL, such as memory-like CTL clonotypes found in long-term diabetics that mediate islet graft rejection (Diz et al., 2012). Therefore, the use of pMHCI multimers to specifically ablate diabetogenic clonotypes may be advantageous for islet transplantation, since islet antigen-specific CTL clonotypes mediate recurrence of T1D (Sibley et al., 1985; Prange et al., 2001; Young et al., 2004; Ishida-Oku et al., 2009; Coppieters et al., 2012). The first description of a toxic pMHCI multimer was published by Yuan et al. (Yuan, 2004) and utilized tetramers conjugated to a radionuclide, which eliminated antigen-specific CTL *in vitro*. Using saporin as a toxic agent, we demonstrated the ablation of transgenic CD8+ T cells in an antigen-specific manner *in vitro* and *in vivo* (Hess et al., 2007). Our group then demonstrated that toxic pMHCI administration killed IGRP-reactive CTL transferred into T-cell deficient NOD.scid recipients (Vincent et al., 2010). Toxic tetramer treatment also resulted in the rapid reduction of cognate CTL (>75% eliminated 72 hours post treatment) from the spleens of lymphoreplete NOD recipients. Furthermore, toxic tetramer-treated WT NOD mice showed delayed onset of T1D (3 of 10 treated animals were euglycemic at study completion, compared to none among the PBS-injected mice), and lasting depletion (for 44 weeks after treatment) of cognate CTL from the islets. Lastly, treatment was initiated at 8 weeks of age, a time point when the autoimmune response is well underway in NOD mice, indicating that this strategy may be applicable to the prevention of disease progression. Thus, immunomodulation and ablation strategies utilizing pMHCI multimers may be suitable for preventing progression or recurrence of T1D.

MULTIMER SUMMARY

In summary, the goals of pMHC multimer usage in T1D are to create a better prognostic indicator for diabetes onset or impending islet transplant rejection; to halt the destructive activity of diabetogenic T-cell clones via anergy induction, phenotype conversion, or clonal deletion; and ultimately, to restore the balance of islet-specific effector and suppressor T cells in at-risk individuals. Future studies should address the following issues with pMHC multimer administration: determining optimal time point of therapy application (is there an ideal time to deplete antigen-specific CTL?) utilizing numerous pMHCI multimers of different specificities simultaneously (can we modulate multiple CTL populations?) combining therapies that target CD4+ and CD8+ T cells (would targeting TH and CTL have a synergistic effect?); combining therapies that target other cell types (will B cell-depleting antibodies prevent epitope spreading?) and producing next generation recombinant pMHC molecules (can we more effectively target islet-reactive T cells?). Therefore, we believe that this technology will continue to evolve and perhaps be used in conjunction with existing therapies to treat or prevent T cell-mediated autoimmune disorders such as T1D.

Islet cell transplantation as therapy

The above sections in this chapter describe putative therapies utilizing MHC multimers to modify autoreactive responses directly, yet none have been applied to islet transplantation therapies in efforts to prevent diabetes recurrence, only for monitoring disease progression. Furthermore, most such efforts are intended for use in preventing the onset of overt diabetes, which does not help individuals who have been diabetic for years. For long-term diabetics, the primary therapy involves use of exogenous insulin delivery to counteract hyperglycemia. Islet cell transplantation offers hope of insulin-injection independence, but requires simultaneous immunosuppressive therapy due to the allo- and autoimmune responses that ensue post-transplantation [reviewed in (Ricordi and Strom, 2004)]. While modifications to transplantation protocols have increased the success rate in islet graft survival (Barton et al., 2012), issues have been described that may concern recipients, such as increased risks of nephrotoxicity and cancer, and increased numbers of autoreactive T cells following immunosuppressive regimens (Wang et al., 2011; Monti et al., 2008). Thus, alternative means of quelling the immune response in diabetics receiving insulin producing transplants are needed.

The proportional effects of direct and indirect CTL killing mechanisms in diabetics are dependent upon factors such as the stage of disease, cytokine microenvironment of the islets, and, most importantly, the direct interaction of the CTL and pMHCI complexes on β cells. Studies that attempted to prevent destruction of islets by knocking out direct or indirect mechanisms of diabetogenic CTLs have achieved variable success [reviewed in(Tsai et al., 2008)]. Most therapeutic strategies for T1D have been directed at modulating responses of effector cells, such as described above, but what if one focused instead on the target of autoimmunity, the β cells? In fact, diabetic NOD mice who received MHCI^{null} islets from transgenic, syngeneic donors displayed minimal recurrence of T1D [5 of 27 mice across three studies (Xiang et al., 2008; Prange et al., 2001; Young et al., 2004)]. Other techniques to disrupt the MHCI-mediated CTL destruction of grafts have also been successful that do not require creation of transgenic mice strains, which is obviously not applicable to human disease. For example, by utilizing retroviral gene-insertion strategies that prevent pMHCI display, destruction of transplanted tissues by CTLs was prevented (Busch et al., 2004; de la Garza-Rodea et al., 2011; Hacke et al., 2008). However, islet tissues, which need to be MHC-matched in order to prevent allograft rejection, are acquired from cadavers and are extremely scarce, thus preventing engineering strategies from being feasible due to incomplete transduction efficiencies in such cells (Ju et al., 1998; Zaldumbide et al., 2013). Therefore, the ability to provide T1D patients with abundant islet tissues that evade CTL destruction offers challenges, but also great hopes of preventing T1D recurrence.

Studies have attempted to increase the abundance of insulin producing cells for use in transplantation by differentiating stem cell progenitors or by utilizing xenogeneic tissues, both of which still require immunosuppressive or encapsulation strategies to prevent recipient immune responses (Eventov-Friedman and Reisner, 2013). While xenogeneic tissues and stem cells may ultimately provide abundant graft material, the issue of graft survivability still remains. Two recent studies have provided proof of concept for modifying islet grafts prior to transplantation for increased protection from immune responses (Kumagai-Braesch et al., 2013; Zaldumbide et al., 2013). While such studies employ encapsulation and lentiviraltransduced immunevasin gene insertion strategies, respectively, to escape immune responses, and do provide hope for clinical applications; limitations in these experiments include the lack of addressing durability of encapsulated islets, and the possibility of immunevasin genes being immunogenic or lentiviral-modified grafts being recognized by NK cells. In the next chapter, we will attempt *in vitro* experiments to achieve further proof of immunoevasive grafts by utilizing TALEN technology to modify grafts and will directly monitor CTL and NK cell recognition of MHCI-KO cells.

The 8.3-NOD mouse model for T1D studies

To increase understanding of experiments to be described in the next chapter, I will briefly describe the spontaneously diabetic 8.3-NOD mouse strain, which was created by introduction of TCR alpha and beta transgenes into the NOD mouse background (Verdaguer et al., 1997), resulting in a majority of CD8+ T cells within this strain recognizing murine MHCI-restricted beta cell-specific antigen. The expression of the 8.3TCR transgenes by NOD mice results in a nearly complete population of CD8+ T cells restricted by the K^d variant of murine MHCI (depending upon Rag gene expression) within the animal that are specific for IGRP peptides and the high-affinity NRP mimotopes (Anderson et al., 1999). Such CTL have been determined to be present at varying frequencies within insulitic lesions across individual mice, but avidity maturation of this clonotype occurs during progression of disease (Lieberman et al., 2004; Amrani et al., 2000a). The K^d complex in the NOD mouse as been determined to be the restrictive MHCI element for most of the described diabetogenic clonotypes involved in pathogenesis (Tsai et al., 2008), and is thought to restrict CTL clonotypes involved in initiation of disease in NOD mice (Krishnamurthy et al., 2006, 2008). Thus, the 8.3-NOD-derived CTL are ideal model effectors for use in studies monitoring destruction of β cells, as recent studies in mice and humans have determined that autoreactive CTL populations found at initial disease onset and recurrence following transplantation are highly identical in composition for islet-specificities within the individual (Diz et al., 2012; Unger et al., 2011).

Summary

The major effectors of T1D onset and recurrence are CD8+ T cells specific for islet antigens presented by MHCI on β cells. Understanding of disease etiology has been enhanced by pMHC multimers, which may also provide therapies for amelioration of human disease. Most treatments have targeted the effectors for activity modulation to prevent disease progression with minimal clinical efficacy to date, but data exist that support the notion of therapeutically targeting the β cell itself in order to prevent effector recognition. In the next chapter, we will describe our efforts using TALEN technology to genetically modify murine insulin producing cells to protect such cells from recognition by the 8.3-NOD CTL, a representative effector population that accurately and stringently models effector cells found during islet graft rejection.

References

Altman, J., P. Moss, P. Goulder, D. Barouch, M. McHeyzer-Williams, J. Bell, A. McMichael, and M. Davis. 1996. Phenotypic Analysis of Antigen-Specific T Lymphocytes. *Science*. 274:94–6.

Amrani, A., J. Verdaguer, P. Serra, S. Tafuro, R. Tan, and P. Santamaria. 2000a. Progression of autoimmune diabetes driven by avidity maturation of a T-cell population. *Nature*. 406. doi:Letter.

Amrani, A., J. Verdaguer, S. Thiessen, S. Bou, and P. Santamaria. 2000b. IL-1a, IL-1b, and IFN-g mark b cells for Fas-dependent destruction by diabetogenic CD4+ T lymphocytes. *J. Clin. Invest.* 105:459–68.

Anderson, B., B.J. Park, J. Verdaguer, A. Amrani, and P. Santamaria. 1999. Prevalent CD8(+) T cell response against one peptide/MHC complex in autoimmune diabetes. *Proc. Natl. Acad. Sci. U. S. A.* 96:9311–9316.

Angelov, G., P. Guillaume, M. Cebecauer, G. Bosshard, D. Dojcinovic, P. Baumgaertner, and I. Luescher. 2006. Soluble MHC-Peptide Complexes Containing Long Rigid Linkers Abolish CTL-Mediated Cytotoxicity. *J. Immunol.* 176:3356–65.

Baker, P.R., and A.K. Steck. 2011. The Past, Present, and Future of Genetic Associations in Type 1 Diabetes. *Curr. Diab. Rep.* 11:445–453. doi:10.1007/s11892-011-0212-0.

Barton, F.B., M.R. Rickels, R. Alejandro, B.J. Hering, S. Wease, B. Naziruddin, J. Oberholzer, J.S. Odorico, M.R. Garfinkel, M. Levy, F. Pattou, T. Berney, A. Secchi, S. Messinger, P.A. Senior, P. Maffi, A. Posselt, P.G. Stock, D.B. Kaufman, X. Luo, F. Kandeel, E. Cagliero, N.A. Turgeon, P. Witkowski, A. Naji, P.J. O’Connell, C. Greenbaum, Y.C. Kudva, K.L. Brayman, M.J. Aull, C. Larsen, T.W.H. Kay, L.A. Fernandez, M.-C. Vantyghem, M. Bellin, and A.M.J. Shapiro. 2012. Improvement in Outcomes of Clinical Islet Transplantation: 1999–2010. *Diabetes Care*. 35:1436–1445. doi:10.2337/dc12-0063.

Busch, A., W. Marasco, C. Doebis, H. Volk, and M. Seifert. 2004. MHC class I manipulation on cell surfaces by gene transfer of anti-MHC class I intrabodies: a tool for decreased immunogenicity of allogeneic tissue and cell transplants. *Methods*. 34:240–249. doi:10.1016/j.ymeth.2004.03.017.

Casares, S., A. Hurtado, R.C. McEvoy, A. Sarukhan, H. von Boehmer, and T.-D. Brumeanu. 2002. Down-regulation of diabetogenic CD4+ T cells by a soluble dimeric peptide–MHC class II chimera. *Nat. Immunol.* 3:383–391. doi:10.1038/ni770.

Casares, S., A. Stan, C. Bona, and T. Brumeanu. 2001. Antigen-specific downregulation of T cells by doxorubicin delivered through a recombinant MHC II–peptide chimera. *Nat. Biotechnol.* 19:142–7.

Cebecauer, M., P. Guillaume, P. Hozák, S. Mark, H. Everett, P. Schneider, and I. Luescher. 2005. Soluble MHC-Peptide Complexes Induce Rapid Death of CD8+ CTL. *J. Immunol.* 174:6809–19.

Clark, B., S. Deshpande, S. Sharma, and B. Nag. 1994. Antigen-specific Deletion of Cloned T Cells Using Peptide-Toxin Conjugate Complexed with Purified Class II Major Histocompatibility Complex Antigen. *J. Biol. Chem.* 269:94–9.

Coppieters, K.T., F. Dotta, N. Amirian, P.D. Campbell, T.W.H. Kay, M.A. Atkinson, B.O. Roep, and M.G. von Herrath. 2012. Demonstration of islet-autoreactive CD8 T cells in insulitic lesions from recent onset and long-term type 1 diabetes patients. *J. Exp. Med.* 209:51–60. doi:10.1084/jem.20111187.

Crawford, F., B. Stadinski, N. Jin, A. Michels, M. Nakayama, P. Pratt, P. Marrack, G. Eisenbarth, and J.W. Kappler. 2011. Specificity and detection of insulin-reactive CD4+ T cells in type 1 diabetes in the nonobese diabetic (NOD) mouse. *Proc. Natl. Acad. Sci.* 108:16729–16734. doi:10.1073/pnas.1113954108.

Culina, S., C. Boitard, and R. Mallone. 2011. Antigen-Based Immune Therapeutics for Type 1 Diabetes: Magic Bullets or Ordinary Blanks? *Clin. Dev. Immunol.* 2011:1–15. doi:10.1155/2011/286248.

DeWitt, D., and I. Hirsch. 2003. Outpatient Insulin Therapy in Type 1 and Type 2 Diabetes Mellitus. *J. Am. Med. Assoc.* 289:2254–64.

Diz, R., A. Garland, B.G. Vincent, M.C. Johnson, N. Spidale, B. Wang, and R. Tisch. 2012. Autoreactive Effector/Memory CD4+ and CD8+ T Cells Infiltrating Grafted and Endogenous Islets in Diabetic NOD Mice Exhibit Similar T Cell Receptor Usage. *PLoS ONE*. 7:e52054. doi:10.1371/journal.pone.0052054.

Drake, D., R. Ream, C. Lawrence, and T. Braciale. 2005. Transient loss of MHC class I tetramer binding after CD8+ T cell activation reflects altered T cell effector function. *J. Immunol.* 175.

Eventov-Friedman, S., and Y. Reisner. 2013. Fetal Pancreas as a Source for Islet Transplantation Sweet Promise and Current Challenges. *Diabetes*. 62:1382–1383. doi:10.2337/db13-0018.

De la Garza-Rodea, A., M. Verweij, H. Boersma, I. van der Velde-van Dijke, A. de Vries, R. Hoeben, D. van Bekkum, E.J. Wiertz, S. Knaän-Shanzer, and D. Unutmaz. 2011. Exploitation of Herpesvirus Immune Evasion Strategies to Modify the Immunogenicity of Human Mesenchymal Stem Cell Transplants. *PLoS ONE*. 6:e14493. doi:10.1371/journal.pone.0014493.

Ge, Q., J. Stone, M. Thompson, J. Cochran, M. Rushe, H. Eisen, J. Chen, and L. Stern. 2002. Soluble peptide-MHC monomers cause activation of CD8+ T cells through transfer of the peptide to T cell MHC molecules. *Proc. Natl. Acad. Sci.* 99:13729–13734. doi:10.1073/pnas.212515299.

Gojanovich, G.S., and P.R. Hess. 2012. Making the most of major histocompatibility complex molecule multimers: applications in type 1 diabetes. *Clin. Dev. Immunol.* 2012:380289. doi:10.1155/2012/380289.

Gojanovich, G.S., S.L. Murray, A.S. Buntzman, E.F. Young, B.G. Vincent, and P.R. Hess. 2012. The use of peptide-major-histocompatibility-complex multimers in type 1 diabetes mellitus. *J. Diabetes Sci. Technol.* 6:515–524.

Hacke, K., R. Falahati, L. Flebbe-Rehwaldt, N. Kasahara, and K. Gaensler. 2008. Suppression of HLA expression by lentivirus-mediated gene transfer of siRNA cassettes and in vivo chemoselection to enhance hematopoietic stem cell transplantation. *Immunol. Res.* 44:112–126. doi:10.1007/s12026-008-8088-z.

Han, B., P. Serra, J. Yamanouchi, A. Amrani, J. Elliott, P. Dickie, T. DiLorenzo, and P. Santamaria. 2005. Developmental control of CD8+ T cell–avidity maturation in autoimmune diabetes. *J. Clin. Invest.* 115:1879–1887. doi:10.1172/jci24219.

Herold, K.C., S. Gitelman, C. Greenbaum, J. Puck, W. Hagopian, P. Gottlieb, P. Sayre, P. Bianchine, E. Wong, V. Seyfert-Margolis, K. Bourcier, and J.A. Bluestone. 2009. Treatment of patients with new onset Type 1 diabetes with a single course of anti-CD3 mAb teplizumab preserves insulin production for up to 5 years. *Clin. Immunol.* 132:166–173. doi:10.1016/j.clim.2009.04.007.

Hess, P.R., C. Barnes, M.D. Woolard, M.D.L. Johnson, J.M. Cullen, E.J. Collins, and J.A. Frelinger. 2007. Selective deletion of antigen-specific CD8+ T cells by MHC class I tetramers coupled to the type I ribosome-inactivating protein saporin. *Blood*. 109:3300–3307. doi:10.1182/blood-2006-06-028001.

Ishida-Oku, M., M. Iwase, A. Sugitani, K. Masutani, H. Kitada, M. Tanaka, and and M. Iida. 2009. A case of recurrent type 1 diabetes mellitus with insulitis of transplanted pancreas in simultaneous pancreas–kidney transplantation from cardiac death donor. *Diabetologia*. 53:341–345. doi:10.1007/s00125-009-1593-3.

Itoh, N., T. Hanafusa, A. Miyazaki, J. Miyagawa, K. Yamagata, K. Yamamoto, M. Waguri, A. Imagawa, S. Tamura, and M. Inada. 1993. Mononuclear cell infiltration and its relation to the expression of major histocompatibility complex antigens and adhesion molecules in pancreas biopsy specimens from newly diagnosed insulin-dependent diabetes mellitus patients. *J. Clin. Invest.* 92:2313–2322. doi:10.1172/JCI116835.

Ju, Q., D. Edelstein, M.D. Brendel, D. Brandhorst, H. Brandhorst, R.G. Bretzel, and M. Brownlee. 1998. Transduction of non-dividing adult human pancreatic beta cells by an integrating lentiviral vector. *Diabetologia*. 41:736–739. doi:10.1007/s001250050977.

Juvenile Diabetes Research Foundation. Type 1 Diabetes Facts.

Katz, J., C. Benoist, and D. Mathis. 1993. Major histocompatibility complex class I molecules are required for the development of insulitis in non-obese diabetic mice. *Eur. J. Immunol.* 23:3358–3360.

Keymeulen, B., S. Candon, S. Fafi-Kremer, A. Ziegler, M. Leruez-Ville, C. Mathieu, E. Vandemeulebroucke, M. Walter, L. Crenier, E. Thervet, C. Legendre, D. Pierard, G. Hale, H. Waldmann, J.F. Bach, J.M. Seigneurin, D. Pipeleers, and L. Chatenoud. 2009. Transient Epstein-Barr virus reactivation in CD3 monoclonal antibody-treated patients. *Blood*. 115:1145–1155. doi:10.1182/blood-2009-02-204875.

Kotani, R., M. Nagata, H. Moriyama, M. Nakayama, K. Yamada, S.A. Chowdhury, S. Chakrabarty, Z. Jin, H. Yasuda, and K. Yokono. 2002. Detection of GAD65-Reactive T-Cells in Type 1 Diabetes by Immunoglobulin-Free ELISPOT Assays. *Diabetes Care*. 25:1390–7.

Krishnamurthy, B., N.L. Dudek, M.D. McKenzie, A.W. Purcell, A.G. Brooks, S. Gellert, P.G. Colman, L.C. Harrison, A.M. Lew, H.E. Thomas, and T.W.H. Kay. 2006. Responses against islet antigens in NOD mice are prevented by tolerance to proinsulin but not IGRP. *J. Clin. Invest.* 116:3258–3265. doi:10.1172/jci29602.

Krishnamurthy, B., L. Mariana, S.A. Gellert, P.G. Colman, L.C. Harrison, A.M. Lew, P. Santamaria, H.E. Thomas, and T.W. Kay. 2008. Autoimmunity to both proinsulin and IGRP is required for diabetes in nonobese diabetic 8.3 TCR transgenic mice. *J. Immunol.* 180:4458–4464.

Kumagai-Braesch, M., S. Jacobson, H. Mori, X. Jia, T. Takahashi, A. Wernerson, M. Flodström-Tullberg, and A. Tibell. 2013. The TheraCyte™ device protects against islet allograft rejection in immunized hosts. *Cell Transplant.* 22:1137–1146. doi:10.3727/096368912X657486.

Lehuen, A., J. Diana, P. Zaccone, and A. Cooke. 2010. Immune cell crosstalk in type 1 diabetes. *Nat. Rev. Immunol.* 10:501–513. doi:10.1038/nri2787.

Li, L., Z. Yi, B. Wang, and R. Tisch. 2009. Suppression of Ongoing T Cell-Mediated Autoimmunity by Peptide-MHC Class II Dimer Vaccination. *J. Immunol.* 183:4809–4816. doi:10.4049/jimmunol.0901616.

Lieberman, S.M., T. Takaki, B. Han, P. Santamaria, D.V. Serreze, and T.P. and DiLorenzo. 2004. Individual Nonobese Diabetic Mice Exhibit Unique Patterns of CD8+ T Cell Reactivity to Three Islet Antigens, Including the Newly Identified Widely Expressed Dystrophia Myotonica Kinase. *J. Immunol.* 173:6727–34.

Liu, C., K. Jiang, C. Wu, W. Lee, and W. Lin. 2000. Detection of glutamic acid decarboxylase-activated T cells with I-Ag7 tetramers. *Proc. Natl. Acad. Sci.* 97:14596–14601. doi:10.1073/pnas.250390997.

Di Lorenzo, T., R. Graser, T. Ono, G. Christianson, H. Chapman, D. Roopenian, S. Nathenson, and D. Serreze. 1998. Major histocompatibility complex class I-restricted T cells are required for all but the end stages of diabetes development in nonobese diabetic mice and use a prevalent T cell receptor alpha chain gene rearrangement. *Proc. Natl. Acad. Sci.* 95:12538–43.

Di Lorenzo, T., M. Peakman, and B. Roep. 2007. Translational Mini-Review Series on Type 1 Diabetes: Systematic analysis of T cell epitopes in autoimmune diabetes. *Clin. Exp. Immunol.* 148:1–16. doi:10.1111/j.1365-2249.2006.03244.x 10.1111/j.1365-2249.2007.03328.x.

Ludvigsson, J. 2009. The role of immunomodulation in autoimmune diabetes. *J. Diabetes Sci. Technol.* 3:320–30.

Maile, R., S. Pop, R. Tisch, E. Collins, B. Cairns, and J. Frelinger. 2006. Low-avidity CD8lo T cells induced by incomplete antigen stimulation in vivo regulate naive higher avidity CD8hi T cell responses to the same antigen. *Eur. J. Immunol.* 36:397–410. doi:10.1002/eji200535797 10.1002/eji.200535064.

Mallone, R. 2005. Functional avidity directs T-cell fate in autoreactive CD4+ T cells. *Blood*. 106:2798–2805. doi:10.1182/blood-2004-12-4848.

Mallone, R., V. Brezar, and C. Boitard. 2011. T Cell Recognition of Autoantigens in Human Type 1 Diabetes: Clinical Perspectives. *Clin. Dev. Immunol.* 2011:1–16. doi:10.1155/2011/513210.

Mallone, R., S. Kochik, E. Laughlin, V. Gersuk, H. Reijonen, W. Kwok, and G. Nepom. 2004. Differential Recognition and Activation Thresholds in Human Autoreactive GAD-Specific T-Cells. *Diabetes*. 53.

Mallone, R., and G. Nepom. 2004. MHC Class II tetramers and the pursuit of antigen-specific T cells: define, deviate, delete. *Clin. Immunol.* 110:232–242. doi:10.1016/j.clim.2003.11.004.

Martinuzzi, E., G. Novelli, M. Scotto, P. Blancou, J.M. Bach, L. Chaillous, G. Bruno, L. Chatenoud, P. van Endert, and and R. Mallone. 2008. The Frequency and Immunodominance of Islet-Specific CD8+ T-cell Responses Change after Type 1 Diabetes Diagnosis and Treatment. *Diabetes*. 57:1312–1320. doi:10.2337/db07-1594.

Masteller, E., M. Warner, W. Ferlin, V. Judkowski, D. Wilson, N. Glaichenhaus, and J. Bluestone. 2003. Peptide-MHC Class II Dimers as Therapeutics to Modulate Antigen-Specific T Cell Responses in Autoimmune Diabetes. *J. Immunol.* 171:5587–95.

Medarova, Z., S. Tsai, N. Evgenov, P. Santamaria, and A. Moore. 2008. In vivo imaging of a diabetogenic CD8+ T cell response during type 1 diabetes progression. *Magn. Reson. Med.* 59:712–720. doi:10.1002/mrm.21494.

Monti, P., M. Scirpoli, P. Maffi, N. Ghidoli, F. De Taddeo, F. Bertuzzi, L. Piemonti, M. Falcone, A. Secchi, and E. Bonifacio. 2008. Islet transplantation in patients with autoimmune diabetes induces homeostatic cytokines that expand autoreactive memory T cells. *J. Clin. Invest.* doi:10.1172/jci35197.

Moore, A., J. Grimm, B. Han, and P. Santamaria. 2004. Tracking the Recruitment of Diabetogenic CD8+ T-Cells to the Pancreas in Real Time. *Diabetes*. 53:1459–66.

Moriwaki, M., N. Itoh, J. Miyagawa, K. Yamamoto, A. Imagawa, K. Yamagata, H. Iwahashi, H. Nakajima, M. Namba, S. Nagata, T. Hanafusa, and Y. Matsuzawa. 1999. Fas and Fas ligand expression in inflamed islets in pancreas sections of patients with recent-onset Type I diabetes mellitus. *Diabetologia*. 42:1332–40.

National diabetes fact sheet: national estimates and general information on diabetes and prediabetes in the United States. 2011.

Nikoopour, E., C. Sandrock, K. Huszarik, O. Krougly, E. Lee-Chan, E. Masteller, J. Bluestone, and B. Singh. 2011. Cutting Edge: Vasostatin-1-Derived Peptide ChgA29-42 Is an Antigenic Epitope of Diabetogenic BDC2.5 T Cells in Nonobese Diabetic Mice. *J. Immunol.* 186:3831–3835. doi:10.4049/jimmunol.1003617.

O'Herrin, S., J. Slansky, Q. Tang, M. Markiewicz, T. Gajewski, D. Pardoll, J. Schneck, and J. Bluestone. 2001. Antigen-Specific Blockade of T Cells In Vivo Using Dimeric MHC Peptide. *J. Immunol.* 167:2555–60.

Penaloza-MacMaster, P., D. Masopust, and R. Ahmed. 2009. T-cell reconstitution without T-cell immunopathology in two models of T-cell-mediated tissue destruction. *Immunology*. 128:164–171. doi:10.1111/j.1365-2567.2009.03080.x.

Polychronakos, C., and Q. Li. 2011. Understanding type 1 diabetes through genetics: advances and prospects. *Nat. Rev. Genet.* 12:781–792. doi:10.1038/nrg3069.

Dal Porto, J., T. Johansen, B. Catipovic, D. Parfiit, D. Tuveson, U. Gether, S. Kozlowski, D. Fearon, and J. Schneck. 1993. A soluble divalent class I major histocompatibility complex molecule inhibits alloreactive T cells at nanomolar concentrations. *Proc. Natl. Acad. Sci.* 90:6671–5.

Prange, S., P. Zucker, A. Jevnikar, and B. Singh. 2001. Transplanted MHC class I-deficient nonobese diabetic mouse islets are protected from autoimmune injury in diabetic nonobese recipients. *Transplantation*. 71:982–5.

Preda-Pais, A., A. Stan, S. Casares, C. Bona, and T. Brumeanu. 2005. Efficacy of clonal deletion vs. anergy of self-reactive CD4 T-cells for the prevention and reversal of autoimmune diabetes. *J. Autoimmun.* 25:21–32. doi:10.1016/j.jaut.2005.04.003.

Reijonen, H., E. Novak, S. Kochik, A. Heninger, A. Liu, W. Kwok, and G. Nepom. 2002. Detection of GAD65-Specific T-Cells by Major Histocompatibility Complex Class II Tetramers in Type 1 Diabetic Patients and At-Risk Subjects. *Diabetes*. 51.

Ricordi, C., and T.B. Strom. 2004. Clinical islet transplantation: advances and immunological challenges. *Nat. Rev. Immunol.* 4:259–268. doi:10.1038/nri1332.

Roep, B., and M. Peakman. 2012. Antigen targets of type 1 diabetes autoimmunity. *Cold Spring Harb. Perspect. Med.* doi:Advanced online article.

Samanta, D., D. Mukherjee, U. Ramagopal, R. Chaparro, S. Nathenson, T. DiLorenzo, and S. Almo. 2011. Structural and functional characterization of a single-chain peptide–MHC molecule that modulates both naive and activated CD8+ T cells. *Proc. Natl. Acad. Sci.* 108:13682–7.

Sibley, R., D. Sutherland, F. Goetz, and A. Michael. 1985. Recurrent diabetes mellitus in the pancreas iso- and allograft. A light and electron microscopic and immunohistochemical analysis of four cases. *Lab. Investig.* 53:132–144.

Toebes, M., B. Rodenko, H. Ovaa, and T.N.M. Schumacher. 2009. Generation of Peptide MHC Class I Monomers and Multimers Through Ligand Exchange. doi:10.1002/0471142735.im1816s87.

Trudeau, J.D., C. Kelly-Smith, C.B. Verchere, J.F. Elliott, J.P. Dutz, D.T. Finegood, P. Santamaria, and and R. Tan. 2003. Prediction of spontaneous autoimmune diabetes in NOD mice by quantification of autoreactive T cells in peripheral blood. *J. Clin. Invest.* 111:217–223. doi:10.1172/jci200316409.

Tsai, S., A. Shameli, and and P. Santamaria. 2008. Chapter 4 CD8+ T Cells in Type 1 Diabetes. 100:79–124. doi:10.1016/s0065-2776(08)00804-3.

Tsai, S., A. Shameli, J. Yamanouchi, X. Clemente-Casares, J. Wang, P. Serra, Y. Yang, Z. Medarova, A. Moore, and P. Santamaria. 2010. Reversal of Autoimmunity by Boosting Memory-like Autoregulatory T Cells. *Immunity*. 32:568–580. doi:10.1016/j.immuni.2010.03.015.

Unger, W.W., J. Velthuis, J.R.F. Abreu, S. Laban, E. Quinten, M.G.D. Kester, S. Reker-Hadrup, A.H. Bakker, G. Duinkerken, A. Mulder, K.L.M.C. Franken, R. Hilbrands, B. Keymeulen, M. Peakman, F. Ossendorp, J.W. Drijfhout, T.N. Schumacher, and B.O. Roep. 2011. Discovery of low-affinity preproinsulin epitopes and detection of autoreactive CD8 T-cells using combinatorial MHC multimers. *J. Autoimmun.* 37:151–159. doi:10.1016/j.jaut.2011.05.012.

Velthuis, J., W. Unger, J. Abreu, G. Duinkerken, K. Franken, M. Peakman, A. Bakker, S. Reker-Hadrup, B. Keymeulen, J. Drijfhout, T. Schumacher, and B. Roep. 2010. Simultaneous Detection of Circulating Autoreactive CD8+ T-Cells Specific for Different Islet Cell-Associated Epitopes Using Combinatorial MHC Multimers. *Diabetes*. 59:1721–1730. doi:10.2337/db09-1486.

Verdaguer, J., D. Schmidt, A. Amrani, B. Anderson, N. Averill, and and P. Santamaria. 1997. Spontaneous Autoimmune Diabetes in Monoclonal T Cell Nonobese Diabetic Mice. *J. Exp. Med.* 186:1663–76.

Vincent, B.G., E.F. Young, A.S. Buntzman, R. Stevens, T.B. Kepler, R.M. Tisch, J.A. Frelinger, and P.R. Hess. 2010. Toxin-coupled MHC class I tetramers can specifically ablate autoreactive CD8+ T cells and delay diabetes in nonobese diabetic mice. *J. Immunol. Baltim. Md 1950*. 184:4196–4204. doi:10.4049/jimmunol.0903931.

Waldron-Lynch, F., and K.C. Herold. 2011. Immunomodulatory therapy to preserve pancreatic β-cell function in type 1 diabetes. *Nat. Rev. Drug Discov.* 10:439–452. doi:10.1038/nrd3402.

Wang, B., R. Maile, R. Greenwood, E. Collins, and J. Frelinger. 2000. Naive CD8+ T cells do not require costimulation for proliferation and differentiation into cytotoxic effector cells. *J. Immunol.* 164.

Wang, J., S. Tsai, A. Shameli, J. Yamanouchi, G. Alkemade, and P. Santamaria. 2010. In situ recognition of autoantigen as an essential gatekeeper in autoimmune CD8+ T cell inflammation. *Proc. Natl. Acad. Sci.* 107:9317–9322. doi:10.1073/pnas.0913835107.

Wang, X., J. Hao, D.L. Metzger, Z. Ao, M. Meloche, C.B. Verchere, L. Chen, D. Ou, A. Mui, and G.L. Warnock. 2011. B7-H4 Pathway in Islet Transplantation and β-Cell Replacement Therapies. *J. Transplant.* 2011:1–8. doi:10.1155/2011/418902.

Wong, F., I. Visintin, L. Wen, R. Flavell, and J.C. Janeway. 1996. CD8 T Cell Clones from Young Nonobese Diabetic (NOD) Islets Can Transfer Rapid Onset of Diabetes in NOD Mice in the Absence of CD4 Cells. *J. Exp. Med.* 183:67–76.

Wong, F.S., J. Karttunen, C. Dumont, I. Wen, L. Visintin, I.M. Pilip, N. Shastri, E.G. Pamer, and and C.A.J. Jr. 1999. Identification of an MHC class I-restricted autoantigen in type 1 diabetes by screening an organ-specific cDNA library. *Nat. Med.* 5:1026–31.

Wooldridge, L., A. Lissina, D.K. Cole, H.A. van den Berg, D.A. Price, and A.K. Sewell. 2009. Tricks with tetramers: how to get the most from multimeric peptide-MHC. *Immunology*. 126:147–164. doi:10.1111/j.1365-2567.2008.02848.x.

World Health Organization. 10 facts about diabetes.

Xiang, Z., L. Ma, S. Manicassamy, B. Ganesh, P. Williams, R. Chari, A. Chong, and D. Yin. 2008. CD4+ T Cells Are Sufficient to Elicit Allograft Rejection and Major Histocompatibility Complex Class I Molecule Is Required to Induce Recurrent Autoimmune Diabetes After Pancreas Transplantation in Mice. *Transplantation*. 85:1205–1211. doi:10.1097/TP.0b013e31816b70bf.

Yagi, H., M. Matsumoto, K. Kunimoto, J. Kawaguchi, S. Makino, and M. Harada. 1992. Analysis of the roles of CD4+ and CD8+ T cells in autoimmune diabetes of NOD mice using transfer to NOD athymic nude mice. *Eur. J. Immunol.* 22:2387–2393. doi:10.1002/eji.1830220931.

Young, H., P. Zucker, R. Flavell, A. Jevnikar, and B. Singh. 2004. Characterization of the Role of Major Histocompatibility Complex in Type 1 Diabetes Recurrence after Islet Transplantation. *Transplantation*. 78:509–515. doi:10.1097/01.tp.0000128907.83111.c6.

Yuan, R.R. 2004. Targeted deletion of T-cell clones using alpha-emitting suicide MHC tetramers. *Blood*. 104:2397–2402. doi:10.1182/blood-2004-01-0324.

Zaldumbide, A., G. Alkemade, F. Carlotti, T. Nikolic, J.R. Abreu, M.A. Engelse, A. Skowera, E.J. de Koning, M. Peakman, B.O. Roep, R.C. Hoeben, and E.J. Wiertz. 2013. Genetically Engineered Human Islets Protected From CD8-mediated Autoimmune Destruction In Vivo. *Mol. Ther.* 21:1592–1601. doi:10.1038/mt.2013.105.

Zekzer, D., F. Wong, O. Ayalon, I. Millet, M. Altieri, S. Shintani, M. Solimena, and R. Sherwin. 1998. GAD-reactive CD4+ Th1 Cells Induce Diabetes in NOD/SCID Mice. *J. Clin. Invest.* 101:68–73.

CHAPTER 6: Eradication of MHC class Ia surface expression by TALEN-targeted bicistronic gene deletions in an insulinoma cell clone inhibits killing by diabetogenic CTL

NOTE: This chapter is formatted for submission for publication.

Abstract

In type 1 diabetes, transplantation of islets offers hope of insulin-injection independence to the patient, but long term outcomes have not been successful primarily due to the allo- and auto-immune responses that ensue. Classical MHC class I (MHCI) presentation on the surface of transplanted islets allows for recognition of these tissues by autoreactive CD8+ or alloreactive CD4+ T cells, thereby requiring life-long immunosuppressive drug therapies. Genetic engineering strategies to reduce recognition of transplanted tissues by the immune system have shown promise in model settings. We hypothesized that application of transcription activator-like effector nucleases (TALENs) would prevent expression of classical MHCI proteins on the surface of NIT-1 cells, a murine model islet cell line, thereby rendering these cells invisible to islet-specific CD8+ T cells from 8.3-NOD mice. By adapting a GFP reporter plasmid assay, we sorted TALEN-transfected cells based on GFP expression to isolate cell clones that do not present either $K^{d/b}$ or D^b variants of classical MHCI. We confirmed that the genomic loci of H2-K1 and –D1 in the knock out cell clone, NIT-KG, were disrupted by loss of restriction enzyme sites and

by sequencing each locus to discover the novel alleles produced following TALEN-mediated DNA modification. *In vitro* co-culture experiments verified that CD8+ T cells did not undergo proliferation or produce IFNγ in the presence of the NIT-KG clone. These data constitute proof of concept that TALEN-mediated modification of the genome of transplantable cells could prevent CD8+ T-cell mediated rejection following grafting.

Keywords: CD8+ T cells, graft rejection, immune evasion, TALENs, type 1 diabetes

1. Introduction

Transplantation of pancreatic islets, and the insulin-producing beta cells specifically, offers the hope of insulin-injection independence to patients of type 1 diabetes (T1D), but has been hampered by scarcity of donor tissues, the need for life-long immunosuppressive drug regimens to reduce allo- and auto -reactive immune responses, and the limited half-life of tissue functionality as a result of immune responses and transplant-associated trauma, such as graft hypoxia and non-specific inflammation (Baiu et al., 2011). The recent era of islet transplantation has yielded improvements in duration of insulin independence, but even with optimal immunosuppressive regimens only 44% of recipients remain independent at three years (Barton et al., 2012). Recent efforts have been made to find alternative sources, such as stem cells and xenogeneic tissues, as transplantable insulin-producing tissues, but the need for therapeutics to prevent allo- and auto-immune response are still required (Eventov-Friedman and Reisner, 2013). Strategies of replacing insulin production without the need for immunosuppression have involved the differentiation of stem cells into insulin-producing cell populations (Anzalone et al., 2010; Chandra et al., 2011) and the use of encapsulation techniques to isolate xenogeneic and stem cell-derived tissues from the immune responses (O'Sullivan et al., 2011; Kumagai-Braesch et al., 2013), but minimal clinical data are available (Ludwig et al., 2013; Colton, 2014).Thus, the demand for beta cells capable of evading the immune responses associated with transplantation into diabetic recipients still exists.

T cells are important effectors in T1D pathogenesis, with autoreactive, islet-specific CD8+ T cells displaying direct cytotoxic effects on beta cells during disease onset and recurrence following transplant rejection (Sibley et al., 1985; Sutherland et al., 1989; Katz et al., 1993; Xiang et al., 2008; Coppieters et al., 2012). Furthermore, recent studies have determined that the composition of islet-specific CD8+ T-cell clonotypes found during disease onset correlates with specificities found during islet graft rejection (Diz et al., 2012), and that frequencies of such clonotypes may be reliable indicators for the likelihood of graft survival (Velthuis et al., 2010). Diabetogenic CD8+ T-cell responses are restricted by classical class I major histocompatibility (MHCI) complexes, which display beta cell-derived peptide fragments, such as insulin $B_{10\text{-}18}$ in humans or $IGRP_{206\text{-}214}$ in mice, at the surface of the cell (Roep and Peakman, 2012). Thusly, numerous antigen-specific therapies have been targeted at CD8+ T cells in efforts to tolerize or delete diabetogenic effectors, but no therapies have been able to prevent onset or recurrence of T1D in humans (Gojanovich et al., 2012; Culina et al., 2011). Although there are data to support that CD4+ T cells are capable of rejecting MHC-disparate islet grafts, likely through direct and indirect allograft recognition pathways (Kupfer et al., 2005; Xiang et al., 2008), multiple murine studies indicate that removal of classical MHCI from the surface of transplanted islets is sufficient for promoting their survival (Prange et al., 2001; Young et al., 2004; Xiang et al., 2008), highlighting the importance of MHCI complex expression and CD8+ T-cell responses in T1D.

Several biotechnological strategies, such as “intrabodies” or virus-derived immune evasion proteins, have been employed to minimize MHCI expression on transplanted cells to enhance survival (Busch et al., 2004; Kim et al., 2005; Hacke et al., 2008; de la Garza-Rodea et al., 2011), but none to date have utilized transcription activator-like effector nucleases (TALENs) to accomplish this objective. TALEN technology is a relatively new addition to the genome-editing toolbox, and has been utilized in numerous species to alter expression by way of target gene deletion, addition, and correction [reviewed in (Gaj et al., 2013)]. Endonucleases linked to each of the DNA-binding arms can induce double strand breaks (DSBs) in the region between where each TALEN arm recognizes the genomic sequence. Such DSB formation results in activation of cellular DNA repair mechanisms, such as non-homologous end joining (NHEJ) or homology-directed recombination (HDR), that may not correct the sequence with high fidelity, as seen in the specialized situation of T-cell receptor V(D)J recombination in which (Lieber, 2010).

Furthermore, a recent study has shown the capacity of increasing targeted gene correction efficiency by introducing TALENs and homologous repair templates during the cell cycle stage in which there are higher rates of HDR usage (Strouse et al., 2014). Thus, TALENs can target genomic loci and prevent, insert, or correct protein expression as a result of DSB formation and the resulting activation of DNA repair mechanisms. This technology may therefore offer means of disrupting expression of the classical MHCI heavy chain genes in beta cells, thereby preventing CD8+ T cell-mediated rejection.

Here, using a model murine-derived beta cell line, NIT-1, we show that TALEN-induced modifications to the classical murine MHCI heavy chain genes, H2-K1 and –D1, result in a cell clone, NIT-KG, that escapes recognition by diabetogenic CD8+ T cells. We also provide a method for fluorescence-activated cell sorting for enrichment of cells with high TALEN activity. This study provides proof of concept for the usefulness of TALEN-mediated engineering of tissues for evasion of rejection responses that could be expanded into efforts that promote survival following transplantation of stem cells and xenogeneic tissues.

2. Methods and materials

2.1. Cell care

The NOD mouse-derived insulinoma cell line, NIT-1, was purchased from ATCC and cultured in Kaighn’s modification of Ham’s F-12K medium (ATCC) supplemented with 10% heat-inactivated FBS, L-glutamine, and 1% penicillin and streptomycin (P/S). Cells were subcultured at a ratio of 1:3 after plate removal by use of 0.05% trypsin in HBSS (Caisson) for 10 minutes at 37C, followed by neutralization with FBS-containing medium. Transfection of NIT-1 cells was performed using Lipofectamine LTX Plus™ (Life Technologies) per manufacturer recommendations at 2µl of LTX per 1µg DNA; TALEN and SSA GFP reporter plasmids (see sections 2.3 and 2.4, respectively) were co-transfected at a ratio of 1:1:1. Following transfection, cells were monitored and selected for GFP expression, and surface K^d expression in some experiments, via fluorescence-activated cell sorting (see section 2.5). For single cell ring-cloning, $3x10^3$ cells sorted for GFP positivity were seeded into a 150 mm culture plate, where they were expanded for two weeks. Individual colonies visible to the naked eye were isolated in cloning rings, removed from the plate by exposure to trypsin, and transferred to 24-well culture plates.

2.2. H2-D1 AND –K1 PRIMER DESIGN, LOSS OF RESTRICTION SITE ASSAYS, AND DNA SEQUENCING

For generation of primers specific for the heavy chain genes in NIT-1 cells, the GenBank accession #**NT_187004** (NOD/ShiLtJ) and #**NT_187027** (NOD/MrkTac) sequences were used as references. Access to these reference sequences and alignment of nucleotides was performed using Geneious v.6.1 software by Biomatters (http://www.geneious.com/). The alignment of H2-K1 and -D1 sequences and locus-specific primers can be seen in Supplemental Figure 1.

The genomic 5`K1 primer sequence, 5`-CTTCAGTGGACAAGGGGGTC-3`, was designed to anneal 819 base pairs (bp) upstream of the start codon, while the 3`K1 primer sequence, 5`-TTGTAGTATCTCTGTGCGGTCC-3`, annealed 517bp downstream of the start codon. The genomic 5`D1 primer sequence, 5`-ACAAACTGCTCTCTGTCCGCAGT-3`, annealed 277bp upstream of the start codon, and the 3`D1 primer sequence, 5`-TTCAGGTCTTCGTTCAGGGC-3`, annealed 846bp downstream of the ATG site. The NIT-1 genomic sequences spanning the intended TALEN target site was confirmed to match reference sequences prior to TALEN construction. Genomic DNA was isolated from cells using the Quick-gDNA MiniPrep kit (Zymo) and used at 100ng per PCR reaction. For amplification of each locus, the JumpStart™ TAQ polymerase (Sigma Aldrich) was used in the presence of 1x OneTaq™ GC buffer (NEB) for 30 cycles according to manufacturer protocols. For loss of restriction site assays, half of each PCR product volume was split into two tubes, to which 10x NEBuffer 3 (NEB) was diluted to 1x in the absence (water instead) or presence of the *BglI* restriction enzyme (NEB) and incubated at 37C for 90 minutes. Following digestion, samples of each product were run on 1.5% agarose gels and analyzed using Image Lab v.2.0.1 (Bio-Rad) and GelQuant.NET v1.8.2 (BiochemLabSolutions.com). Remaining amplimers were purified and ligated into the pGEM-T Easy Vector (Promega), which was transformed into DH5α competent cells (Life Technologies), screened by blue/white analysis. The presence of inserts within purified plasmids was confirmed by *EcoRI* digestion (NEB). For each locus, >10 pGEM clones underwent Sanger DNA sequencing (Eurofins MWG Operon). PCR reactions of WT gDNA were performed side-by-side with reactions using gDNA from the cloned cell lines.

2.3. TALEN DESIGN AND PREPARATION

Exon 1 of the H2-D1 (GenBank accession# **14964**) and H2-K1 (GenBank accession# **101056305**) genes from the NOD/ShiLtJ genome were aligned and analyzed for restriction enzyme recognition sites (Figure 1). Nucleotide sequences flanking the *BglI* consensus recognition sites were entered into the ZiFiT Targeter v.4.2 (Sander et al., 2010) and TALEN pairs were constructed using the REAL protocol (Reyon et al., 2012). The TALENs designed to flank the *BglI* consensus site were named the Bgl left and right TALEN plasmids and the nucleotide sequences of each arm are shown in supplemental data (Figures 2 and 3, respectively). The left TALEN was ligated into the JDS74 expression plasmid, while the right TALEN was ligated into JDS70 vector. All TALEN materials were kindly shared by Jorge Piedrahita (NCSU). *In silico* off-target site TALEN-interactions were predicted using the TALENT 2.0 (Doyle et al., 2012).

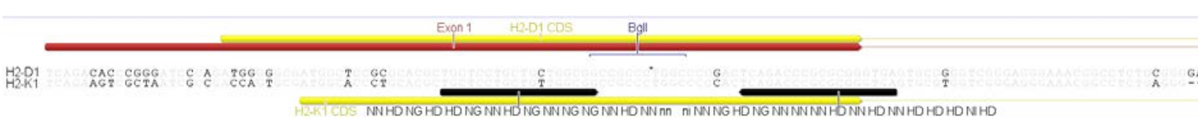

Figure 1. TALEN design for the NIT-1, classical MHCI genes**.** Alignment of genomic exon 1 sequences (red arrow) shows ~80% identity for H2-K1 and H2-D1 loci (GenBank ID# 101056305 and 14964, respectively). The amino acid sequence of the repeat variable domains of each Bgl TALEN are annotated and are responsible for interaction with cognate DNA sequences (black arrows).The Bgl TALEN pair was designed using the ZiFiT program to flank the *BglI* restriction enzyme recognition site (shown in bracket; carrot indicates cleavage site) within the coding sequence of the K1 locus (yellow bar) and constructed using the REAL method.

2.4. GFP REPORTER ASSAY

A protocol using single-strand annealing plasmids (Perez-Pinera et al., 2012) was modified as described below and performed as the readout for TALEN activity in cells. Briefly, the GFP reporter pSSA plasmid (kind gift from Odessa Marks, NCSU; see Supplemental Figure 4 for sequence) was modified to contain a segment of exon 1 from the K1 locus (see Figure 2a), and renamed the pH2 GFP plasmid. A reverse primer encoding the K1 target sequence (5`-CTCCTCGAATTCTCACCCGCGCGGGTCTGAGTGGGGGCCAGGGCGGCCGCCAACAGCAGGAGCATCACTGCTTGTCGGCCATGATATAGACG-3`; K1 nucleotides underlined) was produced by Eurofins MWG Operon and used to amplify a segment from the pSSA plasmid in conjunction with the EGFPA 5` primer, 5`-GAGGAGGCTAGCGGATCCATGGTGAGCAAGGGCGAGGAGC-3`. The PCR amplimers were then digested and ligated to pre-digested pSSA plasmids, and the presence of K1 target sequences were confirmed via Sanger sequencing after plasmid purification processes. Following co-transfection with the Bgl TALEN pair, nuclease-mediated disruption of the pH2 target sequence may result in restoration of the GFP coding sequence by cellular repair mechanisms, and thereby indicate TALEN activity within a single cell. To control for random GFP gene repair, the pSSA plasmid was also co-transfected with the Bgl TALEN pair and GFP expression was monitored by flow cytometry. To confirm that pH2 GFP conversion was Bgl TALEN-specific, we performed experiments in which unrelated TALENs (Bam) were co-transfected into cells as well.

Figure 2. The co-transfection of Bgl left and right TALEN plasmids with the GFP reporter plasmid into NIT-1 cells increases GFP+ cells, genomic modifications, and the percentage of cells that display modified levels of MHCI surface protein. *A)* The pSSA GFP reporter plasmid (green) allows for ligation of the H2-K1 target sequence (cognate TALEN-recognition nucleotides in bold, restriction enzyme recognition site in italics with dash indicating cleavage position) between two dysfunctional GFP coding regions, thus renamed the pH2 GFP plasmid. *B)* Transfection of NIT-1 cells with the incorrect combination of TALEN and GFP reporters (pTAP2 + Bgl, and pH2 + Bam) or the correct combination (pH2 + Bgl) yields higher percentages of GFP+ cells (left panel), but the MFI of these GFP+ cells (right panel) is significantly higher only in cells receiving the correct combination of H2 TALEN and reporter plasmids ($P<0.0001$). Three replicate transfections of each TALEN/GFP reporter combination were performed. *C)* Loss of restriction site analyses of the H2 loci (K1, left panel; D1, right panel) show higher percentages of modifications in pooled genomic DNA from recipients of the Bgl TALEN pair (bulk pH2 + Bgl gDNA) than Bam TALEN recipients (Bulk Bam gDNA). Sorting for GFP+ cells from Bgl co-transfectants (GFP+ pH2 Bgl gDNA) results in higher percentages of genomic modifications at both loci than in unsorted Bgl TALEN-recipients. Genomic DNA was pooled from multiple transfections for each group. *D)* Expression of the K^d and D^b proteins on the surface of Bgl TALEN-recipients is lower than parental or Bam TALEN-recipient cells. Data shown are representative of results from three replicate transfections. Numbers in dot plot indicate the percentage of cells found within the region. *E)* When normalized to protein levels found on the parental WT cells, MFI for K^d (left panel) and D^b (right panel) expression was significantly lower on the surface of Bgl TALEN-recipients (dark bars) than on Bam TALEN-recipients (light bars). Significance values are indicated by the * symbol and indicate the following values: $*P \leq 0.05$; $**P \leq 0.01$; $***P \leq 0.001$; $****P \leq 0.0001$.

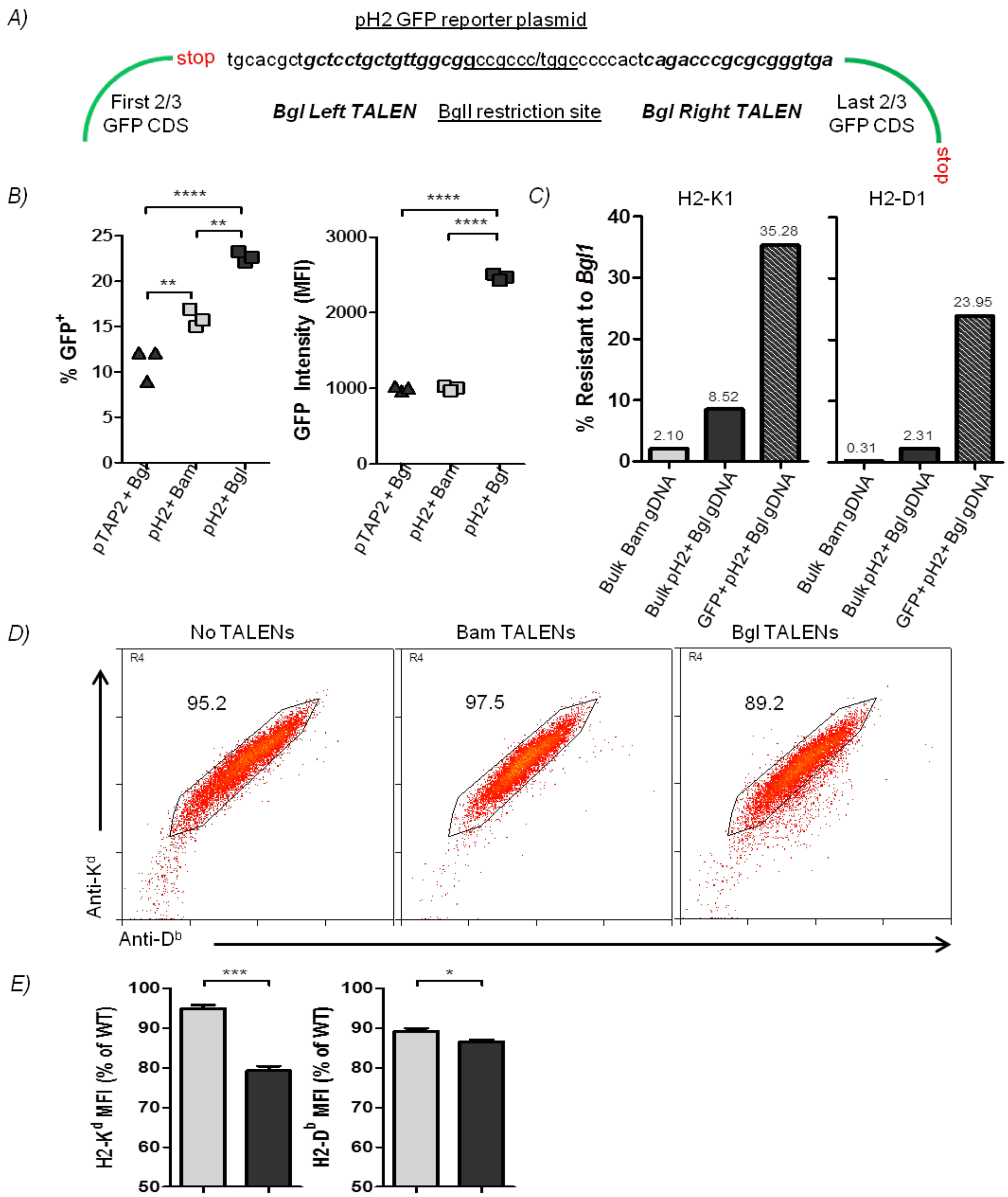

A)
pH2 GFP reporter plasmid
stop
tgcacgctgctcctgctgttggcggccgccc/tggcccccactcagacccgcgcgggtga
First 2/3 GFP CDS
Bgl Left TALEN
BglI restriction site
Bgl Right TALEN
Last 2/3 GFP CDS
stop
B)
% GFP+
GFP Intensity (MFI)
pTAP2+Bgl
pH2+Bam
pH2+Bgl
C)
H2-K1
H2-D1
% Resistant to Bgl1
2.10
8.52
35.28
0.31
2.31
23.95
Bulk Bam gDNA
Bulk pH2+Bgl gDNA
GFP+ pH2+Bgl gDNA
D)
No TALENs
Bam TALENs
Bgl TALENs
95.2
97.5
89.2
Anti-Kd
Anti-Db
E)
H2-Kd MFI (% of WT)
H2-Db MFI (% of WT)

2.5. Flow cytometry

Surface expression of classical MHCI molecules was detected using antibodies (Ab) against H2-K$^{d/b}$ (34-1-2S, BioLegend) conjugated to Alexa Fluor 647(AF647) and H2-D^{b} Ab conjugated to R-phycoerythrin (PE; 28-12-8, Southern Biotech). Flow cytometry data were acquired on a FACSCalibur flow cytometer (BD Biosciences), while fluorescence-based cell sorting (FACSorting) used a Beckman Coulter MoFlo Legacy flow cytometer operated by the NCSU facility. In some experiments, unconjugated primary Ab was used in combination with an AF647-labeled donkey ant-mouse IgG Ab (Jackson ImmunoResearch). Data analysis was performed using Summit software v5.2 (Beckman Coulter). For background fluorescence, labeled cells were compared to unstained cells or cells receiving secondary Ab only. Detection of CD8+ T cells was performed using Ab against CD8α conjugated to allophycocyanin (APC; clone 53-6.7, eBioscience)

2.6. Immune cell isolation and CD8α + cell proliferation and marker expression

The 8.3-NOD strain [NOD.Cg-Tg(TcraTcrbNY8.3)1Pesa/DvsJ] mice were acquired from Jackson Laboratories (and in some cases, 8.3-NOD spleens were kind gifts from Dr. Roland Tisch, UNC-CH) and housed briefly in an Association for Assessment and Accreditation of Laboratory Animal Care-accredited, specific pathogen-free facility. The mice were typically used at 6–8 weeks of age in experiments that were approved by the Institutional Animal Care and Use

Committee of North Carolina State University and adhered to published principles of laboratory animal care. Mice spleens were isolated and disaggregated by manual forceps disruption, and depleted of erythrocytes with ammonium chloride lysis buffer. Cells were washed and resuspended in PBS buffer supplemented with 1% FBS and 2mM EDTA. Enrichment was achieved by magnetic-activated cell sorting (MACS) using CD8α microbeads (130-049-401, Miltenyi Biotec) with LS MACS separation columns (130-042-401, Miltenyi Biotec). Following enrichment, 1×10^7 CD8α+ cells/ml were resuspended in PBS supplemented with 0.1% BSA and labeled with carboxyfluorescein diacetate, succinimidyl ester (CFSE, Life Technologies) at 10µM for 10 minutes at 37C prior to washing with pre-warmed media three times. NIT-1 and -KG cells were pulsed for 3 hours in a 37C water bath with media containing 10µM of the influenza hemagglutinin peptide ($HA_{512\text{-}520}$, GenScript) or in media containing 10 µM NRP-V7 peptide (high antagonism mimotope of $IGRP_{206\text{-}214}$; KYNKANVFL, GenScript) and washed three times prior to seeding in triplicate wells of 96-well plates. $1x10^5$ CD8α+ cells were then seeded with $1x10^5$ peptide-pulsed NIT-1 or -KG lineages; co-cultures were incubated for 48 hours at 37C and 5% CO_2.

For detection of surface activation markers on CD8α+ cells, antibody against CD62L conjugated to PE was applied to non-CFSE-labeled, CD8α+cells that had been co-cultured with NIT cells for three days in conditions as described above. Anti-CD8α antibody conjugated to APC was used to identify positive cells for gating to exclude other cell types found within the culture.

2.7. Interferon gamma (IFNγ) ELISA

Supernatants used in ELISA assays were collected from triplicate wells in co-culture experiments as described in 2.6., but using non-CFSE-labeled CD8+ cells as effectors. The ELISA assay was performed as described previously (Moran et al., 2009). Briefly, plates were coated with anti-mouse IFNγ Ab (clone R4-6A2, BD Pharmingen) and IFNγ protein was detected using a biotin-labeled Ab (XMG1.2, BD Biosciences Pharmingen), followed by incubation with streptavidin-linked horseradish peroxidase then substrate. Standard curves were generated using diluted recombinant murine IFNγ and compared against for quantification of IFNγ in supernatants.

2.8. Statistical analysis

Two-way ANOVA analyses followed by Bonferroni post-test were performed on data from TALEN and GFP co-transfectant assays for comparison of TALEN-mediated changes in GFP expression. Similar analyses were performed for T-cell proliferation and surface marker expression. The Students *t* test was used to compare changes in MHCI MFI on polyclonal BgI TALEN-recipient cells versus the control Bam TALEN-recipient cells.

3. Results

3.1. H2-TARGETING TALEN DESIGN AND GFP REPORTER-BASED SORTING

Regions of interest in the classical H2 loci (H2-K1 and H2-D1) were amplified by PCR of NIT-1 genomic DNA and confirmed to match the reference genomic scaffold sequence (GenBank accession # **NT_187004**, data not shown). Supplemental Figure 1 shows the design of primer sequences used to amplify the genomic H2 loci. When comparing the H2-K1 locus with the H2-D1 locus, we found the sequences share 89% identity across the aligned regions and that exons 1 of each gene contain a *BglI* restriction enzyme recognition site, which is useful in downstream assays used to detect modifications (Bedell et al., 2012). We elected to target our TALENs to exon 1 in order to increase the chances of inducing premature translation disruption through frame-shift mutation events created by faulty cell-intrinsic DNA repair of double-strand breaks (DSB). Figure 1 aligns the exon 1 regions of the NOD classical class I H2 loci, highlights the cognate nucleotide sequences with which the Bgl TALENs interact, and annotates the amino acid sequences of each repeat variable diresidue (RVD) domain found within each TALEN arm. Note that there is one nucleotide difference in the left Bgl TALEN arm recognition region between K1 and D1, and that the TALEN was designed to have greater affinity for the K1 locus.

As a reporter for episomal TALEN activity, we modified a single-strand annealing (SSA) GFP plasmid [sequence available in Supplemental Figure 4; (Perez-Pinera et al., 2012)] to include the TALEN-targeted nucleotide sequence of

H2-K1 into the parental pSSA plasmid between two partially duplicated, dysfunctional GFP coding segments, and we renamed this plasmid pH2 (Figure 2A). When co-transfected with the left and right pair of TALEN plasmids into cells, the episomal SSA GFP coding sequence may be corrected by DNA repair mechanisms to yield functional GFP expression following TALEN-targeted sequence cleavage. To confirm the functional ability of our Bgl TALENs to convert the pH2 reporter, we performed an experiment in which NIT-1 cells were co-transfected with an unrelated SSA GFP reporter construct (pTAP2) and the Bgl TALENs, the pH2 reporter and an unrelated TALEN pair (Bam TALENS), or the pH2 reporter and the Bgl TALEN pair. As seen in the left panel of Figure 2B, when TALEN pairs were unable to recognize the plasmid target sequences (pTAP2 + Bgl or pH2 + Bam), 10-15% of cells became positive for GFP expression. However, when the TALEN pair was able to interact with the target sequence (pH2 + Bgl), a significantly higher proportion (~22%; P<0.01) of cells expressed GFP. Notably, there was significantly higher background conversion of the pH2 GFP reporter compared to the pTAP2 reporter, as seen in cells receiving the wrong TALEN and GFP reporter plasmids. To further characterize the GFP+ co-transfectants, we analyzed the mean fluorescence intensity (MFI) across samples (Figure 2B right panel) and determined that the cells receiving the correct combination of Bgl TALEN and pH2 GFP reporter expressed significantly higher levels of protein (P<0.0001). These data indicate that the Bgl TALENs were able to properly target the nucleotide sequence of interest within the reporter plasmid, and that expression of high levels of GFP within transfectants was TALEN-specific.

To confirm that the Bgl TALENs were able to modify the genomic H2 loci, we utilized a loss of restriction site assay in which genomic DNA is amplified by locus-specific primer sets and the PCR products are then exposed to restriction enzyme digestion prior to gel electrophoresis. If cellular DNA repair mechanisms have introduced insertions/deletions during repair of Bgl TALEN-mediated DSBs, then the *BglI* restriction enzyme recognition site within exon 1 may be disrupted, resulting in amplimers unable to be cut by the enzyme. Figure 2C shows that when cells were transfected with the Bgl TALENs (Bulk pH2+ Bgl gDNA), a modest percentage of each H2 locus PCR product (K1 left panel; D1 right panel) remained uncleaved following exposure to enzyme digestion, while transfection of unrelated TALENs (bulk Bam gDNA) showed similar percentages of H2 loci modifications as untransfected cells (not shown). Genomic DNA for each group was pooled from at least three replicate transfections. The K1 locus showed ~4-fold higher levels of modification than control samples and the D1 locus ~7-fold higher; the percentage of modifications appears low, but our data are in accordance with other studies utilizing TALEN technology to induce genomic modification (Miller et al., 2010) and are likely a result of low co-transfection efficiency, overall low TALEN-mediated disruption of the genome, and apoptotic mechanisms induced by DSB resulting in modified DNA not being retrievable at the time of extraction. Overall, these data indicate that Bgl TALENs successfully induced genomic modifications at the H2 loci.

To confirm the ability of the Bgl TALEN pair to disrupt surface protein expression of the NOD H2-K1 and –D1 gene products (K^d and D^b, respectively), we performed flow cytometry-based analyses of cells from triplicate co-transfection experiments (Figure 2D; representative shown). When the unrelated TALEN pair was co-transfected into NIT-1 cells, recipients showed similar expression profiles for surface MHCI to untransfected cells (Figure 2D, middle and left panels, respectively). Specifically greater than 95% of cells fell within the defined region of MHCI expression. However, Bgl TALEN-recipients showed a lower proportion of cells within this same gate (89.2%), indicating altered protein expression (Figure 2D, right panel). Across transfections, the normalized MFI of K^d expression was significantly lower ($P<0.001$) on Bgl TALEN-recipients than on Bam TALEN-recipients, and D^b expression was also significantly lower ($P<0.05$; Figure 2 E, left and right panels, respectively). Thus, Bgl TALENs successfully lower the surface expression of targeted gene products in a polyclonal population of transfected cells.

To determine whether GFP expression following pH2 and Bgl TALEN co-transfection can identify cells with a higher percentage of genomic modifications, we performed fluorescent-activated cell sorting (FACS) of GFP+ transfectants and screened gDNA from these cells for loss of restriction sites at both loci (Figure 2C, far right bars of each panel). Replicate transfections were performed and cells were pooled during sorting prior to gDNA modification analysis. While bulk Bgl TALEN transfectants displayed 8.52% and 2.31% (K1 and D1 loci, respectively) of uncut product compared to the 2.1% and 0.31% found in samples receiving the wrong

TALENs, the GFP+ samples displayed 35.28% and 23.95% *BglI* resistance. These data indicate that enrichment for genomic modifications at the H2 loci can be achieved by sorting for GFP expression in Bgl TALEN-recipients, with an ~4-fold and ~10-fold increase in modification found at the K1 and D1 loci, respectively, compared to unsorted Bgl TALEN-recipients.

We therefore hypothesized that the strategy of FACS-based enrichment for GFP+ Bgl TALEN-transfectants would result in cell clones with lower expression of surface MHCI proteins. To reduce the effect of the natural distribution seen for MHCI expression on NIT-1 cells (Figure 2D, left panel), we performed MACS-based enrichment to produce a polyclonal NIT-1 group with high MHCI expression (data not shown). We then co-transfected this line with Bgl TALENs and the GFP reporter plasmids, sorted based on GFP expression, and isolated clones for flow cytometry analyses of K^d and D^b proteins (Figure 3). When normalized to expression values of an untransfected $MHCI^{high}$ NIT-1 cell clone, 7 of the 19 (36.8%) TALEN-transfected NIT-1 clones screened expressed <34% of the normalized K^d or D^b protein values, while only 15.8% of clones expressed both proteins at >66% of the normalized values. Interestingly, most clones appeared to simultaneously express lower levels of both proteins, likely indicating that when Bgl TALEN presence is high within a cell, both H2 loci will be modified.

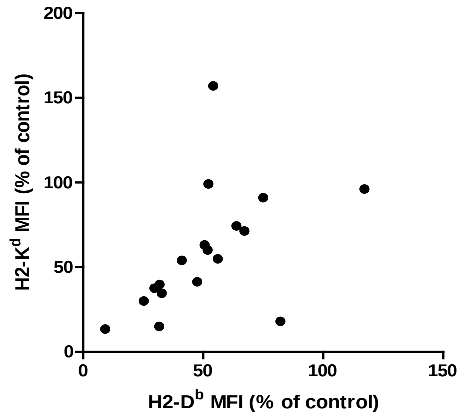

Figure 3. GFP-sorted, TALEN-transfected NIT-1 cell clones express altered surface protein values compared to a MHCI^{high} clone. A polyclonal MHCI^{high} population of NIT-1 cells was transfected with the Bgl TALENs and pH2 reporter constructs, sorted for GFP expression, and ring-isolated to produce clones. Twenty clones were selected based upon growth kinetics similar to the parental line and screened for K^{d} and D^{b} expression via flow cytometry: one cell line turned out to be a dual population, while the remaining 19 clones were normalized to protein expression values of an unmanipulated MHCI^{high} clone.

Overall, TALENs designed to target exon 1 regions in the H2 loci within NIT-1 cells are capable of modifying the genomic sequences and disrupting surface protein expression; the use of a GFP reporter and FACS selection techniques can enrich the proportion of cells possessing TALEN-mediated modification; ultimately, transfectants sorted for increased TALEN activity yield cell clones with altered H2 protein expression profiles.

3.2. THE NIT-KG CELL LINE LACKS H2 PROTEIN EXPRESSION DUE TO TALEN-MEDIATED GENOMIC LOCI MODIFICATIONS

We selected a cell clone, derived from WT co-transfected NIT-1 cells sorted for GFP expression, for further characterization and for use in experiments measuring diabetogenic CD8+ T-cell recognition. This clone, designated KG, expresses neither K^d nor D^b proteins (Figure 4) even when exposed to interferon gamma (IFNγ), a cytokine well known to upregulate classical MHCI gene expression in NIT-1 cells (Hamaguchi et al., 1991).

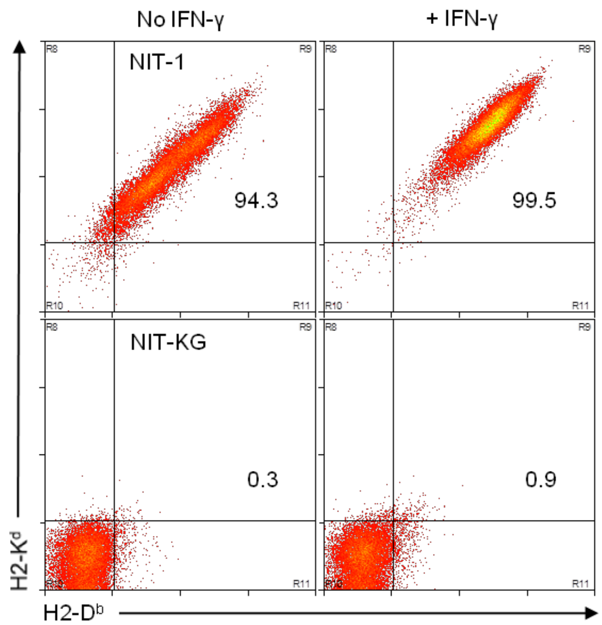

Figure 4. The GFP+, TALEN-recipient cell clone, NIT-KG, lacks surface MHCI protein. The parental NIT-1 cells (WT, top left panel) increase expression of both K^d (Y axis) and D^b (X axis) MHCI proteins following exposure to 100 units/ml of IFNγ overnight (top right). Yet, the KG cell line (bottom left) lacks expression of both proteins, even following IFNγ treatment (bottom right).

We next sought to confirm that the H2 loci within KG cells contained modifications at both alleles of each gene, as the flow cytometry results indicated. Figure 5A depicts the possible results of single allele or double allele modifications occurring at either locus during the loss of restriction site assay. Analysis of the K1 locus of KG determined that both chromosomal sequences were disrupted (Figure 5B). Interestingly, results shown in Figure 5C indicate that only one allele of the D1 locus was modified. This result seemingly contradicts the above flow cytometry data; however, certain genomic modifications may yield false negatives due to limitations in our loss of restriction site assay, as will be discussed in section 4.

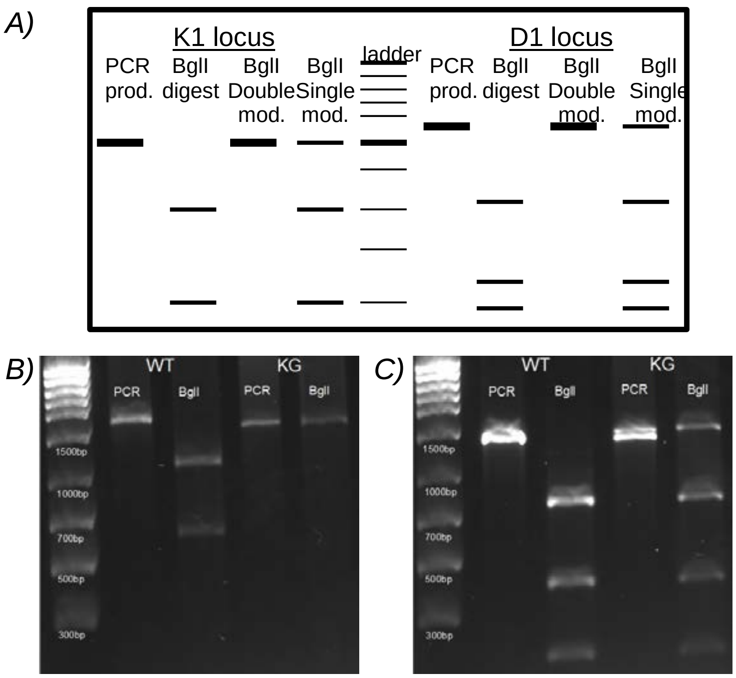

Figure 5. The loss of restriction site assay indicates the NIT-KG clone contains modified genomic MHCI loci. *A)* Cartoon schematic depicting the bands produced following PCR amplification of genomic DNA and subsequent restriction enzyme digestion on an electrophoresed agarose gel. PCR amplicon bands from the genomic K1 and D1 loci without digestion enzyme (PCR prod.) or digested with the *BglI* enzyme for 90 minutes are shown. If the locus is unmodified by TALEN activity, the amplicons are completely fragmented within the agarose gel following enzyme exposure (BglI digest). However, if TALEN activity has induced modifications, the *BglI* recognition site may be lost, resulting in the inability of the product to be fragmented. *B)* The loss of restriction site assay indicates modification of both K1 alleles within the KG clone. *C)* Analysis of the D1 locus of KG detects one allele incapable of being digested. Also note that there are two bands present in the KG PCR product and the slightly larger product is indigestible.

To determine the exact genomic modifications within the KG cell clone, we performed DNA sequencing of TA clones containing amplimers from each H2 locus. Of importance, we never found any DNA sequences (>10 pGEM clones screened) from WT loci other than those matching the reference data. As expected, the K1 locus within KG contained two alleles possessing modified sequences (named Kd mod. 1 and 2; Figure 6A). Surprisingly, the K1 alleles detected were novel, hybrid sequences that appear to have undergone gene conversion downstream of the TALEN-mediated DSBs. Figure 6B proposes the truncated coding sequences of each novel allele as based on analyses of translations utilizing the exonic structure of the K2 locus, the template used for gene repair as determined by BLAST analysis. Sequencing of the D locus within KG, Figure 6C, also returned two modified alleles, indicated as Db mod. 1 and 2. The insertion of 4 base pairs (bp) at the TALEN-targeted site within Db mod. 1 yields a frame shift and formation of a premature stop codon in exon 2, Figure 6D. This modification results in a sequence still recognizable by the *BglI* restriction enzyme, explaining the anomaly seen in the loss of restriction site analysis (Figure 5C). The Db mod. 2 allele possesses insertion of an exogenous sequence that matches a portion of the simian virus 40 (SV40) polyadenylation signal found within the TALEN expression constructs. Furthermore, following the insertion event appears a recombined sequence that matches the H2-Q4 locus; nonetheless, translation of the novel Db mod. 2 allele results in gene truncation. The likelihood that hybrid sequences were created by template switching during PCR amplification reactions is low, as we routinely sequenced numerous TA clones from concurrent WT reactions and never found such recombination. All of these results indicate that the KG cell line lacks the ability to express classical MHCI proteins as a result of modifications of H2 genes induced by TALEN activity.

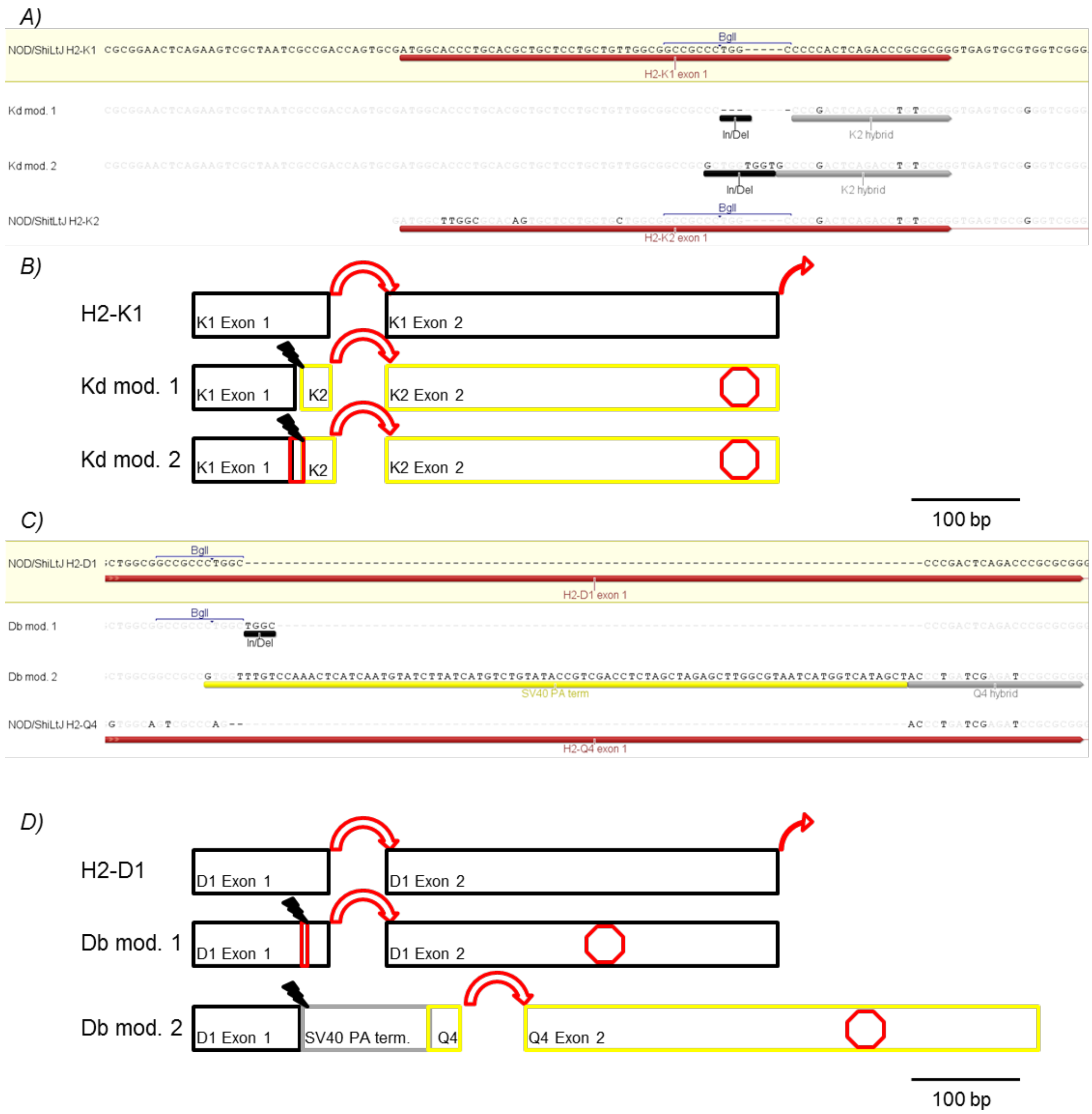

Figure 6. The NIT-KG clone possesses modified genomic MHCI loci that result in frame-shift mutations. *A)* Sequencing of 12 pGEM clones containing K1 amplicons detects 2 novel alleles (Kd mod. 1 and 2) that contain sequences identical to the K2 locus downstream of the TALEN target site. The Kd mod. 1 allele is comprised of a 4 bp deletion event followed by the K2 template. The Kd mod. 2 allele contains a single bp substitution and a 5 bp insertion prior to the K2 template. *B)* Schematic depicting the coding sequences of the modified alleles compared to the reference structure highlighting that the altered reading frames result in stop codons being produced 231 bp into exon 2 of each novel allele. *Note*: introns are not to scale. *C)* D1 amplicon sequencing from the KG clone also shows modifications, such as a 4 bp insertion in the Db mod. 1 allele, and insertion and recombination events in the Db mod. 2 allele. The Db mod. 2 allele includes 88 bp of the SV40 polyA termination sequence and contains sequences identical to the H2-Q4 locus 3` of the TALEN recognition site. *D)* Cartoon schematics highlight the new stop codons created post-modification. The Db mod. 1 allele retains the D1 sequence 3` of the TALEN site, but a frame-shift results in a stop codon 138 bp into exon 2. The Db mod. 2 allele introduces 29 new amino acids but creates a stop codon 222 bp into exon 2 of the Q4 locus. *Note:* More than 10 pGEM clones were sequenced for each WT locus and never returned a sequence other than expected.

3.3. KG CELLS ESCAPE RECOGNITION BY CD8+ T CELLS

We next sought to determine whether the KG cell clone would fail to stimulate K^d-restricted CD8+ T cells specific for islet antigen. To accomplish this, we isolated CD8α+ cells by positive magnetic selection from splenocytes of 8.3-NOD mice, which express a transgenic TCR that recognizes IGRP peptide and its high affinity mimotope NRP-V7 (Lieberman et al., 2003; Verdaguer et al., 1997). As seen in Figure 7A, co-culture of 8.3-NOD CD8+ cells with NRP-V7-pulsed NIT-1 cells results in significantly higher (P>0.0001) proliferation compared with NIT-KG cells. Similarly significant results are found when effector cells are monitored for shedding of surface CD62L in the presence of NIT-1 cells pulsed with cognate antigen, Figure 7B. Interestingly, loss of CD62L was also found to be significantly higher for NIT-1 cells pulsed with HA peptide compared to KG pulsed with either peptide (P<0.001; note that this statistical result is not depicted on graph), indicating endogenously expressed IGRP that is presented by MHCI on NIT-1 cells can induce loss of this marker on effectors but does not induce detectable proliferation, as seen in Figure 7A. Finally, effector cells cultured with WT NIT-1 cells produced IFNγ at detectable levels, while minimal IFNγ was detected following culture with KG cells, Figure 7C. These data indicate that KO of the H2-K1 locus within the KG cell line effectively protects this clone from K^d-restricted, diabetogenic CD8+ T cell recognition.

Figure 7. CD8+ T cells specific for IGRP-K^d do not respond to the KG cell line pulsed with the high affinity cognate peptide (NRP-V7). A) Effector cells proliferate in the presence of NRP-V7-pulsed WT NIT-1 cells, but not when exposed to KG cells pulsed with cognate antigen. Representative flow cytometry histogram of biological replicates from one experiment, left panel. Effector cells proliferate significantly less in the presence of KG cells pulsed with peptide than WT cells pulsed with peptide, right panel. B) Shedding of the CD62L surface marker by effector cells occurs only in cultures containing NRP-V7-pulsed NIT-1 cells; left panel depicts representative sample from two experiments. Right panel shows significant differences in CD62L expression on effector cells cultured with cognate peptide-pulsed WT cells. *C)* Diabetogenic effectors produce IFNγ protein above the level of ELISA detection limits in the presence of NRP-V7-pulsed NIT-1 cells. Supernatants were pooled from two wells of six replicate co-cultures that were then assayed in duplicate on ELISA plates. Assay duplicates were then averaged to represent a single dot on the chart.

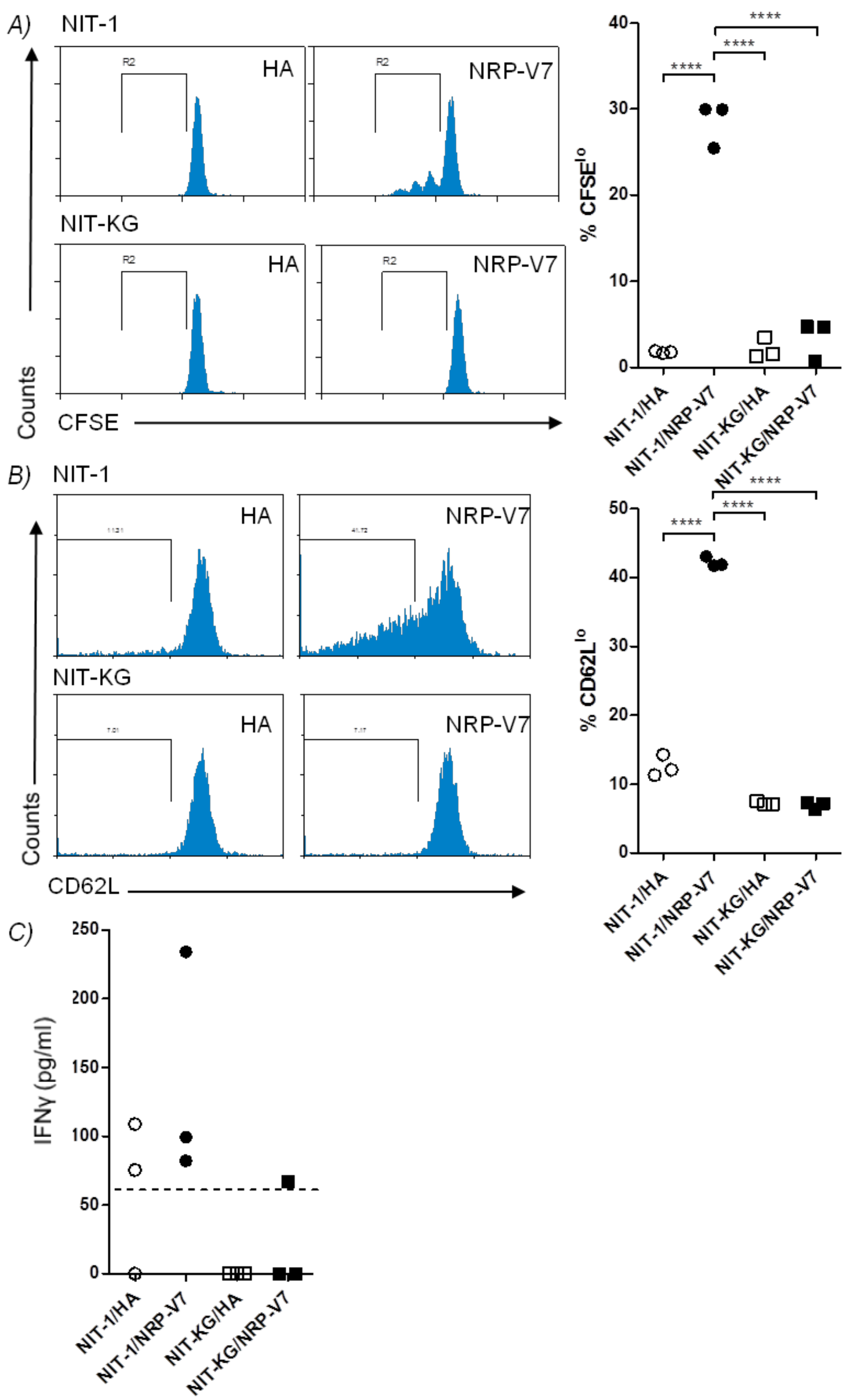
A)
NIT-1
HA
NRP-V7
NIT-KG
HA
NRP-V7
Counts
CFSE
% CFSE^{lo}
NIT-1/HA
NIT-1/NRP-V7
NIT-KG/HA
NIT-KG/NRP-V7
B)
NIT-1
HA
NRP-V7
NIT-KG
HA
NRP-V7
Counts
CD62L
% CD62L^{lo}
NIT-1/HA
NIT-1/NRP-V7
NIT-KG/HA
NIT-KG/NRP-V7
C)
IFNγ (pg/ml)
NIT-1/HA
NIT-1/NRP-V7
NIT-KG/HA
NIT-KG/NRP-V7

4. Discussion

In this study, we addressed the question of whether TALEN-mediated modifications of the classical H2 loci in insulin producing cells result in escape from recognition by diabetogenic T cells. Data shown here reaffirm the usefulness of TALEN-mediated re-engineering of genes related to disease (Liu et al., 2012; Ma et al., 2013; Ousterout et al., 2013), though certain precautions, discussed herein, must be taken before utilizing TALENs to KO genes within a highly homologous family. We provide further proof of concept that genetically engineering beta cells to prevent classical MHCI expression results in escape from CD8+ T-cell autoreactivity in a murine diabetes model (Prange et al., 2001; Xiang et al., 2008; Young et al., 2004), and provide groundwork for *in vivo* studies to expand these results, possibly in the realm of stem cells differentiated into physiologically-responsive insulin producing cells.

The abilities to detect and enrich for TALEN activity are important due to the low frequency at which TALEN-mediated modifications may occur (Miller et al., 2010), thus robust and high-throughput assays are necessary. In this study we performed loss of restriction site analyses and GFP reporter assays for detecting TALEN activity, but the following points should be considered. Specifically, the *BglI* enzyme that we applied in this study for loss of restriction site detection recognizes the promiscuous sequence of 5`-GCCNNNN▼NGGC-3`, thereby allowing some insertion/deletion and homology-directed recombination (HDR) events, which may ultimately disrupt the coding sequence, to retain cleavability. Thus, other means [e.g.

the Surveyor nuclease assay (Guschin et al., 2010); or high-resolution melt analysis (Panda et al., 2013)] of detecting genomic modifications in TALEN-recipient populations may be more useful in certain circumstances, though each assay will inherently have its own limitations. Enrichment of TALEN-modified cell clones via drug resistance and exogenous protein induction has been shown previously (Kim et al., 2013; Wang et al., 2013), and we utilized a similar concept by way of a modified SSA GFP reporter construct. The SSA GFP plasmid was initially used as a measure of DNA repair activity following zinc-finger nuclease transfection (Perez-Pinera et al., 2012), but here we show further usefulness of this reporter for enrichment purposes (Figure 2C). As our goal was to select clones with low surface H2 protein expression, we could have directly selected $H2^{low}$ TALEN-recipients by cell sorting, however we intended to determine the spectrum of possible KO phenotypes. Yet, as seen in Figure 3, enrichment of cells for TALEN activity resulted primarily in modifications at both loci, indicating the high efficiency of the Bgl TALENs at both loci within transfectants. The overall efficiency-limiting step in generating KO clones appears to be the TALEN activity as seen by the difference in TALEN-specific GFP conversion versus random conversion in transfected NIT-1 cells (~7%, Figure 2B), and also measurable by *BglI* resistance (Figure 2C). Therefore, future experiments creating new modification-detecting assays or enrichment strategies are warranted and will be advantageous to the process of genetically engineering tissues.

The issue of HDR in genes following TALEN-induced DSB repair is of special importance to our study when one considers that the Major Histocompatibility

Complex is thought to have evolved primarily by gene duplication events and exon shuffling [reviewed in (Danchin et al., 2004)]. Firstly, design of PCR primers for the targeted loci was difficult because of high identity values between genes, and the inability for the designed primers to cross-react with other loci may have been a cause for amplification resistance of modified loci in some screened cell clones (data not shown). Secondly, HDR events, such as those seen in the KG clone (Figure 6), could result in hybrid gene products being translated, which may in turn allow *de novo* antigen presentation and rejection responses similar to those seen during other gene correction strategies (Mendell et al., 2010). Thus, more stringent clone selection strategies involving sequencing of the target locus to eliminate clones possessing such recombination would lower the overall efficiency by reducing the actual amount of useful clones. In the KG clone scenario however, immunogenicity of putative *de novo* antigens would likely not be an issue due to the modified cell being invisible to CD8+ T-cell recognition (Figure 7), unless the hybrid MHCI product is expressed at the cell surface and recognizable by alloreactive cells, which is also unlikely here due to stop codon creation early in the modified coding sequences. Thirdly, the possibility of off-target TALEN-modifications is increased when targeting genes in a family with high homology, though *in silico* tools are available to reduce such interactions (Doyle et al., 2012) and our *in silico* analyses determined that no other sites within the NOD/ShiLtJ genome are recognized by the Bgl TALENs (data not shown). Conversely, the build-a-block characteristic of TALEN construction allows one to intentionally discriminate between loci, allowing for very precise gene targeting (Mak et al., 2013; Wicky et al., 2013). Additionally, the intentional manipulation of HDR events has allowed for the use of homology arm-containing plasmids to be co-transfected with TALENs to introduce exogenous sequences at the site of gene disruption (Miller et al., 2010). Thus, one must thoroughly analyze such considerations in order to design TALENs specific to the target locus and to attain the intended effects without off-target manipulations occurring simultaneously.

Our TALEN design was successful in disrupting classical MHCI expression in NIT-1 cells, but such manipulation could have been achieved by targeting various other components within the class I antigen processing pathway; the transporters associated with antigen processing (TAP), the beta-2-microglobulin (β2M) light chain, or the class I heavy chains ($K^{d/b}$ and D^{b}) have all been disrupted previously to create MHCI-deficient cells/organisms (Powis et al., 1991; Zijlstra et al., 1990; Vugmeyster et al., 1998; Kärre et al., 1986). The heterodimeric TAP complex shuttles peptides into the endoplasmic reticulum for association with MHCI complexes, however TAP function is required for the presentation of peptides by the non-classical murine Qa-1 and -2 molecules (Aldrich et al., 1994; Tabaczewski and Stroynowski, 1994), and some diabetogenic CD8+ T cells recognize TAP-independent epitopes presented by classical MHCI (Skowera et al., 2008), thus KO of this gene could still result in rejection of modified beta cells. The β2M light chain molecule stabilizes a trimolecular complex with classical MHCI heavy chain and peptide to allow surface expression but is required for stabilization of other MHCI-like complexes as well (Hassan and Ahmad, 2011; Robinson et al., 1998), thereby making it a poor choice if one intends to retain non-classical MHCI expression. Furthermore, in certain circumstances cells are capable of utilizing cross-species β2M molecules found in sera used for cell cultures to stabilize MHCI expression (Bernabeu et al., 1984), thereby possibly counteracting such a β2M-KO strategy *in vitro* or *in vivo*. Although transplantation studies have shown survival of β2M-KO islet and pancreas grafts in diabetic NOD mice (Prange et al., 2001; Xiang et al., 2008, respectively), the precise mechanisms by which graft rejection occurred in 25% of the combined recipients (2 of 6, and 3 of 14, respectively) was not determined. We therefore elected to target our Bgl TALENs to disrupt the heavy chain molecules themselves, attempting to leave intact the ability to express non-classical MHCI complexes at the cell surface.

We show here the ability of Bgl TALEN-modifications to protect a murine beta cell line from diabetogenic CD8+ T-cell recognition (Figure 7). This type of evasive strategy naturally occurs during certain types of viral infection and malignant transformation of cells (Maudsley and Pound, 1991), indicating it as an evolutionarily intelligent approach to apply to grafts in hopes of preventing immune-mediated rejection (Horst et al., 2011). However, this strategy of modifying grafts could theoretically result in transplanted cells that either transform into malignancies or are capable of being viral reservoirs due to non-recognition by immune cells that normally inhibit development of these pathologic conditions and will need to be addressed in future studies. Thusly, the addition of exogenous genes that cause transplanted cells to become susceptible to targeted destruction via pharmaceutical therapies while leaving normal recipient cells safe would be highly valuable in such MHCI-KO cells (Di Stasi et al., 2011), and these “kill switch” genes could be inserted via TALEN technology at the time of gene disruption by way of HDR. Ideally, TALEN-modified graft tissues should be rigidly screened prior to transplantation to insure minimal genomic aberrations have arisen during the clonal selection processes. The use of comparative genomic hybridization, exome sequencing, high resolution melting analysis, and other as-yet defined techniques would be highly valuable prior to clinical transplantation of engineered tissues.

4.1. Conclusions

TALEN-mediated modification of the MHCI genes in a murine insulinoma cell line results in non-recognition by beta cell-specific CD8+ T cells. The results of this study support further *in vivo* experiments using TALENized beta cells as grafts to further elucidate rejection requirements for immunologic acceptance of the grafted cells in diabetic recipients. Alternative strategies of confirming and enriching for TALEN-mediated modifications will be useful in the creation of other genetically engineered tissues, which should be screened thoroughly and incorporate fail-safe components in order to prevent adverse reactions, for use in disease amelioration.

Supplemental Data

Supplemental Figure 1. Alignment of genomic sequences from H2-K1 and –D1 (GenBank ID# **101056305** and **14964**, respectively)flanking the TALEN target site indicates 89% identity of nucleotides shared. Primer pairs for each loci are highlighted along with the primer name. Note that the D1 amplicon contains 2 *BglI* recognition sites, while the K1 locus only possesses this site in the spacer between the TALEN pair.

GCTAGCACCATGGACTACAAAGACCATGACGGTGATTATAAAGATCATGACATCGAT
TACAAGGATGACGATGACAAGATGGCCCCCAAGAAGAAGAGGAAGGTGGGCATTCA
CCGCGGGGTACCTATGGTGGACTTGAGGACACTCGGTTATTCGCAACAGCAACAGG
AGAAAATCAAGCCTAAGGTCAGGAGCACCGTCGCGCAACACCACGAGGCGCTTGT
GGGGCATGGCTTCACTCATGCGCATATTGTCGCGCTTTCACAGCACCCTGCGGCGC
TTGGGACGGTGGCTGTCAAATACCAAGATATGATTGCGGCCCTGCCCGAAGCCACG
CACGAGGCAATTGTAGGGGTCGGTAAACAGTGGTCGGGAGCGCGAGCACTTGAGG
CGCTGCTGACTGTGGCGGGTGAGCTTAGGGGGCCTCCGCTCCAGCTCGACACCGG
GCAGCTGCTGAAGATCGCGAAGAGAGGGGGAGTAACAGCGGTAGAGGCAGTGCAC
GCCTGGCGCAATGCGCTCACCGGGGCCCCCTTGAACCTGACCCCAGACCAGGTAG
TCGCAATCGCGAACAATAATGGGGGAAAGCAAGCCCTGGAAACCGTGCAAAGGTTG
TTGCCGGTCCTTTGTCAAGACCACGGCCTTACACCGGAGCAAGTCGTGGCCATTGC
ATCCCACGACGGTGGCAAACAGGCTCTTGAGACGGTTCAGAGACTTCTCCCAGTTC
TCTGTCAAGCCCACGGGCTGACTCCCGATCAAGTTGTAGCGATTGCGTCCAACGGT
GGAGGGAAACAAGCATTGGAGACTGTCCAACGGCTCCTTCCCGTGTTGTGTCAAGC
CCACGGTTTGACGCCTGCACAAGTGGTCGCCATCGCCAGCCATGATGGCGGTAAG
CAGGCGCTGGAAACAGTACAGCGCCTGCTGCCTGTACTGTGCCAGGATCATGGACT

Supplemental figure 2. Nucleotide sequence of the BglI TALEN left insert that was ligated into the JDS74 expression construct prior to co-transfection. The TALEN sequenced was designed using the ZiFiT software available online and constructed using the Joung lab REAL TALEN assembly protocol.

GCTAGCACCATGGACTACAAAGACCATGACGGTGATTATAAAGATCATGACATCGAT
TACAAGGATGACGATGACAAGATGGCCCCCAAGAAGAAGAGGAAGGTGGGCATTCA
CCGCGGGGTACCTATGGTGGACTTGAGGACACTCGGTTATTCGCAACAGCAACAGG
AGAAAATCAAGCCTAAGGTCAGGAGCACCGTCGCGCAACACCACGAGGCGCTTGT
GGGGCATGGCTTCACTCATGCGCATATTGTCGCGCTTTCACAGCACCCTGCGGCGC
TTGGGACGGTGGCTGTCAAATACCAAGATATGATTGCGGCCCTGCCCGAAGCCACG
CACGAGGCAATTGTAGGGGTCGGTAAACAGTGGTCGGGAGCGCGAGCACTTGAGG
CGCTGCTGACTGTGGCGGGTGAGCTTAGGGGGCCTCCGCTCCAGCTCGACACCGG
GCAGCTGCTGAAGATCGCGAAGAGAGGGGGAGTAACAGCGGTAGAGGCAGTGCAC
GCCTGGCGCAATGCGCTCACCGGGGCCCCCTTGAACCTGACCCCAGACCAGGTAG
TCGCAATCGCGTCACATGACGGGGGAAAGCAAGCCCTGGAAACCGTGCAAAGGTT
GTTGCCGGTCCTTTGTCAAGACCACGGCCTTACACCGGAGCAAGTCGTGGCCATTG
CAAGCAACATCGGTGGCAAACAGGCTCTTGAGACGGTTCAGAGACTTCTCCCAGTT
CTCTGTCAAGCCCACGGGCTGACTCCCGATCAAGTTGTAGCGATTGCGTCGCATGA
CGGAGGGAAACAAGCATTGGAGACTGTCCAACGGCTCCTTCCCGTGTTGTGTCAAG
CCCACGGTTTGACGCCTGCACAAGTGGTCGCCATCGCCAGCCATGATGGCGGTAA
GCAGGCGCTGGAAACAGTACAGCGCCTGCTGCCTGTACTGTGCCAGGATCATGGA

Supplemental figure 3. Nucleotide sequence of the BglI TALEN right insert that was ligated into the JDS70 expression construct prior to co-transfection. The TALEN sequenced was designed using the ZiFiT software available online and constructed using the Joung lab REAL TALEN assembly protocol.

TTCGAGCTCGCCCGAATTGATTATTGACAGTTATTAATAGTAATCATTACGGGGTCATTAGTTCATAGCCCATATATGGAGTTCCGCGTTA
CATAACTTACGGTAAATGGCCCGCCTGGCTGACCGCCCAACGACCCCCGCCCATTGACGTCAATAATGACGTATGTTCCCATAGTAACG
CCAATAGGGACTTTCCATTGACGTCAATGGGTGGAGTATTTACGGTAAACTGCCCACTTGGCAGTACATCAAGTGTATCATATGCCAAGT
ACGCCCCCTATTGACGTCAATGACGGTAAATGGCCCGCCTGGCATTATGCCCAGTACATGACCTTATGGGACTTTCCTACTTGGCAGTA
CATCTACGTATTAGTCATCGCTATTACCATGGTGATGCGGTTTTGGCAGTACATCAATGGGCGTGGATAGCGGTTTGACTCACGGGGAT
TTCCAAGTCTCCACCCCATTGACGTCAATGGGAGTTTGTTTTGGCACCAAAATCAACGGGACTTTCCAAAATGTCGTAACAACTCCGCCC
CATTGACGCAAATGGGCGGTAGGCGTGTACGGTGGGAGGTCTATATAAGCAGAGCTCGTTTAGTGAACCGTCAGATCGCCTGGAGACG
CCATCCACGCTGTTTTGACCTCCATAGAAGACACCGGGACCGATCCAGCCTCCGCGGCCGGGAACGGTGCATTGGAACGCGGATTCCC
CGTGCCAAGAGTGACGTAAGTACCGCCTATAGAGTCTATAGGCCCACCCCCTTGGAATTCGCCATGGACTACAAAGACCATGACGGTGA
TTATAAAGATCATGACATCGATTACAAGGATGACGATGACAAGATGGCCCCCAAGAAGAAGAGGAAGGTGGGCCGCCTCGAGCACCAC
ACCGGTGCGGCCGCCCGCGCCCTGGTGAAGAGCGAGCTGGAGGAGAAGAAGTCCGAGCTGCGGCACAAGCTGAAGTACGTGCCCCA
CGAGTACATCGAGCTGATCGAGATCGCCAGGAACCCCACCCAGGACCGCATCCTGGAGATGAAGGTGATGGAGTTCTTCATGAAGGTG
TACGGCTACAGGGGAGAGCACCTGGGCGGAAGCAGAAAGCCTGACGGCGCCATCTATACAGTGGGCAGCCCCATCGATTACGGCGTG
ATCGTGGACACAAAGGCCTACAGCGGCGGCTACAATCTGCCTATCGGCCAGGCCGACGAGATGCAGAGATACGTGAAGGAGAACCAG
ACCCGGAATAAGCACATCAACCCCAACGAGTGGTGGAAGGTGTACCCTAGCAGCGTGACCGAGTTCAAGTTCCTGTTCGTGAGCGGCC
ACTTCAAGGGCAACTACAAGGCCCAGCTGACCAGGCTGAACCGCAAAACCAACTGCAATGGCGCCGTGCTGAGCGTGGAGGAGCTGC
TGATCGGCGGCGAGATGATCAAAGCCGGCACCCTGACACTGGAGGAGGTGCGGCGCAAGTTCAACAACGGCGAGATCAACTTCTGATT
AATTAACTATCTAGAGTCGACCGCAGAAGCTTGGCGGGCATGGCCCAACTTGTTTATTGCAGCTTATAATGGTTACAAATAAAGCAATAG
CATCACAAATTTCACAAATAAAGCATTTTTTTCACTGCATTCTAGTTGTGGTTTGTCCAAACTCATCAATGTATCTTATCATGTCTGGATCG
ATCGGGAATTAATTCGGCGCAGCACCATGGCCTGAAATAACCTCTGAAAGAGGAACTTGGTTAGGTACCTTCTGAGGCGGAAAGAACCA
GCTGTGGAATGTGTGTCAGTTAGGGTGTGGAAAGTCCCCAGGCTCCCCAGCAGGCAGAAGTATGCAAAGCATGCATCTCAATTAGTCA
GCAACCAGGTGTGGAAAGTCCCCAGGCTCCCCAGCAGGCAGAAGTATGCAAAGCATGCATCTCAATTAGTCAGCAACCATAGTCCCGC
CCCTAACTCCGCCCATCCCGCCCCTAACTCCGCCCAGTTCCGCCCATTCTCCGCCCCATGGCTGACTAATTTTTTTTATTTATGCAGAGG
CCGAGGCCGCCTCGGCCTCTGAGCTATTCCAGAAGTAGTGAGGAGGCTTTTTTGGAGGCCTAGGCATTTGCAAAAAGCTGTTAACAGCT
TGGCACTGGCCGTCGTTTTACAACGTCGTGACTGGGAAAACCCTGGCGTTACCCAACTTAATCGCCTTGCAGCACATCCCCCCTTCGCC
AGCTGGCGTAATAGCGAAGAGGCCCGCACCGATCGCCCTTCCCAACAGTTGCGTAGCCTGAATGGCGAATGGCGCCTGATGCGGTATT
TTCTCCTTACGCATCTGTGCGGTATTTCACACCGCATACGTCAAAGCAACCATAGTACGCGCCCTGTAGCGGCGCATTAAGCGCGGCGG
GTGTGGTGGTTACGCGCAGCGTGACCGCTACACTTGCCAGCGCCCTAGCGCCCGCTCCTTTCGCTTTCTTCCCTTCCTTTCTCGCCACG
TTCGCCGGCTTTCCCCGTCAAGCTCTAAATCGGGGGCTCCCTTTAGGGTTCCGATTTAGTGCTTTACGGCACCTCGACCCCAAAAAACT
TGATTTGGGTGATGGTTCACGTAGTGGGCCATCGCCCTGATAGACGGTTTTTCGCCCTTTGACGTTGGAGTCCACGTTCTTTAATAGTG
GACTCTTGTTCCAAACTGGAACAACACTCAACCCTATCTCGGGCTATTCTTTTGATTTATAAGGGATTTTGCCGATTTCGGCCTATTGGTT
AAAAAATGAGCTGATTTAACAAAAATTTAACGCGAATTTTAACAAAATATTAACGTTTACAATTTTATGGTGCACTCTCAGTACAATCTGCT
CTGATGCCGCATAGTTAAGCCAACTCCGCTATCGCTACGTGACTGGGTCATGGCTGCGCCCCGACACCCGCCAACACCCGCTGACGCG
CCCTGACGGGCTTGTCTGCTCCCGGCATCCGCTTACAGACAAGCTGTGACCGTCTCCGGGAGCTGCATGTGTCAGAGGTTTTCACCGT
CATCACCGAAACGCGCGAGGCAGTATTCTTGAAGACGAAAGGGCCTCGTGATACGCCTATTTTTATAGGTTAATGTCATGATAATAATGG
TTTCTTAGACGTCAGGTGGCACTTTTCGGGGAAATGTGCGCGGAACCCCTATTTGTTTATTTTTCTAAATACATTCAAATATGTATCCGCT
CATGAGACAATAACCCTGATAAATGCTTCAATAATATTGAAAAAGGAAGAGTATGAGTATTCAACATTTCCGTGTCGCCCTTATTCCCTTT
TTTGCGGCATTTTGCCTTCCTGTTTTTGCTCACCCAGAAACGCTGGTGAAAGTAAAAGATGCTGAAGATCAGTTGGGTGCACGAGTGGG
TTACATCGAACTGGATCTCAACAGCGGTAAGATCCTTTGAGAGTTTTCGCCCCGAAGAACGTTTTCCAATGATGAGCACTTTTAAAGTTCT
GCTATGTGGCGCGGTATTATCCCGTGATGACGCCGGGCAAGAGCAACTCGGTCGCCGCATACACTATTCTCAGAATGACTTGGTTGAGT
ACTCACCAGTCACAGAAAAGCATCTTACGGATGGCATGACAGTAAGAGAATTATGCAGTGCTGCCATAACCATGAGTGATAACACTGCG
GCCAACTTACTTCTGACAACGATCGGAGGACCGAAGGAGCTAACCGCTTTTTTGCACAACATGGGGGATCATGTAACTCGCCTTGATCG
TTGGGAACCGGAGCTGAATGAAGCCATACCAAACGACGAGCGTGACACCACGATGCCAGCAGCAATGGCAACAACGTTGCGCAAACTA
TTAACTGGCGAACTACTTACTCTAGCTTCCCGGCAACAATTAATAGACTGGATGGAGGCGGATAAAGTTGCAGGACCACTTCTGCGCTC
GGCCCTTCCGGCTGGCTGGTTTATTGCTGATAAATCTGGAGCCGGTGAGCGTGGGTCTCGCGGTATCATTGCAGCACTGGGGCCAGAT
GGTAAGCCCTCCCGTATCGTAGTTATCTACACGACGGGGAGTCAGGCAACTATGGATGAACGAAATAGACAGATCGCTGAGATAGGTG
CCTCACTGATTAAGCATTGGTAACTGTCAGACCAAGTTTACTCATATATACTTTAGATTGATTTAAAACTTCATTTTTAATTTAAAAGGATCT
AGGTGAAGATCCTTTTTGATAATCTCATGACCAAAATCCCTTAACGTGAGTTTTCGTTCCACTGAGCGTCAGACCCCGTAGAAAAGATCA
AAGGATCTTCTTCAGATCCTTTTTTTCTGCGCGTAATCTGCTGCTTGCAAACAAAAAAACCACCGCTACCAGCGGTGGTTTGTTTGCCGG
ATCAAGAGCTACCAACTCTTTTTCCGAAGGTAACTGGCTTCAGCAGAGCGCAGATACCAAATACTGTCCTTCTAGTGTAGCCGTAGTTAG
GCCACCACTTCAAGAACTCTGTAGCACCGCCTACATACCTCGCTCTGCTAATCCTGTTACCAGTGGCTGCTGCCAGTGGCGATAAGTCG
TGTCTTACCGGGTTGGACTCAAGACGATAGTTACCGGATAAGGCGCAGCGGTCGGGCTGAACGGGGGGTTCGTGCACACAGCCCAGC
TTGGAGCGAACGACCTACACCGAACTGAGATACCTACAGCGTGAGCATTGAGAAAGCGCCACGCTTCCCGAAGGGAGAAAGGCGGACA
GGTATCCGGTAAGCGGCAGGGTCGGAACAGGAGAGCGCACGAGGGAGCTTCCAGGGGGAAACGCCTGGTATCTTTATAGTCCTGTCG
GGTTTCGCCACCTCTGACTTGAGCGTCGATTTTTGTGATGCTCGTCAGGGGGGCGGAGCCTATGGAAAAACGCCAGCAACGCGGCCTT
TTTACGGTTCCTGGCCTTTTGCTGGCCTTTTGCTCACATGTTCTTTCCTGCGTTATCCCCTGATTCTGTGGATAACCGTATTACCGCCTTT
GAGTGAGCTGATACCGCTCGCCGCAGCCGAACGACCGAGCGCAGCGAGTCAGTGAGCGAGGAAGCGGAAGAGCGCCCAATACGCAA
ACCGCCTCTCCCCGCGCGTTGGCCGATTCATTAATCCAGCTGGCACGACAGGTTTCCCGACTGGAAAGCGGGCAGTGAGCGCAACGC
AATTAATGTGAGTTACCTCACTCATTAGGCACCCCAGGCTTTACACTTTATGCTTCCGGCTCGTATGTTGTGTGGAATTGTGAGCGGATA
ACAATTTCACACAGGAAACAGCTATGACCATGATTACGAATTAA

Supplemental figure 4. Nucleotide sequence of the pSSA GFP plasmid.

References

Aldrich, C.J., A. DeCloux, A.S. Woods, R.J. Cotter, M.J. Soloski, and J. Forman. 1994. Identification of a tap-dependent leader peptide recognized by alloreactive T cells specific for a class Ib antigen. *Cell*. 79:649–658. doi:10.1016/0092-8674(94)90550-9.

Anzalone, R., M. Lo Iacono, T. Loria, A. Di Stefano, P. Giannuzzi, F. Farina, and G. La Rocca. 2010. Wharton's Jelly Mesenchymal Stem Cells as Candidates for Beta Cells Regeneration: Extending the Differentiative and Immunomodulatory Benefits of Adult Mesenchymal Stem Cells for the Treatment of Type 1 Diabetes. *Stem Cell Rev. Rep.* 7:342–363. doi:10.1007/s12015-010-9196-4.

Baiu, D., F. Merriam, and J. Odorico. 2011. Potential Pathways to Restore β-Cell Mass: Pluripotent Stem Cells, Reprogramming, and Endogenous Regeneration. *Curr. Diab. Rep.* 11:392–401. doi:10.1007/s11892-011-0218-7.

Barton, F.B., M.R. Rickels, R. Alejandro, B.J. Hering, S. Wease, B. Naziruddin, J. Oberholzer, J.S. Odorico, M.R. Garfinkel, M. Levy, F. Pattou, T. Berney, A. Secchi, S. Messinger, P.A. Senior, P. Maffi, A. Posselt, P.G. Stock, D.B. Kaufman, X. Luo, F. Kandeel, E. Cagliero, N.A. Turgeon, P. Witkowski, A. Naji, P.J. O'Connell, C. Greenbaum, Y.C. Kudva, K.L. Brayman, M.J. Aull, C. Larsen, T.W.H. Kay, L.A. Fernandez, M.-C. Vantyghem, M. Bellin, and A.M.J. Shapiro. 2012. Improvement in Outcomes of Clinical Islet Transplantation: 1999–2010. *Diabetes Care*. 35:1436–1445. doi:10.2337/dc12-0063.

Bedell, V.M., Y. Wang, J.M. Campbell, T.L. Poshusta, C.G. Starker, R.G. Krug Ii, W. Tan, S.G. Penheiter, A.C. Ma, A.Y.H. Leung, S.C. Fahrenkrug, D.F. Carlson, D.F. Voytas, K.J. Clark, J.J. Essner, and S.C. Ekker. 2012. In vivo genome editing using a high-efficiency TALEN system. *Nature*. advance online publication. doi:10.1038/nature11537.

Bernabeu, C., M. van de Rijn, P.G. Lerch, and C.P. Terhorst. 1984. β2-Microglobulin from serum associates with MHC class I antigens on the surface of cultured cells. *Nature*. 308:642–645. doi:10.1038/308642a0.

Busch, A., W. Marasco, C. Doebis, H. Volk, and M. Seifert. 2004. MHC class I manipulation on cell surfaces by gene transfer of anti-MHC class I intrabodies: a tool for decreased immunogenicity of allogeneic tissue and cell transplants. *Methods*. 34:240–249. doi:10.1016/j.ymeth.2004.03.017.

Chandra, V., S. G, S. Muthyala, A.K. Jaiswal, J.R. Bellare, P.D. Nair, and R.R. Bhonde. 2011. Islet-Like Cell Aggregates Generated from Human Adipose

Tissue Derived Stem Cells Ameliorate Experimental Diabetes in Mice. *PLoS ONE*. 6:e20615. doi:10.1371/journal.pone.0020615.

Chun, T., E. Hermel, R.H. Gaskins, and C. Aldrich. 2001. Cytotoxic T lymphocyte and cDNA sequence analyses of the MHC class Ib molecule Qa1 in nonobese diabetic mice. *Immunogenetics*. 53:506–510. doi:10.1007/s002510100357.

Colton, C.K. 2014. Oxygen supply to encapsulated therapeutic cells. *Adv. Drug Deliv. Rev.* doi:10.1016/j.addr.2014.02.007.

Coppieters, K.T., F. Dotta, N. Amirian, P.D. Campbell, T.W.H. Kay, M.A. Atkinson, B.O. Roep, and M.G. von Herrath. 2012. Demonstration of islet-autoreactive CD8 T cells in insulitic lesions from recent onset and long-term type 1 diabetes patients. *J. Exp. Med.* 209:51–60. doi:10.1084/jem.20111187.

Culina, S., C. Boitard, and R. Mallone. 2011. Antigen-Based Immune Therapeutics for Type 1 Diabetes: Magic Bullets or Ordinary Blanks? *Clin. Dev. Immunol.* 2011:1–15. doi:10.1155/2011/286248.

Danchin, E., V. Vitiello, A. Vienne, O. Richard, P. Gouret, M.F. McDermott, and P. Pontarotti. 2004. The major histocompatibility complex origin. *Immunol. Rev.* 198:216–232. doi:10.1111/j.0105-2896.2004.00132.x.

Diz, R., A. Garland, B.G. Vincent, M.C. Johnson, N. Spidale, B. Wang, and R. Tisch. 2012. Autoreactive Effector/Memory CD4+ and CD8+ T Cells Infiltrating Grafted and Endogenous Islets in Diabetic NOD Mice Exhibit Similar T Cell Receptor Usage. *PLoS ONE*. 7:e52054. doi:10.1371/journal.pone.0052054.

Doyle, E.L., N.J. Booher, D.S. Standage, D.F. Voytas, V.P. Brendel, J.K. Vandyk, and A.J. Bogdanove. 2012. TAL Effector-Nucleotide Targeter (TALE-NT) 2.0: tools for TAL effector design and target prediction. *Nucleic Acids Res.* 40:W117–122. doi:10.1093/nar/gks608.

Eventov-Friedman, S., and Y. Reisner. 2013. Fetal Pancreas as a Source for Islet Transplantation Sweet Promise and Current Challenges. *Diabetes*. 62:1382–1383. doi:10.2337/db13-0018.

Frances Gays, Meera Unnikrishnan, Sunil Shrestha, Karen P. Fraser, Adam R. Brown, Colin M. G. Tristram, Z.M.A. Chrzanowska-Lightowlers, and and C.G. Brooks. 2000. The Mouse Tumor Cell Lines EL4 and RMA Display Mosaic Expression of NK-Related and Certain Other Surface Molecules and Appear to Have a Common Origin. *J. Immunol.* 164:5094–102.

Gaj, T., C.A. Gersbach, and C.F. Barbas III. 2013. ZFN, TALEN, and CRISPR/Cas-based methods for genome engineering. *Trends Biotechnol.* 31:397–405. doi:10.1016/j.tibtech.2013.04.004.

De la Garza-Rodea, A., M. Verweij, H. Boersma, I. van der Velde-van Dijke, A. de Vries, R. Hoeben, D. van Bekkum, E.J. Wiertz, S. Knaän-Shanzer, and D. Unutmaz. 2011. Exploitation of Herpesvirus Immune Evasion Strategies to Modify the Immunogenicity of Human Mesenchymal Stem Cell Transplants. *PLoS ONE*. 6:e14493. doi:10.1371/journal.pone.0014493.

Gojanovich, G.S., S.L. Murray, A.S. Buntzman, E.F. Young, B.G. Vincent, and P.R. Hess. 2012. The use of peptide-major-histocompatibility-complex multimers in type 1 diabetes mellitus. *J. Diabetes Sci. Technol.* 6:515–524.

Guschin, D.Y., A.J. Waite, G.E. Katibah, J.C. Miller, M.C. Holmes, and E.J. Rebar. 2010. A rapid and general assay for monitoring endogenous gene modification. *Methods Mol. Biol. Clifton NJ*. 649:247–256. doi:10.1007/978-1-60761-753-2_15.

Hacke, K., R. Falahati, L. Flebbe-Rehwaldt, N. Kasahara, and K. Gaensler. 2008. Suppression of HLA expression by lentivirus-mediated gene transfer of siRNA cassettes and in vivo chemoselection to enhance hematopoietic stem cell transplantation. *Immunol. Res.* 44:112–126. doi:10.1007/s12026-008-8088-z.

Hamaguchi, K., H.R. Gaskins, and E.H. Leiter. 1991. NIT-1, a pancreatic β-cell line established from a transgenic NOD/Lt mouse. *Diabetes*. 40:842–849.

Hassan, M.I., and F. Ahmad. 2011. Chapter 6 - Structural diversity of class I MHC-like molecules and its implications in binding specificities. *In* Advances in Protein Chemistry and Structural Biology. Rossen Donev, editor. Academic Press. 223–270.

Horst, D., M.E. Ressing, and E.J.H.J. Wiertz. 2011. Exploiting human herpesvirus immune evasion for therapeutic gain: potential and pitfalls. *Immunol. Cell Biol.* 89:359–366. doi:10.1038/icb.2010.129.

Kärre, K., H.G. Ljunggren, G. Piontek, and R. Kiessling. 1986. Selective rejection of H–2-deficient lymphoma variants suggests alternative immune defence strategy. *Nature*. 319:675–678. doi:10.1038/319675a0.

Katz, J., C. Benoist, and D. Mathis. 1993. Major histocompatibility complex class I molecules are required for the development of insulitis in non-obese diabetic mice. *Eur. J. Immunol.* 23:3358–3360.

Kim, H., M.-S. Kim, G. Wee, C. Lee, H. Kim, and J.-S. Kim. 2013. Magnetic Separation and Antibiotics Selection Enable Enrichment of Cells with ZFN/TALEN-Induced Mutations. *PLoS ONE*. 8. doi:10.1371/journal.pone.0056476.

Kim, J.Y., D. Kim, I. Choi, J.S. Yang, D.-S. Lee, J.R. Lee, K. Kang, S. Kim, W.S. Hwang, J.S. Lee, and C. Ahn. 2005. MHC expression in a human adult stem cell line and its down-regulation by hCMV US gene transfection. *Int. J. Biochem. Cell Biol.* 37:69–78. doi:10.1016/j.biocel.2004.04.024.

Kupfer, T.M., M.L. Crawford, K. Pham, and R.G. Gill. 2005. MHC-Mismatched Islet Allografts Are Vulnerable to Autoimmune Recognition In Vivo. *J. Immunol.* 175:2309–2316.

Lieber, M.R. 2010. The Mechanism of Double-Strand DNA Break Repair by the Nonhomologous DNA End Joining Pathway. *Annu. Rev. Biochem.* 79:181–211. doi:10.1146/annurev.biochem.052308.093131.

Lieberman, S.M., A.M. Evans, B. Han, T. Takaki, Y. Vinnitskaya, J.A. Caldwell, D.V. Serreze, J. Shabanowitz, D.F. Hunt, S.G. Nathenson, P. Santamaria, and and T.P. DiLorenzo. 2003. Identification of the beta cell antigen targeted by a prevalent population of pathogenic CD8+ T cells in autoimmune diabetes. *Proc. Natl. Acad. Sci.* 100:8384–8388. doi:10.1073/pnas.0932778100.

Liu, G.-H., I. Sancho-Martinez, and J.C.I. Belmonte. 2012. Cut and Paste: restoring cellular function by gene correction. *Cell Res.* 22:283–284. doi:10.1038/cr.2011.192.

Di Lorenzo, T., R. Graser, T. Ono, G. Christianson, H. Chapman, D. Roopenian, S. Nathenson, and D. Serreze. 1998. Major histocompatibility complex class I-restricted T cells are required for all but the end stages of diabetes development in nonobese diabetic mice and use a prevalent T cell receptor alpha chain gene rearrangement. *Proc. Natl. Acad. Sci.* 95:12538–43.

Ludwig, B., A. Reichel, A. Steffen, B. Zimerman, A.V. Schally, N.L. Block, C.K. Colton, S. Ludwig, S. Kersting, E. Bonifacio, M. Solimena, Z. Gendler, A. Rotem, U. Barkai, and S.R. Bornstein. 2013. Transplantation of human islets without immunosuppression. *Proc. Natl. Acad. Sci.* 201317561. doi:10.1073/pnas.1317561110.

Ma, N., B. Liao, H. Zhang, L. Wang, Y. Shan, Y. Xue, K. Huang, S. Chen, X. Zhou, Y. Chen, D. Pei, and G. Pan. 2013. Transcription activator-like effector nuclease (TALEN)-mediated gene correction in integration-free β-thalassemia induced pluripotent stem cells. *J. Biol. Chem.* 288:34671–34679. doi:10.1074/jbc.M113.496174.

Mak, A.N.-S., P. Bradley, A.J. Bogdanove, and B.L. Stoddard. 2013. TAL effectors: function, structure, engineering and applications. *Curr. Opin. Struct. Biol.* 23:93–99. doi:10.1016/j.sbi.2012.11.001.

Maudsley, D.J., and J.D. Pound. 1991. Modulation of MHC antigen expression by viruses and oncogenes. *Immunol. Today*. 12:429–431. doi:10.1016/0167-5699(91)90013-J.

Mendell, J.R., K. Campbell, L. Rodino-Klapac, Z. Sahenk, C. Shilling, S. Lewis, D. Bowles, S. Gray, C. Li, G. Galloway, V. Malik, B. Coley, K.R. Clark, J. Li, X. Xiao, J. Samulski, S.W. McPhee, R.J. Samulski, and C.M. Walker. 2010. Dystrophin Immunity in Duchenne's Muscular Dystrophy. *N. Engl. J. Med.* 363:1429–1437. doi:10.1056/NEJMoa1000228.

Miller, J.C., S. Tan, G. Qiao, K.A. Barlow, J. Wang, D.F. Xia, X. Meng, D.E. Paschon, E. Leung, S.J. Hinkley, G.P. Dulay, K.L. Hua, I. Ankoudinova, G.J. Cost, F.D. Urnov, H.S. Zhang, M.C. Holmes, L. Zhang, P.D. Gregory, and E.J. Rebar. 2010. A TALE nuclease architecture for efficient genome editing. *Nat. Biotechnol.* 29:143–148. doi:10.1038/nbt.1755.

Moran, J.P., J. Walter, G.W. Tannock, S.L. Tonkonogy, and B.R. Sartor. 2009. Bifidobacterium animalis causes extensive duodenitis and mild colonic inflammation in monoassociated interleukin-10-deficient mice: *Inflamm. Bowel Dis.* 15:1022–1031. doi:10.1002/ibd.20900.

O'Sullivan, E., A. Vegas, D. Anderson, and G. Weir. 2011. Islets Transplanted in Immunoisolation Devices: A Review of the Progress and the Challenges that Remain. *Endocr. Rev.* 32. doi:10.1210/er.2010-0026.

Ogasawara, K., J. Hamerman, H. Hsin, S. Chikuma, H. Bour-Jordan, T. Chen, T. Pertel, C. Carnaud, J. Bluestone, and L. Lanier. 2003. Impairment of NK Cell Function by NKG2D Modulation in NOD Mice. *Immunity*. 18:41–51.

Orange, J., M. Fassett, L. Koopman, J. Boyson, and and J. Strominger. 2002. Viral evasion of natural killer cells. *Nat. Immunol.* 3:1006–12.

Ousterout, D.G., P. Perez-Pinera, P.I. Thakore, A.M. Kabadi, M.T. Brown, X. Qin, O. Fedrigo, V. Mouly, J.P. Tremblay, and C.A. Gersbach. 2013. Reading frame correction by targeted genome editing restores dystrophin expression in cells from Duchenne muscular dystrophy patients. *Mol. Ther. J. Am. Soc. Gene Ther.* 21:1718–1726. doi:10.1038/mt.2013.111.

Panda, S.K., B. Wefers, O. Ortiz, T. Floss, B. Schmid, C. Haass, W. Wurst, and R. Kühn. 2013. Highly efficient targeted mutagenesis in mice using TALENs. *Genetics*. 195:703–713. doi:10.1534/genetics.113.156570.

Perez-Pinera, P., D.G. Ousterout, M.T. Brown, and C.A. Gersbach. 2012. Gene targeting to the ROSA26 locus directed by engineered zinc finger nucleases. *Nucleic Acids Res.* 40:3741–3752. doi:10.1093/nar/gkr1214.

Poulton, L., M. Smyth, C. Hawke, P. Silveira, D. Shepherd, O. Naidenko, D. Godfrey, and A. Baxter. 2001. Cytometric and functional analyses of NK and NKT cell deficiencies in NOD mice. *Int. Immunol.* 13:887–96.

Powis, S.J., A.R.M. Townsend, E.V. Deverson, J. Bastin, G.W. Butcher, and J.C. Howard. 1991. Restoration of antigen presentation to the mutant cell line RMA-S by an MHC-linked transporter. *Nature*. 354:528–531.

Prange, S., P. Zucker, A. Jevnikar, and B. Singh. 2001. Transplanted MHC class I-deficient nonobese diabetic mouse islets are protected from autoimmune injury in diabetic nonobese recipients. *Transplantation*. 71:982–5.

Revilleza, M., R. Wang, J. Mans, M. Hong, K. Natarajan, and D. Margulies. 2011. How the Virus Outsmarts the Host: Function and Structure of Cytomegalovirus MHC-I-Like Molecules in the Evasion of Natural Killer Cell Surveillance. *J. Biomed. Biotechnol.* 2011:1–12. doi:10.1155/2011/724607.

Reyon, D., S.Q. Tsai, C. Khayter, J.A. Foden, J.D. Sander, and J.K. Joung. 2012. FLASH assembly of TALENs for high-throughput genome editing. *Nat. Biotechnol.* 30:460–465. doi:10.1038/nbt.2170.

Robinson, P.J., P.J. Travers, A. Stackpoole, L. Flaherty, and and H. Djaballah. 1998. Maturation of Qa-1b Class I Molecules Requires ß2 Microglobulin But Is TAP Independent. *J. Immunol.* 160:3217–24.

Roep, B., and M. Peakman. 2012. Antigen targets of type 1 diabetes autoimmunity. *Cold Spring Harb. Perspect. Med.* doi:Advanced online article.

Sander, J.D., M.L. Maeder, D. Reyon, D.F. Voytas, J.K. Joung, and D. Dobbs. 2010. ZiFiT (Zinc Finger Targeter): an updated zinc finger engineering tool. *Nucleic Acids Res.* gkq319. doi:10.1093/nar/gkq319.

Sibley, R., D. Sutherland, F. Goetz, and A. Michael. 1985. Recurrent diabetes mellitus in the pancreas iso- and allograft. A light and electron microscopic and immunohistochemical analysis of four cases. *Lab. Investig.* 53:132–144.

Skowera, A., R. Ellis, R. Varela-Calviño, S. Arif, G. Huang, C. Van-Krinks, A. Zaremba, C. Rackham, J. Allen, T. Tree, M. Zhao, C. Dayan, A. Sewell, W. Unger, J. Drijfhout, F. Ossendorp, B. Roep, and M. Peakman. 2008. CTLs are targeted to kill β cells in patients with type 1 diabetes through recognition of a glucose-regulated preproinsulin epitope. *J. Clin. Invest.* 118:3390–402. doi:10.1172/jci35449ds1.

Di Stasi, A., S.-K. Tey, G. Dotti, Y. Fujita, A. Kennedy-Nasser, C. Martinez, K. Straathof, E. Liu, A.G. Durett, B. Grilley, H. Liu, C.R. Cruz, B. Savoldo, A.P. Gee, J. Schindler, R.A. Krance, H.E. Heslop, D.M. Spencer, C.M. Rooney, and M.K. Brenner. 2011. Inducible Apoptosis as a Safety Switch for Adoptive Cell Therapy. *N. Engl. J. Med.* 365:1673–1683. doi:10.1056/NEJMoa1106152.

Strouse, B., P. Bialk, R.A. Niamat, N. Rivera-Torres, and E.B. Kmiec. 2014. Combinatorial gene editing in mammalian cells using ssODNs and TALENs. *Sci. Rep.* 4. doi:10.1038/srep03791.

Sutherland, D., F. Goetz, and R. Sibley. 1989. Recurrence of disease in pancreas transplants. *Diabetes*. 38:85–87.

Tabaczewski, P., and I. Stroynowski. 1994. Expression of secreted and glycosylphosphatidylinositol-bound Qa-2 molecules is dependent on functional TAP-2 peptide transporter. *J. Immunol.* 152:5268–5274.

Vance, R.E., J.R. Kraft, J.D. Altman, P.E. Jensen, and D.H. Raulet. 1998. Mouse CD94/NKG2A is a natural killer cell receptor for the nonclassical major histocompatibility complex (MHC) class I molecule Qa-1(b). *J. Exp. Med.* 188:1841–1848.

Velthuis, J., W. Unger, J. Abreu, G. Duinkerken, K. Franken, M. Peakman, A. Bakker, S. Reker-Hadrup, B. Keymeulen, J. Drijfhout, T. Schumacher, and B. Roep. 2010. Simultaneous Detection of Circulating Autoreactive CD8+ T-Cells Specific for Different Islet Cell-Associated Epitopes Using Combinatorial MHC Multimers. *Diabetes*. 59:1721–1730. doi:10.2337/db09-1486.

Verdaguer, J., D. Schmidt, A. Amrani, B. Anderson, N. Averill, and and P. Santamaria. 1997. Spontaneous Autoimmune Diabetes in Monoclonal T Cell Nonobese Diabetic Mice. *J. Exp. Med.* 186:1663–76.

Vugmeyster, Y., R. Glas, B. Pérarnau, F.A. Lemonnier, H. Eisen, and H. Ploegh. 1998. Major histocompatibility complex (MHC) class I KbDb −/− deficient mice possess functional CD8+ T cells and natural killer cells. *Proc. Natl. Acad. Sci.* 95:12492–12497. doi:10.1073/pnas.95.21.12492.

Wang, H., Y.-C. Hu, S. Markoulaki, G.G. Welstead, A.W. Cheng, C.S. Shivalila, T. Pyntikova, D.B. Dadon, D.F. Voytas, A.J. Bogdanove, D.C. Page, and R. Jaenisch. 2013. TALEN-mediated editing of the mouse Y chromosome. *Nat. Biotechnol.* 31:530–532. doi:10.1038/nbt.2595.

Wicky, B.I.M., M. Stenta, and M. Dal Peraro. 2013. TAL Effectors Specificity Stems from Negative Discrimination. *PLoS ONE*. 8:e80261. doi:10.1371/journal.pone.0080261.

Xiang, Z., L. Ma, S. Manicassamy, B. Ganesh, P. Williams, R. Chari, A. Chong, and D. Yin. 2008. CD4+ T Cells Are Sufficient to Elicit Allograft Rejection and Major Histocompatibility Complex Class I Molecule Is Required to Induce Recurrent Autoimmune Diabetes After Pancreas Transplantation in Mice. *Transplantation*. 85:1205–1211. doi:10.1097/TP.0b013e31816b70bf.

Young, H., P. Zucker, R. Flavell, A. Jevnikar, and B. Singh. 2004. Characterization of the Role of Major Histocompatibility Complex in Type 1 Diabetes Recurrence after Islet Transplantation. *Transplantation*. 78:509–515. doi:10.1097/01.tp.0000128907.83111.c6.

Zijlstra, M., M. Bix, N.E. Simister, J.M. Loring, D.H. Raulet, and R. Jaenisch. 1990. β2-Microglobulin deficient mice lack CD4|[minus]|8+ cytolytic T cells. *Nature*. 344:742–746. doi:10.1038/344742a0.

CHAPTER 7: Future directions for experiments and dissertation summary

In this chapter I present a brief summary of the results described in previous chapters and highlights future experimental directions for the knockout (KO) cell lines in which TALEN technology was utilized to create MHCI^{low} cell lines (chapters 4 and 6). In those chapters, we showed that TALEN-mediated KO of either the feline transporter associated with antigen processing 2 gene (TAP2; chapter 4) or the classical murine MHCI heavy chain loci (H2-K1 and –D1; chapter 6) resulted in cell lines incapable of presenting MHCI proteins at normal levels. These cell lines were created for the intended use in either detecting MHCI-restricted CD8+ T-cell responses and determining FLAI peptide-binding motifs (CRFK-PoBoy clones), or for showing proof of concept that TALEN-modified cells can evade autoimmune responses that could ensue following transplantation into diabetic recipients (NIT-KG).

Canine TAP gene function

Chapter 2 contains a description of the coding sequences and promoter regions of the canine TAP1/2 genes and confirmation of functionality of the commonly expressed TAP2*001A allele via gene complementation in the murine TAP2-KO RMAS cell line. These data will be useful for studies determining the biochemical properties of the canine TAP proteins by providing coding sequences capable of being translated for expression using biotechnological applications. Furthermore, these data provide insights into polymorphisms and splicing variants that occur naturally within the canine breeds and will allow for studies determining any associations of such variants with susceptibility to infectious or malignant pathologies, as has been described in humans (Wang et al., 2012); although, the contribution of TAP gene polymorphisms to disease susceptibility is still debatable (Rueda Faucz et al., 2000). Nonetheless, our results will assist in increasing the understanding of antigen presentation and immune responses in this invaluable companion animal species.

CRFK TAP2-KO CELL LINE APPLICATIONS

In chapter 4, we describe the creation two TAP2-KO cell clones (WT PoBoy1 and 1A3 PoBoy2) that showed the characteristic of increased FLAI expression following incubation at 27C overnight. This result indicates that FLAI complexes on CRFK cells are thermolabile (readily dissociate at physiological temperatures), which will allow for amino acid sequencing of FLAI-bound peptides presented following cold incubation (Silva et al., 1999). This could be performed by incubating the clones overnight at 27C and performing acid elution protocols followed by peptide purification and double mass spectrometry analyses. Such data would be useful in comparisons to the amino acid sequences determined by acid elution of parental, TAP2-replete FLAI peptides for determining variations in peptide motifs presented during TAP2-KO conditions. An issue that could cause difficulty during peptide sequence comparisons would be the fact that numerous FLAI loci are expressed by

CRFK cells [data not shown, (Holmes et al., 2013)], thereby making the presented peptide pool more variable and thus the identification of peptides that bind to specific FLAI allelic product becomes more difficult. Furthermore, studies have shown that TAP-independent antigens presented at the surface may not actually resemble the canonical peptide motif normally associated with the presenting MHCI complex (Mendoza et al., 1997). However, such analyses could result in data indicating that only a single FLAI complex is capable of expression following cold incubation as determined by the identification of the sequence of a restricted peptide-binding motif. Alternatively, the use of the 1A3 PoBoy2 clone in the above analysis allows for determination of FLAI-E allele-specific peptide-binding characteristics following cold incubation to be compared to the TAP2-replete 1A3 cell line. This could be performed by immunoprecipitation of the FLAG-tagged FLAI-E molecules prior to peptide analyses. A drawback to this experimental design is the possibility that this allele is not thermolabile and therefore would not present antigen following cold incubation. However, we currently cannot directly address this due to the lack of antibodies capable of specifically labeling the FLAI-E complex.

Another useful application of the TAP2-KO CRFK clones is the determination of TAP-independent FLAI expression of pathogen-derived peptides following infection. It has been determined previously that the TAP-KO RMAS cell line is capable of presenting MHCI complexes loaded with virus-derived peptides following infection (Esquivel et al., 1992). In fact, such TAP-independent MHCI presentation is not limited to infection but has been shown to occur in autoimmune diabetes

(Skowera et al., 2008). Thus, we could address whether infections of the PoBoy lines with different pathogens result in increased FLAI expression and determine exact epitope sequences bound to either bulk FLAI complexes (PoBoy1) or the FLAI-E allele-specific complex (PoBoy2). Data acquired from the above experiments could be useful in creation of vaccines capable of enhancing beneficial CD8+ T-cell responses that recognize TAP-inhibited, virally-infected cells, a situation which occurs during certain herpesvirus infections (Ahn et al., 1997; Früh et al., 1995; Montagnaro et al., 2009).

TAP GENE CHARACTERIZATION

A wealth of knowledge regarding the antigen processing and presentation pathways involved in MHCI expression has been amassed in the recent years across species [reviewed in (Neefjes et al., 2011; Parcej and Tampe, 2010)], however very little data are available for companion animals. Specifically, the experiments described above may shed light into whether TAP-independent MHCI presentation routes (Snyder et al., 1997) are conserved in these species. The information collected in Chapters 2 and 4 will also help to elucidate the biochemical nature of the TAP complexes in both the canine and feline species. Results of our recent work will allow direct comparisons of the canine and feline TAP complexes to the well-described human proteins in order to determine kinetics of antigen processing and the necessary residues within the heterodimeric pump for peptide recognition and ATP hydrolysis. Furthermore, such comparisons could confirm the presence of accessory membrane-spanning domains within the canine and feline TAP proteins that have been shown in other species to interact with chaperone molecules during MHCI folding to increase peptide loading (Procko et al., 2005) and supplement the core TAP function (Koch et al., 2004). Determining the chaperone-interacting domains in the canine TAP2 gene and comparing these to confirmed residues in other species could provide further insights, beyond transfection efficiency, into why our gene complementation efforts only yielded modest results. Specifically, variation at these residues in the canine TAP2 protein may have been responsible for reduced capacity to load peptides into the clefts of the murine and feline MHCI complexes. Thus, the determination of the coding sequences of TAP genes in canines (Chapter 2) and the confirmation of the TAP2 locus in felines (Chapter 4) has provided data to allow future studies that should expand our knowledge of the peptide loading complex in these species.

FUTURE STUDIES USING THE MURINE MHCI-KO CELL LINES

In Chapter 6 we described the use of TALENs to target the MHCI heavy chain loci in murine insulinoma cell lines. We confirmed TALEN-mediated modifications at the H2-K1, -D1, (and –Kb) loci resulted in disruption of surface MHCI expression. Preliminary data far indicated that the TALEN-modified NIT-KG clone was able to escape recognition by transgenic, autoreactive CD8+ T cells from the 8.3-NOD mouse strain. Future experiments will be necessary to confirm these initial findings.

While the described NIT-KG and NIT-1 cells could be utilized in *in vivo* transplant experiments, long term transplant survival could be hampered by the presence of anti-SV40 T-cell responses and the tumorigenic nature of NIT-1 cells following transplantation (McKenzie et al., 2000). However, the results published previously (Xiang et al., 2008; Prange et al., 2001; Young et al., 2004) show that ~25% of the NOD recipients of MHCI-KO grafts rejected these grafts. NK cells could have caused rejection, as has been noted in other MHCI-KO strategies (de la Garza-Rodea et al., 2011).

As the NOD-derived NIT-1 cells are not ideal for such experiments, future proposed experiments could address *ex vivo* NK-cell analyses using TALEN-modified, MHCI-KO EL4 cell lines. In short, NOD NK cells lack proper activating signals (Poulton et al., 2001) and NIT-1 cells do not present adequate inhibitory signals (Chun et al., 2001). Thus, the approach using EL4 cells as NK cell targets would allow a more thorough evaluation of the necessary expression levels of K^b and D^b surface protein needed to evade recognition by NK cells. This could be achieved by selecting EL4 cell clones with altered expression of one or both MHCI proteins and exposing cells of differing phenotypes to $H2^b$-licensed NK cells. If MHCI-modified clones are found to be rejected by NK cells, the use of homology arm-containing plasmids to introduce virus-derived immunevasin genes into TALEN-disrupted loci via homology-directed recombination could also be envisioned and applied to prevent NK-cell susceptibility (Orange et al., 2002).

The above experiments will be useful in validating the applicability of TALEN-mediated MHCI-modified cells as transplantable tissue capable of escaping autoreactive responses. Data provided by the described experiments could justify the application of this technology to the realm of stem cells, which would be differentiated into insulin producing grafts for use in ameliorating type 1diabetes. While much work lies ahead in differentiating insulin secreting tissues from human stem cells (Ravassard et al., 2011; Trivedi et al., 2008; Chandra et al., 2011), the proof of concept has been shown in murine models (Alipio et al., 2010; Chandra et al., 2009), to which the TALEN strategy could be applied. Thus, following confirmation of immune evasion, murine stem cells could be transfected with MHCI-targeting TALENs, followed by GFP+ cell enrichment, cell cloning, and genomic modification confirmation, and then the cells could be differentiated into clonal insulin producing populations lacking MHCI expression. These MHCI-KO islet-like populations would next need to be evaluated for insulin responsiveness to physiological levels of glucose, and full genome sequencing to insure lack of off-site mutations. Ultimately, such strategies could provide type 1 diabetic patients a means of insulin-injection independence without immunosuppression, which is currently not possible following transplantation.

CONCLUDING REMARKS

The results and discussion present in this dissertation adds to the knowledge base of current immunological understanding by characterizing the TAP genes in canine breeds; by confirming the TAP2 locus in the feline species; by creating TAP2-KO feline cell lines useful for FLAI peptide-binding motif confirmation and detection of FLAI-restricted CD8+ T-cell responses; and by confirming TALENs as a valuable technology for creating immune cell-invisible tissues, which could alleviate diabetes recurrence in graft recipients.

References

Ahn, K., A. Gruhler, B. Galocha, T.R. Jones, E.J.H.J. Wiertz, H.L. Ploegh, P.A. Peterson, Y. Yang, and K. Früh. 1997. The ER-Luminal Domain of the HCMV Glycoprotein US6 Inhibits Peptide Translocation by TAP. *Immunity*. 6:613–621. doi:10.1016/S1074-7613(00)80349-0.

Alipio, Z., W. Liao, E. Roemer, M. Waner, L. Fink, D. Ward, and Y. Ma. 2010. Reversal of hyperglycemia in diabetic mouse models using induced-pluripotent stem (iPS)-derived pancreatic beta-like cells. *Proc. Natl. Acad. Sci.* 107:13426–31.

Chandra, V., S. G, S. Muthyala, A. Jaiswal, J. Bellare, P. Nair, and R. Bhonde. 2011. Islet-like cell aggregates generated from human adipose tissue derived stem cells ameliorate experimental diabetes in mice. *PLoS ONE*. 6:e20615. doi:10.1371/journal.pone.0020615.g001.

Chandra, V., S. G, S. Phadnis, P. Nair, and R. Bhonde. 2009. Generation of Pancreatic Hormone-Expressing Islet-Like Cell Aggregates from Murine Adipose Tissue-Derived Stem Cells. *Stem Cells*. 27:1941–1953. doi:10.1002/stem.117.

Chun, T., E. Hermel, R.H. Gaskins, and C. Aldrich. 2001. Cytotoxic T lymphocyte and cDNA sequence analyses of the MHC class Ib molecule Qa1 in nonobese diabetic mice. *Immunogenetics*. 53:506–510. doi:10.1007/s002510100357.

Esquivel, F., J. Yewdell, and J. Bennink. 1992. RMA/S cells present endogenously synthesized cytosolic proteins to class I-restricted cytotoxic T lymphocytes. *J. Exp. Med.* 175:163–168. doi:10.1084/jem.175.1.163.

Früh, K., K. Ahn, H. Djaballah, P. Sempé, P.M. van Endert, R. Tampé, P.A. Peterson, and Y. Yang. 1995. A viral inhibitor of peptide transporters for antigen presentation. *Nature*. 375:415–418. doi:10.1038/375415a0.

De la Garza-Rodea, A., M. Verweij, H. Boersma, I. van der Velde-van Dijke, A. de Vries, R. Hoeben, D. van Bekkum, E.J. Wiertz, S. Knaän-Shanzer, and D. Unutmaz. 2011. Exploitation of Herpesvirus Immune Evasion Strategies to Modify the Immunogenicity of Human Mesenchymal Stem Cell Transplants. *PLoS ONE*. 6:e14493. doi:10.1371/journal.pone.0014493.

Holmes, J.C., S.G. Holmer, P. Ross, A.S. Buntzman, J.A. Frelinger, and P.R. Hess. 2013. Polymorphisms and tissue expression of the feline leukocyte antigen class I loci FLAI-E, FLAI-H, and FLAI-K. *Immunogenetics*. 65:675–689. doi:10.1007/s00251-013-0711-z.

Koch, J., R. Guntrum, S. Heintke, C. Kyritsis, and R. Tampé. 2004. Functional Dissection of the Transmembrane Domains of the Transporter Associated with Antigen Processing (TAP). *J. Biol. Chem.* 279:10142–10147. doi:10.1074/jbc.M312816200.

McKenzie, A.W., J.L. Brady, R.M. Martin, H.M. Georgiou, and A.M. Lew. 2000. Local secretion of a chimeric anti-CD4 antibody protects against graft rejection in the NOD mouse. *Transplantation*. 69:1745–1748.

Mendoza, L.M., P. Paz, A. Zuberi, G. Christianson, D. Roopenian, and N. Shastri. 1997. Minors Held by Majors: The H13Minor Histocompatibility Locus Defined as a Peptide/MHC Class I Complex. *Immunity*. 7:461–472. doi:10.1016/S1074-7613(00)80368-4.

Montagnaro, S., M. Longo, M. Pacilio, P. Indovina, A. Roberti, L. De Martino, G. Iovane, and U. Pagnini. 2009. Feline herpesvirus-1 down-regulates MHC class I expression in an homologous cell system. *J. Cell. Biochem.* 106:179–185. doi:10.1002/jcb.21986.

Neefjes, J., M.L.M. Jongsma, P. Paul, and O. Bakke. 2011. Towards a systems understanding of MHC class I and MHC class II antigen presentation. *Nat. Rev. Immunol.* 11:823–836. doi:10.1038/nri3084.

Orange, J., M. Fassett, L. Koopman, J. Boyson, and and J. Strominger. 2002. Viral evasion of natural killer cells. *Nat. Immunol.* 3:1006–12.

Parcej, D., and R. Tampe. 2010. ABC proteins in antigen translocation and viral inhibition. *Nat Chem Biol*. 6:572–80. doi:nchembio.410 [pii] 10.1038/nchembio.410.

Poulton, L., M. Smyth, C. Hawke, P. Silveira, D. Shepherd, O. Naidenko, D. Godfrey, and A. Baxter. 2001. Cytometric and functional analyses of NK and NKT cell deficiencies in NOD mice. *Int. Immunol.* 13:887–96.

Prange, S., P. Zucker, A. Jevnikar, and B. Singh. 2001. Transplanted MHC class I-deficient nonobese diabetic mouse islets are protected from autoimmune injury in diabetic nonobese recipients. *Transplantation*. 71:982–5.

Procko, E., G. Raghuraman, D.C. Wiley, M. Raghavan, and R. Gaudet. 2005. Identification of domain boundaries within the N-termini of TAP1 and TAP2 and their importance in tapasin binding and tapasin-mediated increase in peptide loading of MHC class I. *Immunol. Cell Biol.* 83:475–482. doi:10.1111/j.1440-1711.2005.01354.x.

Ravassard, P., Y. Hazhouz, S. Pechberty, E. Bricout-Neveu, M. Armanet, P. Czernichow, and and R. Scharfmann. 2011. A genetically engineered human pancreatic beta cell line exhibiting glucose-inducible insulin secretion. *J. Clin. Invest.* 121:3589–97. doi:10.1172/jci58447ds1.

Rueda Faucz, F., C. Macagnan Probst, and M.L. Petzl-Erler. 2000. Polymorphism of LMP2, TAP1, LMP7 and TAP2 in Brazilian Amerindians and Caucasoids: implications for the evolution of allelic and haplotypic diversity. *Eur. J. Immunogenet.* 27:5–16. doi:10.1046/j.1365-2370.2000.00186.x.

Silva, A.D.D., A. Boesteanu, R. Song, N. Nagy, E. Harhaj, C.V. Harding, and S. Joyce. 1999. Thermolabile H-2Kb Molecules Expressed by Transporter Associated with Antigen Processing-Deficient RMA-S Cells Are Occupied by Low-Affinity Peptides. *J. Immunol.* 163:4413–4420.

Skowera, A., R. Ellis, R. Varela-Calviño, S. Arif, G. Huang, C. Van-Krinks, A. Zaremba, C. Rackham, J. Allen, T. Tree, M. Zhao, C. Dayan, A. Sewell, W. Unger, J. Drijfhout, F. Ossendorp, B. Roep, and M. Peakman. 2008. CTLs are targeted to kill β cells in patients with type 1 diabetes through recognition of a glucose-regulated preproinsulin epitope. *J. Clin. Invest.* 118:3390–402. doi:10.1172/jci35449ds1.

Snyder, H.L., I. Bacik, J.R. Bennink, G. Kearns, T.W. Behrens, T. Bachi, M. Orlowski, and J.W. Yewdell. 1997. Two novel routes of transporter associated with antigen processing (TAP)-independent major histocompatibility complex class I antigen processing. *J Exp Med*. 186:1087–98.

Trivedi, H., A. Vanikar, U. Thakker, A. Firoze, S. Dave, C. Patel, J. Patel, A. Bhargava, and V. Shankar. 2008. Human Adipose Tissue-Derived Mesenchymal Stem Cells Combined With Hematopoietic Stem Cell Transplantation Synthesize Insulin. *Transplant. Proc.* 40:1135–1139. doi:10.1016/j.transproceed.2008.03.113.

Wang, D., Y. Zhou, L. Ji, T. He, F. Lin, R. Lin, T. Lin, and Y. Mo. 2012. Association of LMP/TAP Gene Polymorphisms with Tuberculosis Susceptibility in Li Population in China. *PLoS ONE*. 7:e33051. doi:10.1371/journal.pone.0033051.

Xiang, Z., L. Ma, S. Manicassamy, B. Ganesh, P. Williams, R. Chari, A. Chong, and D. Yin. 2008. CD4+ T Cells Are Sufficient to Elicit Allograft Rejection and Major Histocompatibility Complex Class I Molecule Is Required to Induce

Recurrent Autoimmune Diabetes After Pancreas Transplantation in Mice. *Transplantation*. 85:1205–1211. doi:10.1097/TP.0b013e31816b70bf.

Young, H., P. Zucker, R. Flavell, A. Jevnikar, and B. Singh. 2004. Characterization of the Role of Major Histocompatibility Complex in Type 1 Diabetes Recurrence after Islet Transplantation. *Transplantation*. 78:509–515. doi:10.1097/01.tp.0000128907.83111.c6.